ICARUS 110, 117–154 (1994)

Chemical Models of the Deep Atmospheres of Jupiter and Saturn

BRUCE FEGLEY, JR., AND KATHARINA LODDERS

Department of Earth & Planetary Sciences, Campus Box 1169, Washington University, One Brookings Drive, St. Louis, Missouri 63130-4899
E-mail: bfegley@planet.win.net

Received February 10, 1994; revised May 2, 1994

New and updated chemical kinetic data, elemental abundances, and thermodynamic data are used for thermochemical equilibrium and, where relevant, thermochemical kinetic calculations of gas abundances and condensate stability in the hot, deep atmospheres of Jupiter and Saturn. Over 2000 compounds of all naturally occurring elements in the periodic table are considered. The calculations range from 298 to 2000 K and are done for adiabatic models of the two planetary atmospheres. The results predict the abundances of many gases which are potentially observable by the Galileo probe to Jupiter, by the Cassini mission to Saturn, and by Earth-based and Earth-orbital telescopes. In addition, the results also predict many new species which are potentially observable by a new generation of entry probes capable of penetrating deeper into the atmospheres of Jupiter and Saturn.

INTRODUCTION

During the past 25 years, advances in Earth-based and Earth-orbital spectroscopic techniques and the development of spacecraft remote sensing have led to the discovery of many new molecules in the atmospheres of Jupiter and Saturn. In 1969, only H_2, CH_4, and NH_3 were known on Jupiter and Saturn, while today almost 25 different molecules and isotopically substituted species have been detected in their atmospheres (e.g., see the tabulation by Fegley 1994b). Separately, the development of efficient algorithms for the computation of multicomponent chemical equilibria (e.g., see Smith and Missen 1982; Van Zeggeren and Storey 1970), and the use initially of mainframe computers, and later of powerful personal computers and workstations, has provided the ability to produce chemical models of complex natural thermochemical systems such as the deep atmospheres of the jovian planets (Lewis 1969a,b; Barshay and Lewis 1978). The combination of the spectroscopic observations and the theoretical models has led to significant advances in our knowledge of the outer planets (e.g., see Fegley 1990 and references therein).

Four factors motivated us to reexamine the chemistry of the deep atmospheres of Jupiter and Saturn. First, the continuing improvements in Earth-based observational capabilities, which are exemplified by the detection of AsH_3 and GeH_4 at ppb and sub-ppb levels on Jupiter and Saturn (Bézard *et al.* 1989; Noll *et al.* 1988–1990), point out the necessity for reliable models of the chemistry of trace elements which have similar abundances.

Second, the upcoming entry of the Galileo probe into the atmosphere of Jupiter and the planned Cassini mission to Saturn and Titan hold out the promise of major advances in our knowledge of the chemistry and composition of these two gas giant planets. In particular, the Galileo probe, which may provide chemical analyses down to the 20-bar level of the jovian atmosphere (Hunten *et al.* 1986), could detect many species which are not found in the higher, observable regions of Jupiter's atmosphere.

Third, several major new compilations of thermodynamic data for gases and solids have become available in recent years (e.g., Barin 1989; Chase *et al.* 1985; Cordfunke and Konings 1990; Gurvich *et al.* 1989–1994; Knacke *et al.* 1991). These compilations include both newly compiled and significantly revised thermodynamic data for many volatile trace element compounds. The use of an updated thermodynamic database is important because the previous studies of volatile trace element chemistry on Jupiter and Saturn (e.g., Lewis 1969a; Barshay and Lewis 1978; Fegley and Lewis 1979; Fegley and Prinn 1985) used some data from older compilations dating back to the early 1950s. However, new experimental methods and the improvement of existing techniques have led to significant improvements in the quality and quantity of thermodynamic data over the past 40 years.

In addition, as noted by Barshay and Lewis (1978), "In a number of cases it was necessary to extrapolate the high-temperature equilibrium constants from low-temperature data using the Gibbs-Helmholtz equation, a risky and inaccurate business. For this reason, calculations pertaining to the elements Ge, Se, As, Te, Hg, and Sb are

0019-1035/94 $6.00

not reported for temperatures higher than 1000 K." Fegley and Lewis (1979) also used the Gibbs-Helmholtz equation to extrapolate some thermodynamic data and for this reason also reported results (for Ge, Se, Ga, As, Te, Pb, Sn, Cd, Sb, Tl, In, Bi) up to only 1000 K. However, the new thermodynamic data compilations cited earlier generally give equilibrium constants up to at least 2000 K, thus covering the entire temperature range of interest for atmospheric chemistry on Jupiter and Saturn.

Last, as a result of continuing improvements in analytical studies of chondritic meteorites and in solar spectroscopy, the elemental abundances of solar composition material are now much better known than when the prior models of jovian atmospheric chemistry were done. Some elemental abundances have changed dramatically as a result. For example, Lewis (1969a) presented the only prior calculations for Zn, Li, and Be. He used elemental abundances of 603 Zn atoms, 100 Li atoms, and 20 Be atoms per 10^6 Si atoms (Aller 1961; Suess and Urey 1956) while the currently accepted values are 1260 Zn atoms, 57.1 Li atoms, and 0.73 Be atoms per 10^6 Si atoms (Anders and Grevesse 1989). Likewise, Barshay and Lewis (1978) used B and F elemental abundances of 350 B atoms and 2450 F atoms per 10^6 Si atoms (Cameron 1973) while the currently accepted values are only 21.2 B atoms and 843 F atoms per 10^6 Si atoms (Anders and Grevesse 1989). Other elemental abundances which have been revised by more than 10% since the last thermodynamic calculations were presented are O (11% higher), C (14% lower), N (16% lower), Br (13% lower), and Te (25% lower).

We anticipate that the new and revised results presented in this paper will provide a foundation for interpreting existing spectroscopic observations, for guiding future observations from Earth-based and spacecraft platforms, and for designing experiments on future spacecraft missions. In the short term, the work presented here is important for interpreting atmospheric composition measurements from the upcoming Galileo entry probe into the atmosphere of Jupiter and the Cassini orbiter mission to Saturn. In the longer term these models provide essential information for designing the next generation of entry probes that will study the chemical composition of the deep atmospheres of the jovian planets.

METHOD OF CALCULATION

Adiabatic temperature–pressure profiles for the deep atmospheres of Jupiter and Saturn were calculated as described by Fegley and Prinn (1988b) using H_2 and He mole fractions of 0.898 and 0.102 on Jupiter (Gautier *et al.* 1981) and 0.963 and 0.0325 on Saturn (Conrath *et al.* 1984). The calculated profiles for Jupiter and Saturn are displayed in Fig. 1. We adopted chemical composition models which use the observed abundances of H_2, He, and

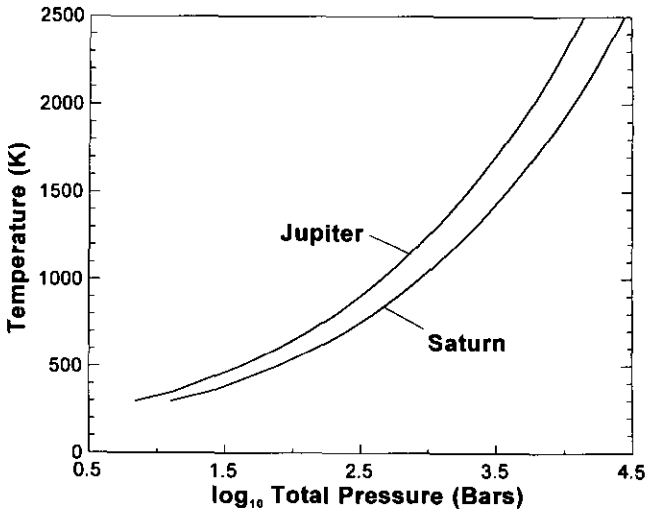

FIG. 1. Temperature–pressure profiles for the deep atmospheres of Jupiter and Saturn. The profiles were calculated as described by Fegley and Prinn (1988b) using H_2 and He mole fractions of 0.898 and 0.102 on Jupiter and 0.963 and 0.0325 on Saturn (Gautier *et al.* 1981, Conrath *et al.* 1984).

CH_4 on Jupiter and Saturn (Gautier *et al.* 1982; Courtin *et al.* 1984; Fegley 1994b), and which otherwise assume equal enrichments of all elements heavier than He in the atmospheres of these two planets (see Table 1). The enrichment factors used for Jupiter and Saturn are 2.3 and 6 times solar, respectively, and are consistent with the methane observations on these planets (Gautier *et al.* 1982; Courtin *et al.* 1984; Fegley 1994b). Following Fegley and Prinn (1988a), we adopt the view that the apparent depletion of water vapor in Jupiter's visible atmosphere (Bjoraker *et al.* 1986b) is due to condensation and/or complex line formation effects and does not reflect a bulk global depletion of water (or oxygen) on Jupiter.

All of the naturally occurring elements in the periodic table were included in the ideal gas thermochemical equi-

TABLE I
Adopted Compositions (Mole Fractions) for Jupiter and Saturn[a]

Gas	Jupiter	Saturn
H_2	0.898	0.963
He	0.102	0.0325
CH_4	$(3.0 \pm 1.0) \times 10^{-3}$	$(4.5^{+2.4}_{-1.9}) \times 10^{-3}$

[a] Data are taken from Gautier *et al.* (1981, 1982), Conrath *et al.* (1984), Courtin *et al.* (1984), and the compilation by Fegley (1993b). As stated in the text, the enrichment factor for carbon is assumed to be valid for all elements heavier than He.

librium calculations. The Appendix gives the data sources for all of the over 2000 compounds included in the calculations. Where possible, data were taken from the JANAF Tables (Chase *et al.* 1985), which has been compiled, revised, and refined by an experienced team over the past three decades. However, data for many compounds of interest are not in the JANAF Tables and must come from other literature sources. Where possible, we compared and quantitatively assessed thermodynamic data from different literature sources and chose what we considered to be the most reliable and accurate thermodynamic data for a particular compound. For example, Fegley (1981) describes the assessment and evaluation of literature data for silicon oxynitride, and later in this paper we discuss the evaluation of thermodynamic data for some phosphorus and arsenic compounds.

The computer program used in the calculations is similar to the code used by Barshay and Lewis (1978), but greatly expanded in scope. The code operates by simultaneously considering the constraints of mass balance and chemical equilibrium. The operation of the code is best illustrated with an example based on a simplified version of Fe chemistry on Jupiter.

Assuming that the total Fe elemental abundance on Jupiter is given by ΣFe and that the only important Fe compounds are Fe (g), $Fe(OH)_2$ (g), and Fe_2Cl_4 (g), the mass balance expression for Fe, which equates the total Fe elemental abundance to the abundance of all Fe compounds, can be written as

$$\sum \mathrm{Fe} = P_{\mathrm{Fe}} + P_{\mathrm{Fe(OH)_2}} + 2P_{\mathrm{Fe_2Cl_4}}, \tag{1}$$

where P_i is the partial pressure of gas i. This mass balance expression can be rewritten in terms of the thermodynamic activity of Fe (a_{Fe}), the equilibrium constants K_i for forming the different gases from the constituent elements in their reference states, and the thermodynamic fugacities (f_i) of the other elements combined with Fe in the gases:

$$\sum \mathrm{Fe} = a_{\mathrm{Fe}}[K_{\mathrm{Fe}} + K_{\mathrm{Fe(OH)_2}}(f_{\mathrm{H_2}})(f_{\mathrm{O_2}}) + 2a_{\mathrm{Fe}}K_{\mathrm{Fe_2Cl_4}}(f_{\mathrm{Cl_2}})^2]. \tag{2}$$

One such equation which contains partial pressure terms for all gases containing the element in question is written for each element in the code. The actual mass balance equation used for Fe in the code contains 19 different gases, while the mass balance equation for H contains several hundred different gases. The equilibrium constants K_i used in the mass balance equations are taken from the thermodynamic data sources listed in the Appendix. An initial guess is assumed for the activity (or fugacity) of each element. These guesses can be optimized if the major gas of each element is known, but this is not essential for the code to operate properly. The code then iteratively solves the set of coupled nonlinear equations and gives the thermodynamic activity (or fugacity) for each element, the abundances of all gases in the code, and information on the quality of the solution for each element. The convergence criterion we used specifies that the code reaches a solution when the calculated abundance and the input abundance for each element agree within 1 part in 100,000, but for all practical purposes the code has reached a solution when abundances agree within 1 part in 1000.

The code also takes possible liquid and solid condensates into account. For example, if the code finds that the thermodynamic activity of Fe (a_{Fe}) is greater than or equal to unity, Fe metal (or liquid depending upon the temperature) can condense out of the atmosphere. The code then computes the temperature at which a_{Fe} first reached unity, resets the thermodynamic activity of iron to unity at all temperatures below this point, and adds a new term to the mass balance expression (A_{Fe}) which takes into account the abundance of condensed iron. The condensates formed by two or more elements are handled in a similar fashion. Because the gas phase and condensation calculations are coupled, they are actually done simultaneously using iterative techniques. A total of 400 liquids and solids are considered in the calculations.

It is important to remember that the total abundance of each condensate is limited by the least abundant element composing the condensate. For example, the abundance of NH_4Br (s), which is formed by the reaction of NH_3 and HBr, is limited by the Br abundance. Because the Br abundance is about 265,000 times lower than the N abundance, NH_4Br condensation removes all HBr, containing 100% of all Br, from the upper atmosphere of Jupiter while leaving the NH_3 abundance virtually unchanged. Similar considerations govern the effects of condensation on the abundances of the other gases illustrated in the following figures.

Where relevant, we also considered the effects of vertical mixing on the abundances of gases which are either observed (e.g., CO, HCN, PH_3, GeH_4, AsH_3) or possible chemical probes of the deep atmospheres of Jupiter and Saturn. These calculations were done using a chemical dynamical model described in earlier publications (e.g., see Prinn and Barshay 1977; Prinn and Olaguer 1981; Fegley and Prinn 1985, 1988a,b; Fegley *et al.* 1991). The basic approach used in the thermochemical kinetic calculations is to compare the time constant (t_{chem}) for the fastest reaction responsible for either producing or destroying a gas to the time constant (t_{mix}) for convectively mixing the gas upward to a cooler region where this reaction is kinetically inhibited. The chemical time constant is calculated from tabulated (or estimated) kinetic data.

The convective mixing time $t_{mix} \sim H^2/K_{eddy}$, where H is the pressure scale height and K_{eddy} is the vertical eddy diffusion coefficient in the deep atmosphere of Jupiter or Saturn. The observed heat fluxes emitted by Jupiter and Saturn and the theory for free convection lead to K_{eddy} values of 10^7–10^9 cm^2 sec^{-1} in their deep atmospheres (Stone 1976, Flasar and Gierasch 1977, Prinn and Barshay 1977, Lewis and Fegley 1984, Fegley and Prinn 1985). Thus, in the deeper regions of the atmospheres of Jupiter and Saturn where thermochemical equilibrium is maintained, $t_{chem} < t_{mix}$ while in the cooler, upper regions of these two planets where thermochemical equilibrium is not reached, $t_{chem} > t_{mix}$. In between these two regions is an intermediate altitude where $t_{chem} = t_{mix}$. This critical altitude, which is different for each species, is the quench level. Once a buoyant air parcel has risen to the quench level, thermochemical reactions with sufficiently large activation energies will be quenched, or frozen in, by further vertical mixing over an altitude increment which is small compared to the scale height H. As a result, the mixing ratios of the quenched gases are then fixed at the values prevailing at the quench level.

DISCUSSION OF THE RESULTS

Table 2 lists the solar elemental abundances of all the elements included in the calculations, the major gases formed by each element, the first condensates (if any), and the figure(s) which illustrate chemistry for a particular element. Several elements, which are italicized in Table 2, were found to be completely or partially condensed out of the atmospheres of Jupiter and Saturn at 2000 K. It is extremely unlikely that any gaseous compounds of these elements can ever be detected by remote sensing techniques or by atmospheric entry probes. Thus, the chemistry of these elements is not discussed further.

Below we describe the results for the more abundant and more volatile elements ordered according to their position in the periodic table. The results of the chemical equilibrium calculations are displayed in graphs which show the mole fractions (defined as P_i/P_{Total} for gas i, and exactly equivalent to the volume mixing ratio) as a function of temperature in the range 298 to 2000 K. The plots extend down to mole fractions of 10^{-20} in order to illustrate trends. In all cases the most abundant gases of an element are included. Furthermore, most of the gases with abundances above 10^{-6} of the total abundance of any element are included.

In general, the results for Jupiter and Saturn are so similar that we omitted separate graphs of Saturn's chemistry in order to conserve space. The condensation temperatures given in the text refer to the jovian atmosphere unless explicitly stated otherwise. However, any important differences between chemistry on Jupiter and Saturn are noted below and the predicted chemical probes of the deep atmospheres of both planets are tabulated later.

Group IA elements (the alkali metals). Our results for Li, Na, K, Rb, and Cs chemistry on Jupiter are displayed in Figs. 2–6. The major gases for the alkalis are generally alkali halides and hydroxides. The alkali metals are removed from the atmospheres of Jupiter and Saturn by condensation as sulfides (M_2S, where M = Li, Na, K) and chlorides (MCl, where M = Rb, Cs). The alkali borates of Li, Na, and K also condense after the alkali sulfides form, but are unimportant for removal of the alkali metals or B from the jovian and saturnian atmospheres. These results differ from those of Lewis (1969a) and Barshay and Lewis (1978) who calculated that Na and K were removed as alkali silicates (M_2SiO_3 and $M_2Si_2O_5$).

As illustrated in the figures, the gaseous Si abundance is much less than the gaseous Na and K abundances at the condensation points of the respective silicates. Thus, alkali silicate condensation is quantitatively unimportant for removing Na and K from the gas phase. This difference results from improvements in the treatment of Mg and Si condensation (see below). Alkali condensation as aluminosilicates (MAlSi$_3$O$_8$ and MAlSiO$_4$) was also considered but is unimportant for analogous reasons. Hibonite ($CaAl_{12}O_{19}$) condensation, which has already taken place by 2000 K, removes essentially all of the Al from the gas phase before any of the alkali aluminosilicates become stable. Our results for Li, Rb, and Cs are the first ones for these elements with the exception of some qualitative statements made by Lewis (1969a) for Li chemistry.

Group IIA elements (the alkaline earths). Our results for the alkaline earths are summarized in Table 2 and Figs. 7 and 8. The major gases are $M(OH)_2$, MOH, M, and MH, where M = any alkaline earth. In some cases, such as Be, the dihydroxide accounts for 99+% of the gaseous element. All of the alkaline earths are refractory and Be, Ca, Sr, and Ba are absent by the 1000-K level of the jovian and saturnian atmospheres. Magnesium is an exception because potentially detectable amounts of $Mg(OH)_2$, the dominant Mg gas, are still present at temperatures below 1300 K. Calcium is removed by condensation as hibonite ($CaAl_{12}O_{19}$, which is Al limited), perovskite ($CaTiO_3$, which is Ti limited), and akermanite ($Ca_2MgSi_2O_7$, the major Ca condensate). Magnesium is removed by condensation as forsterite (Mg_2SiO_4) and enstatite ($MgSiO_3$), which was calculated taking the detailed mass balance between Si and Mg into account. An example of how this is done is in Palme and Fegley (1990). Beryllium condenses as $Be_3B_2O_6$ at 1303 K, which may be a lower limit to the true removal temperature if Be_2SiO_4 dissolves in forsterite to any appreciable extent. Lewis (1969a) also speculated that Be titanates and vanadates

TABLE II
Abundances and Chemistry of Elements Included in the Calculations**

Atomic Number*	Chemical Symbol	Solar Abundance	Major Gas(es) on Jupiter and Saturn	First Condensate on Jupiter and Saturn	Figure Numbers
1	H	2.79×10^{10}	H_2	None	--
2	He	2.72×10^{9}	He	None	--
3	Li	57.1	LiOH, LiCl, LiH, Li	Li_2S	2
4	Be	0.73	$Be(OH)_2$	$Be_3B_2O_6$	7, 12
5	B	21.2	H_3BO_3, $NaBO_2$, KBO_2, HBO_2	$Be_3B_2O_6$, H_3BO_3	3,4,7,12-13
6	C	1.01×10^{7}	CH_4	None	17-19
7	N	3.13×10^{6}	NH_3	aqueous clouds	28-30
8	O	2.38×10^{7}	H_2O	aqueous clouds	39
9	F	843	HF	NH_4F	43
10	Ne	3.44×10^{6}	Ne	None	--
11	Na	5.74×10^{4}	Na, NaOH, $(NaOH)_2$, NaCl	Na_2S	3, 12
12	Mg	1.074×10^{6}	$Mg(OH)_2$, MgOH, Mg, MgH	Mg_2SiO_4, $MgSiO_3$	8
13	Al	8.49×10^{4}	AlOH, Al_2O, AlH, $HAlO_2$	$CaAl_{12}O_{19}$	--
14	Si	1.00×10^{6}	SiH_4, SiO, SiS, SiH_2, $SiFH_3$	Mg_2SiO_4, $MgSiO_3$	20-22
15	P	1.04×10^{4}	PH_3, PH_2	$NH_4H_2PO_4$	31-33
16	S	5.15×10^{5}	H_2S	NH_4SH	40
17	Cl	5,240	HCl, NaCl, KCl	NH_4Cl	44
18	Ar	1.01×10^{5}	Ar	None	--
19	K	3,770	KOH, KCl, K	K-spar in feldspar	4
20	*Ca*	*6.11×10^{4}*	*$Ca(OH)_2$, CaOH, Ca, CaH*	*$CaAl_{12}O_{19}$, $CaTiO_3$, $Ca_2MgSi_2O_7$*	
21	*Sc*	*34.2*	*ScO*	*Sc_2O_3*	--
22	*Ti*	*2,400*	*TiO, TiO_2, Ti*	*$CaTiO_3$*	--
23	*V*	*293*	*VO, VO_2, V*	*diss. in $CaTiO_3$*	--
24	*Cr*	*1.35×10^{4}*	*Cr*	*metal alloy*	--
25	*Mn*	*9,550*	*Mn*	*MnS*	--
26	*Fe*	*9.00×10^{5}*	*Fe, $Fe(OH)_2$*	*metal alloy*	--
27	*Co*	*2,250*	*Co*	*metal alloy*	--
28	*Ni*	*4.93×10^{4}*	*Ni*	*metal alloy*	--
29	Cu	522	CuH	Cu_3P or metal alloy	9
30	Zn	1,260	Zn	ZnS	11
31	Ga	37.8	GaOH	GaS	14
32	Ge	119	GeS, GeH_4, GeSe, GeTe	Ge, GeTe	23-25
33	As	6.56	AsH_3	As or As_2S_2	34-36
34	Se	62.1	H_2Se, GeSe	PbSe	41
35	Br	11.8	HBr, NaBr, KBr	NH_4Br	45
36	Kr	45	Kr	None	--
37	Rb	7.09	RbCl, RbOH, RbBr, $(RbCl)_2$	RbCl	5
38	*Sr*	*23.5*	*$Sr(OH)_2$, SrOH, Sr*	*diss. in $CaTiO_3$*	--
39	*Y*	*4.64*	*YO, YS*	*Y_2O_3*	--

may condense at high temperature. This appears reasonable, but no thermodynamic data are available for these compounds. Our gas phase and condensation chemistry for Mg differs from that of Barshay and Lewis (1978) because of the improved treatment of Mg and Si mass balance during forsterite and enstatite condensation, and updated thermodynamic data for MgOH gas in the third edition of the JANAF Tables (Chase *et al.* 1985).

Group IB elements. Figures 9 and 10 show our results for Cu, Ag, and Au. Lewis (1969a) concluded that Cu is removed from the jovian atmosphere by dissolving in Fe alloy. However, the observations of GeH_4 and AsH_3 on Jupiter and Saturn led us to reexamine this conclusion. Metal-silicate partition coefficients (Schmitt *et al.* 1989; Lodders and Palme 1991) show that Cu is less siderophile than Ge or As, while nebular condensation calculations

TABLE II—*Continued*

Atomic Number*	Chemical Symbol	Solar Abundance	Major Gas(es) on Jupiter and Saturn	First Condensate on Jupiter and Saturn	Figure Numbers
40	*Zr*	*11.4*	*ZrO_2,ZrO, ZrS*	*ZrO_2*	--
41	*Nb*	*0.698*	*NbO_2, NbO*	*diss. in $CaTiO_3$*	--
42	*Mo*	*2.55*	*MoO, H_2MoO_4, Mo, MoO_2*	*metal alloy*	--
44	*Ru*	*1.86*	*Ru*	*metal alloy*	--
45	Rh	0.344	Rh	metal alloy	--
46	Pd	1.39	Pd	metal alloy	--
47	Ag	0.486	Ag	metal alloy	10a
48	Cd	1.61	Cd	CdSe	--
49	In	0.184	InOH, InH	InS	15
50	Sn	3.82	SnS, SnH, SnSe, SnTe	Sn	26
51	Sb	0.309	SbH_3, SbS, Sb_4	Sb	37
52	Te	4.81	H_2Te, GeTe	GeTe, Tl_2Te, PbTe	42
53	I	0.9	HI, NaI, KI	NH_4I	46
54	Xe	4.7	Xe	None	--
55	Cs	0.372	CsCl, CsOH, Cs	CsCl	6
56	*Ba*	*4.49*	*$Ba(OH)_2$, BaOH*	*diss in $CaTiO_3$*	--
57	*La*	*0.446*	*LaO*	*diss in $CaTiO_3$*	--
58	*Ce*	*1.136*	*CeO, CeO_2*	*diss in $CaTiO_3$*	--
59	*Pr*	*0.1669*	*PrO*	*diss in $CaTiO_3$*	--
60	*Nd*	*0.8279*	*NdO*	*diss in $CaTiO_3$*	--
62	*Sm*	*0.2582*	*Sm, SmO, SmS*	*diss in $CaTiO_3$*	--
63	*Eu*	*0.0973*	*Eu*	*diss in $CaTiO_3$*	--
64	*Gd*	*0.33*	*GdO*	*diss in $CaTiO_3$*	--
65	*Tb*	*0.0603*	*TbO*	*diss in $CaTiO_3$*	--
66	*Dy*	*0.3942*	*DyO*	*diss in $CaTiO_3$*	--
67	*Ho*	*0.0889*	*HoO, Ho*	*diss in $CaTiO_3$*	--
68	*Er*	*0.2508*	*ErO*	*diss in $CaTiO_3$*	--
69	*Tm*	*0.0378*	*Tm*	*diss in $CaTiO_3$*	--
70	*Yb*	*0.2479*	*Yb*	*diss in $CaTiO_3$*	--
71	*Lu*	*0.0367*	*LuO*	*diss in $CaTiO_3$*	--
72	*Hf*	*0.154*	*HfO, $HfCl_2$, HfO_2*	*diss. in ZrO_2*	--
73	*Ta*	*0.0207*	*TaO_2, TaO*	*diss. in $CaTiO_3$*	--
74	*W*	*0.133*	*H_2WO_4*	*metal alloy*	--
75	*Re*	*0.0517*	*Re*	*metal alloy*	--
76	*Os*	*0.675*	*Os*	*metal alloy*	--
77	*Ir*	*0.661*	*Ir*	*metal alloy*	--
78	*Pt*	*1.34*	*Pt*	*metal alloy*	--
79	Au	0.187	AuH	metal alloy	10b
80	Hg	0.34	Hg	HgS	--
81	Tl	0.184	Tl, Tl_2S	Tl_2Te	16
82	Pb	3.15	Pb, PbTe, PbSe	Pb	27
83	Bi	0.144	BiH	Bi	38
90	*Th*	*0.0335*	*ThO_2*	*diss in $CaTiO_3$*	--
92	*U*	*0.009*	*UO_2*	*diss in $CaTiO_3$*	--

* The following elements do not occur in nature and were not included in the calculations: Tc (43), Pm (61), Po (84), At (85), Rn (86), Fr (87), Ra (88), Ac (89), Pa (91).

** Italics indicate elements which were found to be completely or partially condensed out of the atmospheres of Jupiter and Saturn at 2000 K.

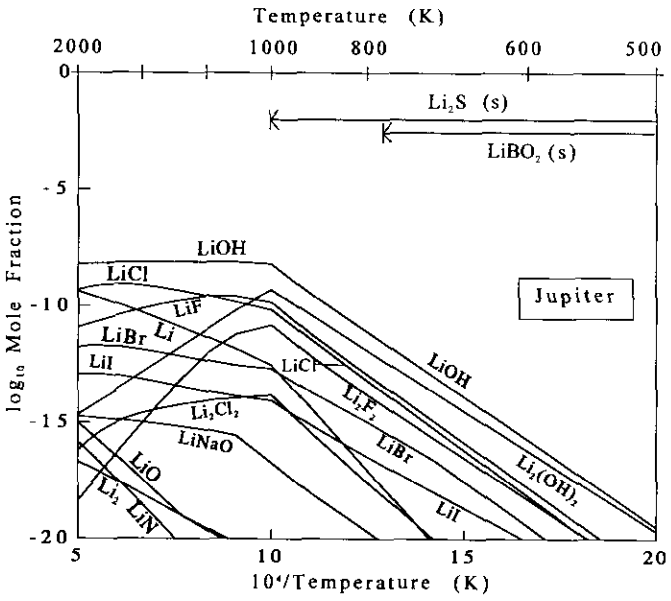

FIG. 2. Lithium equilibrium chemistry along the Jupiter adiabat. Li_2S, which removes most of the Li from the jovian atmosphere, condenses at 1007 K. $LiBO_2$ condenses at 776 K but is unimportant for either the Li or B mass balance. The abundance of LiClF (g) is not graphed because it is very similar to that of Li_2Cl_2 (g). In this and subsequent graphs, the temperature scale is linear in $1/T$, the mole fraction of gas i is defined as $P_i/(P_{Total})$, and the labeled arrows mark condensate stability fields.

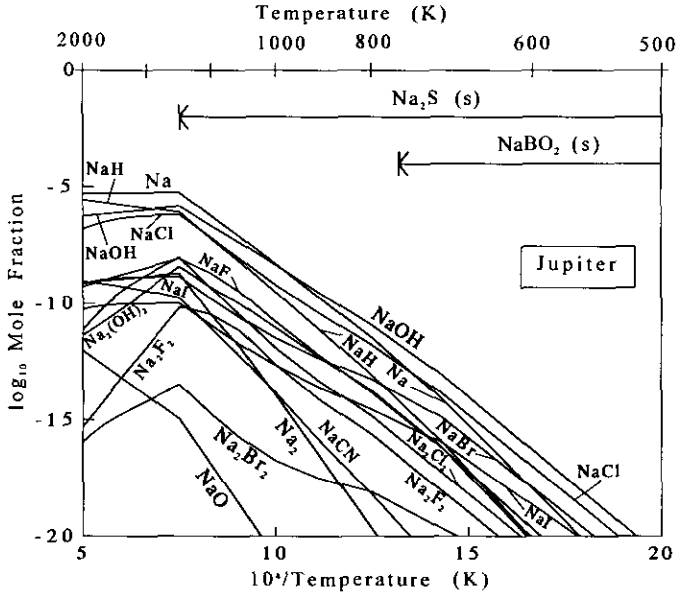

FIG. 3. Sodium equilibrium chemistry along the Jupiter adiabat. Na_2S forms at 1332 K and removes Na from the jovian atmosphere. $NaBO_2$ condensation at 756 K is quantitatively unimportant for Na and B removal.

(Fegley 1994a) show that it is only slightly more refractory than Ge or As. Likewise, Ag is more volatile than Cu, although Au is more refractory (Fegley 1994a). We found that the major gases are CuH, Ag, and AuH and that Cu condenses out of the jovian atmosphere as Cu_3P, while Ag and Au condense out as metals. However metallic Cu would condense only 13° lower than the phosphide. This small difference is within the uncertainties of the thermodynamic data for the Cu compounds. Although CuH and AuH will be difficult to detect, we note that the gaseous metal hydrides CuH, ZnH, GeH, and SnH are observed in the atmospheres of cool stars (Wojslaw and Peery 1976) and that CuCl has been observed in volcanic flames at Kilauea, Hawaii (Murata 1960) and Niragongo, Zaire (Tazieff 1960).

Group IIB elements. Figure 11 displays the equilibrium chemistry for Zn and Table 2 summarizes the results for Cd and Hg. The monatomic elements are the dominant gases for Zn, Cd, and Hg. Zinc and Cd are removed from the atmospheres of Jupiter and Saturn by condensation of sphalerite (ZnS) and CdSe, respectively. In contrast Hg does not condense until HgS forms at 210 K. We suggest that atomic transitions of all three elements may be potentially detectable in the atmospheres of Jupiter and Saturn.

Group IIIA elements. Results for B, Ga, In, and Tl are shown in Figures 12–16; Al chemistry is summarized in Table 2. Boron chemistry is complex with $NaBO_2$ and KBO_2 being important species above the condensation temperatures of the solid alkali borates and H_3BO_3 being

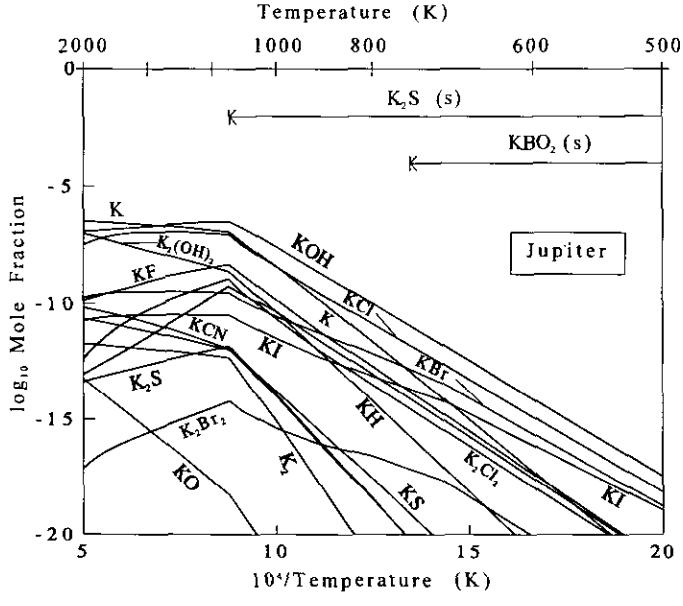

FIG. 4. Potassium equilibrium chemistry along the Jupiter adiabat. K_2S forms at 1142 K and removes K from the jovian atmosphere. KBO_2 condensation at 742 K is quantitatively unimportant for K and B removal.

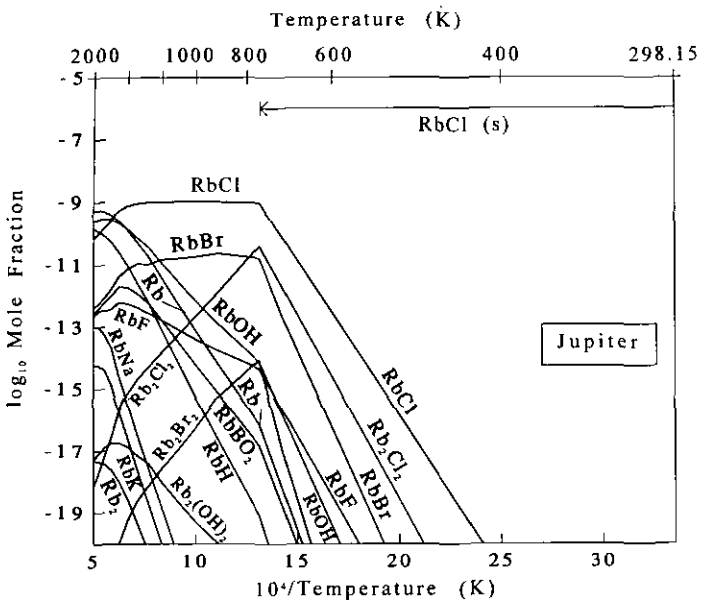

FIG. 5. Rubidium equilibrium chemistry along the Jupiter adiabat. RbCl condenses at 761 K. The abundances of Rb_2 and RbLi (not shown) are overlapping.

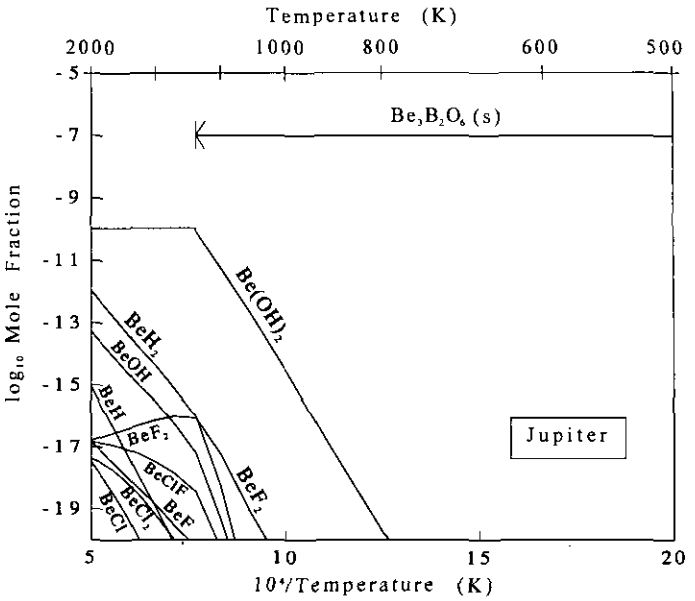

FIG. 7. Beryllium equilibrium chemistry along the Jupiter adiabat. Condensation of $Be_3B_2O_6$ at 1303 K removes all Be but only 3% of B from the jovian atmosphere.

the major gas down to 293 K. This point, which is the aqueous cloud base, is 3° above the condensation temperature of solid boric acid. The solubility of boric acid in water at 303 K is about 6 g per 100 cm^3, which is orders of magnitude larger than the B/H_2O ratio in the atmospheres of Jupiter and Saturn. Thus, all the boric acid is expected to dissolve in the aqueous solution clouds at or close to the cloud base.

Our results differ from those of Barshay and Lewis (1978) who found that 50% of the gaseous boron was removed from the jovian atmosphere by $NaBO_2$ condensation at about 1000 K. Instead we find that the prior

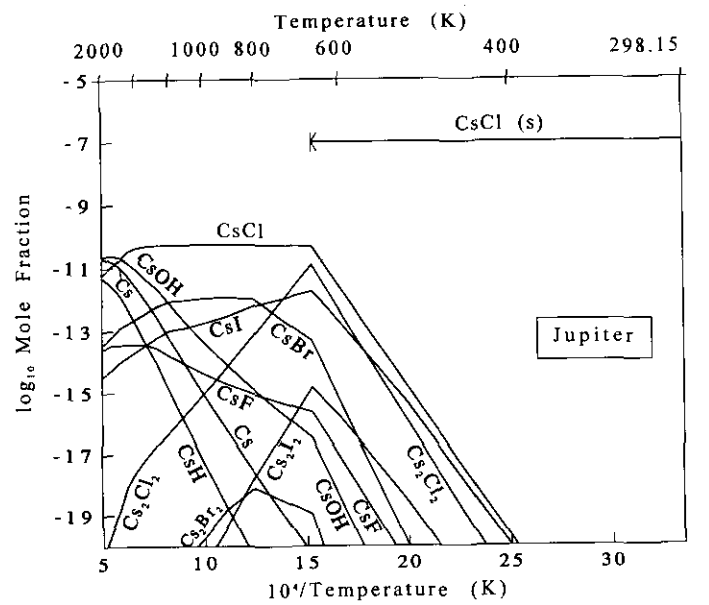

FIG. 6. Cesium equilibrium chemistry along the Jupiter adiabat. CsCl condenses at 654 K.

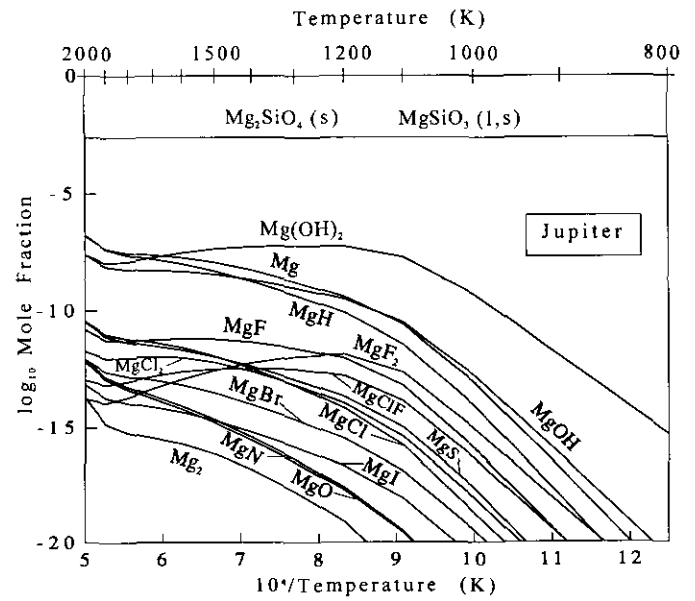

FIG. 8. Magnesium equilibrium chemistry along the Jupiter adiabat. The Mg_2SiO_4 (forsterite) and $MgSiO_3$ (enstatite) stability fields extend above 2000 K. See the text for an explanation of why the present results differ from those of Barshay and Lewis (1978).

condensation of Na_2S dramatically decreases the Na abundance below that of B by 756 K, where we calculate $NaBO_2$ condenses. We have been unable to identify any other boron condensate which is stable in the atmospheres of Jupiter and Saturn. Metal borides and other possible borate condensates do not form because the metals involved are already condensed out of the atmospheres of Jupiter and Saturn at levels far below those where the borides or borates would form. All other boron condensates considered, including carbides, hydroxides, nitrides, oxides, and sulfides are unstable. However, incomplete thermodynamic data are available for ammonium borates, so their condensation temperatures could not be calculated. With this one caveat, we expect that H_3BO_3(g) should be observable in the deep atmospheres of Jupiter and Saturn below the aqueous solution clouds.

Because of the prior condensation of Be, Na, K, and Li borates, the H_3BO_3 mole fraction in the jovian atmosphere is not identical to the total B mole fraction in the jovian atmosphere. But in any case, the predicted H_3BO_3 abundance is only ~ 4% lower and thus to a good first approximation the H_3BO_3 abundance on Jupiter is the same as the total B abundance. However, the jovian B/H ratio may be higher than the primordial solar value due to heavy element enrichment on Jupiter, and thus the jovian B abundance may be several times higher than the solar value. Our calculations confirm the results of Barshay and Lewis (1978) that diborane B_2H_6, which Beer (1976) suggested could be spectroscopically observable on Jupiter, is an insignificant species over the entire temperature range over which gaseous boron compounds exist in the atmospheres of Jupiter and Saturn. The maximum B_2H_6 mole fraction in the jovian atmosphere is about 10^{-19} at 2000 K and decreases rapidly with decreasing temperature. Thus, we urge that efforts to detect boron on Jupiter concentrate on boric acid vapor, H_3BO_3, instead of diborane.

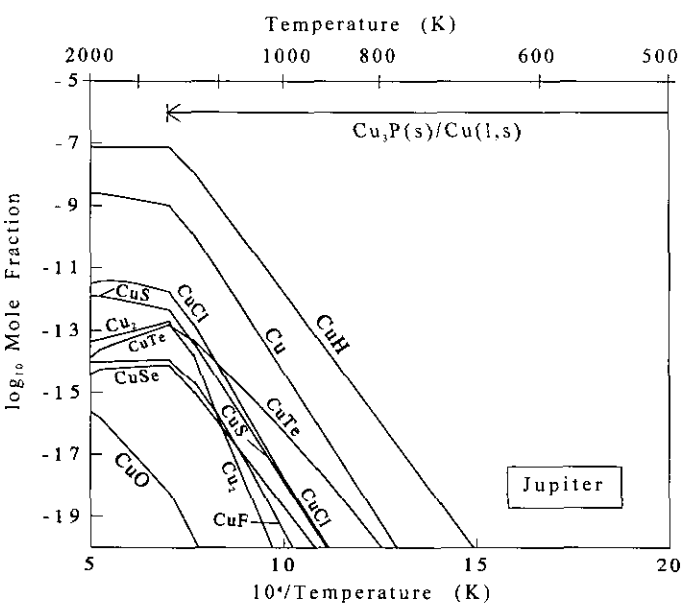

FIG. 9. Copper equilibrium chemistry along the jovian adiabat. Copper phosphide Cu_3P is calculated to condense at 1418 K or metallic Cu condenses 13° lower. The observations of GeH_4 and AsH_3 on Jupiter and Saturn suggest that Cu, which is less siderophile, may be present in the deep atmospheres of these planets instead of being partitioned into Fe alloy in the planetary interiors.

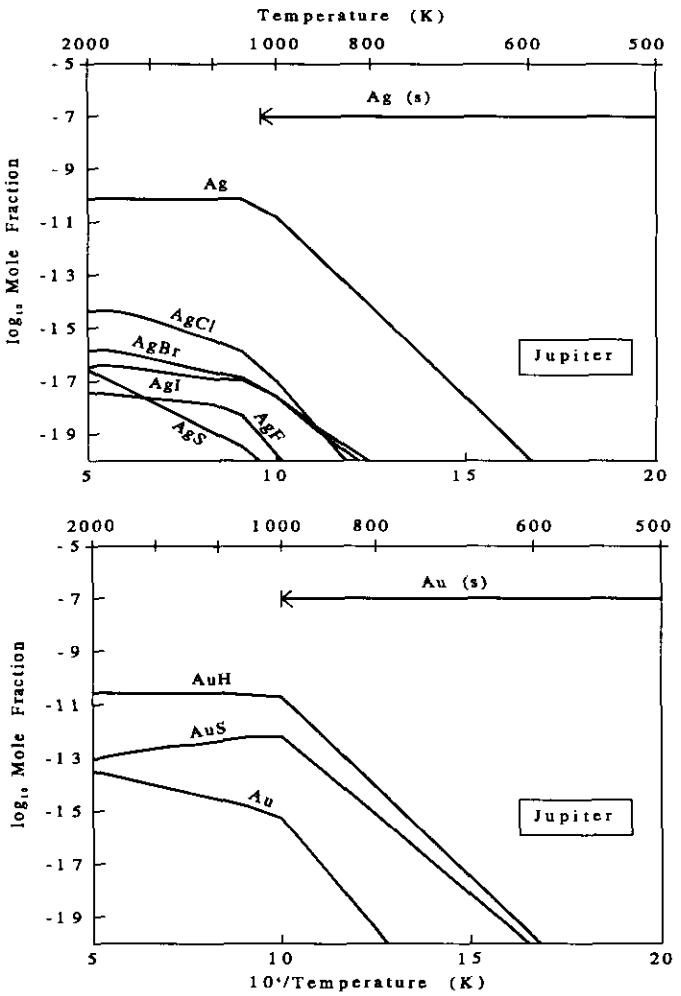

FIG. 10. (top) Silver and (bottom) gold equilibrium chemistry along the jovian adiabat. Metallic Ag and Au condense at 1046 K and 1003 K, respectively.

Gallium and indium have similar chemistry. In both cases *M*OH is the major gas over most of the temperature range studied. The exceptions are at very high temperatures where GaH and InH become dominant and near the GaS condensation point where Ga_2S (g) is about as abundant as GaOH. Gallium and indium initially condense out of the jovian and saturnian atmospheres as GaS (s) and InS (s), respectively. Once this occurs their abundances

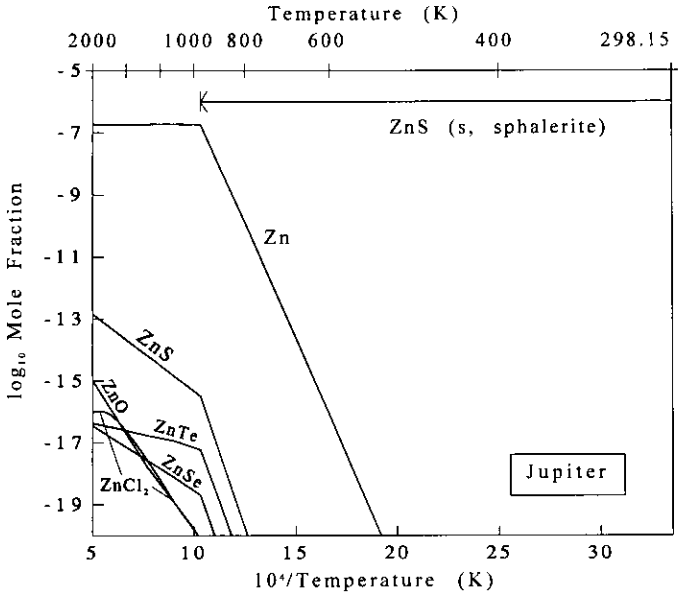

FIG. 11. Zinc equilibrium chemistry along the jovian adiabat. Sphalerite (ZnS) condenses at 968 K.

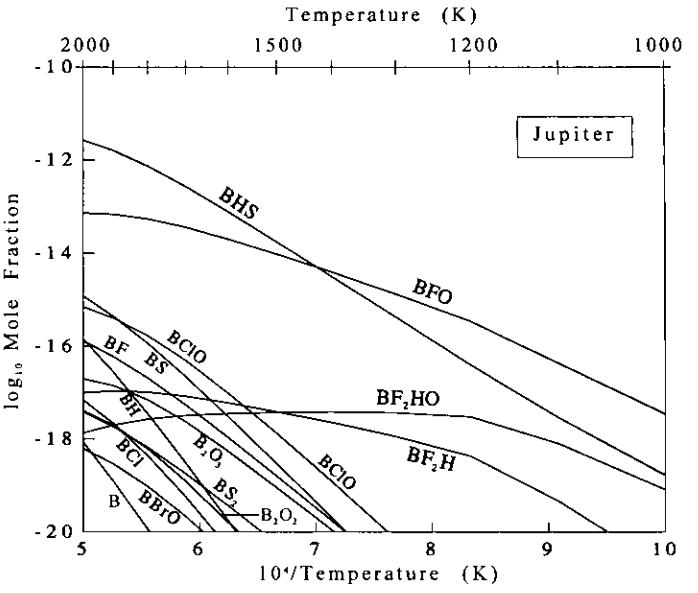

FIG. 13. The second graph illustrating boron equilibrium chemistry along the jovian adiabat. The condensation of Be, Na, and K borates removes several percent of the total B abundance from Jupiter's atmosphere, but most B remains in the gas as H_3BO_3 until it dissolves in the water clouds which form at 293 K.

rapidly drop. At lower temperatures the monosulfides are replaced by Ga_2S_3 and In_2S_3. An important difference between our results for In chemistry and those presented by Fegley and Lewis (1979) is that the calculated abundances of InBr and InI are lower than that previously predicted. This reason for this is that InOH(g) was not included in the earlier calculations.

Thallium equilibrium chemistry is different than that of Ga and In and is also different than that reported by Fegley and Lewis (1979) because of changes in the thermodynamic data for Tl compounds. Monatomic Tl is the

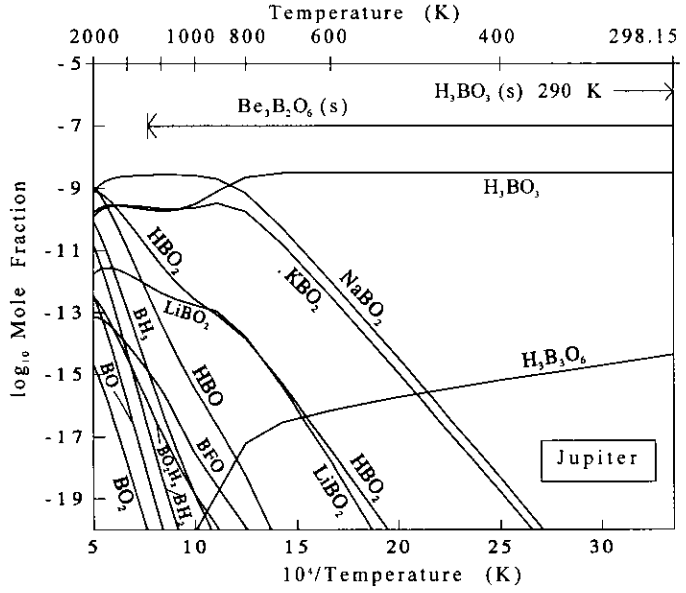

FIG. 12. The first of two graphs illustrating boron equilibrium chemistry along the jovian adiabat. About 3% of total B is consumed by $Be_3B_2O_6$ condensation and about 1% is consumed by condensation of Li, Na, and K borates. Diborane (B_2H_6), which is not graphed, is always insignificant. The B_2H_6 mole fractions vary from $\sim 10^{-19}$ at 2000 K to $\sim 10^{-103}$ at 298 K.

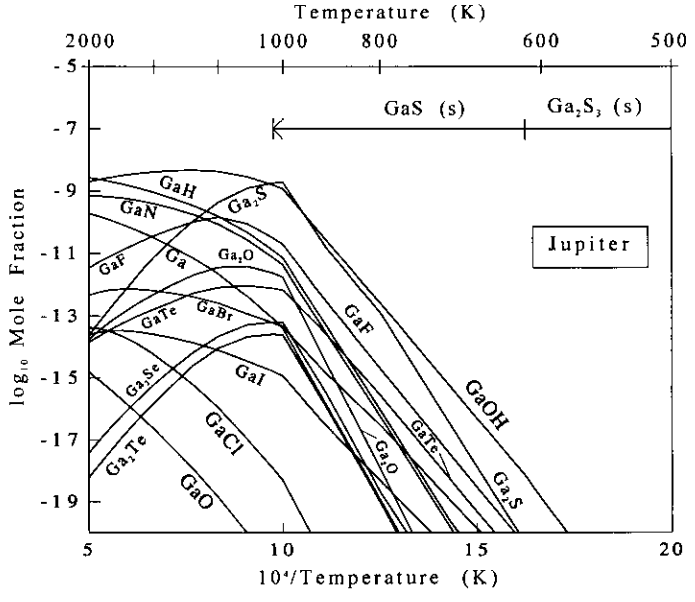

FIG. 14. Gallium chemistry along the jovian adiabat.

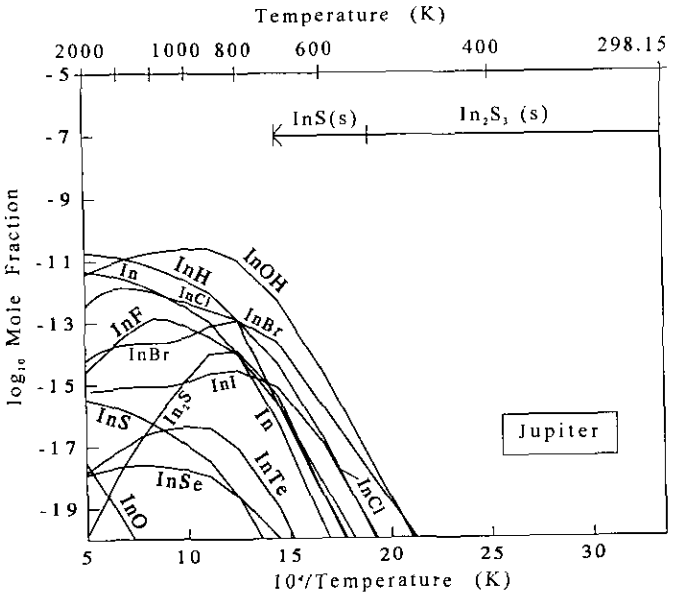

FIG. 15. Indium chemistry along the jovian adiabat. The present results differ from those of Fegley and Lewis (1979) because InOH (g) was not included in the earlier calculations.

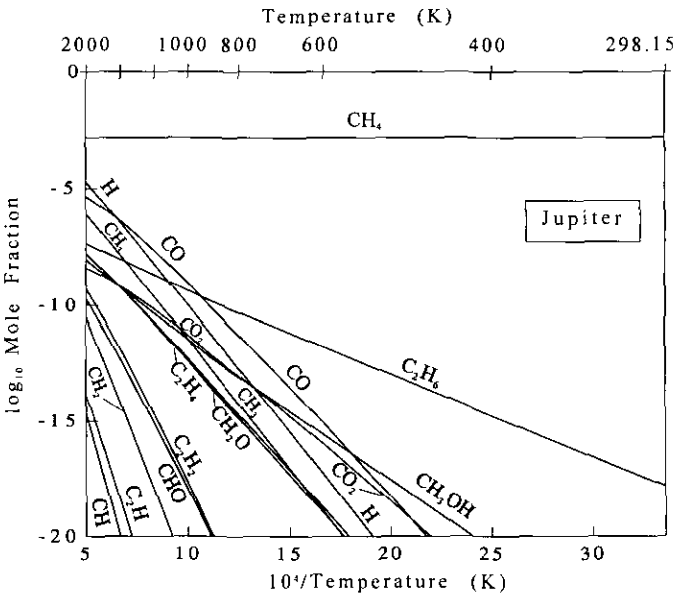

FIG. 17. Carbon equilibrium chemistry along the jovian adiabat.

major gas until shortly after Tl_2Te (s) condenses at 671 K. After Tl_2Te condenses the Tl (g) abundance drops off more rapidly than that of Tl_2S which becomes the major gas.

Group IVA elements. Figures 17–27 show the results for C, Si, Ge, Sn, and Pb. The chemistry of these elements

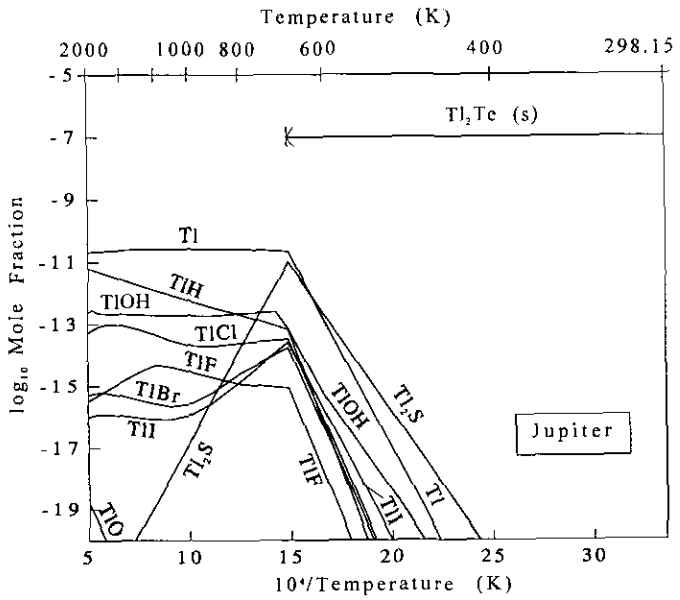

FIG. 16. Thallium chemistry along the jovian adiabat. The present results differ from those of Fegley and Lewis (1979) because of changes in the thermodynamic data for some Tl compounds.

is a good example of periodic trends and how they change with increasing atomic number down a group. For example, CH_4 is the major C gas, SiH_4 is the major Si gas, GeH_4 is the second most important Ge gas, stannane (SnH_4) is a minor Sn gas, and plumbane (PbH_4) is of negligible importance for Pb chemistry. Conversely the monochalcogenide gases (oxide, sulfide, selenide, and telluride) become increasingly important down the group. This is exemplified by the fact that CO is a trace C gas, SiO and SiS are the second and third most abundant Si gases, GeS, GeSe, and GeTe are dominant or major Ge gases, SnS, SnSe, and SnTe are the top three Sn gases over a wide temperature range, and PbTe, PbSe, and PbS are the top three Pb gases over a wide temperature range. Details specific to the chemistry of C, Si, and Ge are discussed at greater length below.

The carbon equilibrium chemistry for Jupiter (see Figure 17) and Saturn is generally similar to prior results (Barshay and Lewis 1978, Fegley and Prinn 1985) except for changes due to the revised temperature–pressure profiles and assumed heavy element enrichment factors in the updated atmospheric models. The chemical equilibrium results are the basis for the kinetic calculations shown in Figs. 18 and 19, which were done using the CO destruction mechanism proposed by Prinn and Barshay (1977):

$$CO + H_2 = H_2CO \quad (3)$$

$$H_2CO + H_2 \rightarrow CH_3 + OH \quad (4)$$

$$CH_3 + H = CH_4. \quad (5)$$

In this scheme, reaction (4) is the rate-determining step and the CO chemical lifetime is

$$t_{chem}(CO) = [CO]/k_4[H_2CO][H_2], \quad (6)$$

where the square brackets denote molecular number densities taken from the chemical equilibrium calculations and $k_4 = 2.3 \times 10^{-10} \exp(-36{,}200/T)$ cm^{3}sec^{-1} from Prinn and Barshay (1977).

As shown in the figures, the kinetic calculations give excellent agreement with the observed CO abundances on both Jupiter and Saturn. Earlier, Prinn and Barshay (1977) and Fegley and Prinn (1985, 1988a,b) found good agreement between the observed and predicted CO abundances on Jupiter. However, Fegley and Prinn (1985) found that the predicted CO abundance on Saturn was significantly smaller than the observed abundance and suggested that the major source of CO on Saturn was CO production in Saturn's upper atmosphere.

Fegley and Prinn (1985) reached this conclusion because on the basis of recommendations made by Prinn *et al.* (1984) for the composition of Saturn's atmosphere, they assumed that C, O, and all other elements heavier than He in Saturn's atmosphere were enriched 2.5 times over the solar values. More recent CH_4 observations summarized in Fegley (1994b) show a carbon enrichment of 6 times solar on Saturn and are the basis for our assumption of a uniform heavy element enrichment factor (E) of 6 times solar.

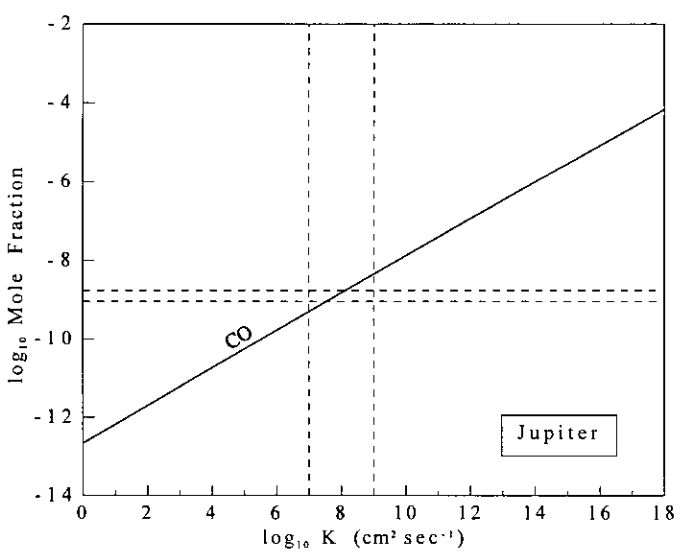

FIG. 18. The predicted CO mixing ratios in the visible atmosphere of Jupiter as a function of K_{eddy} the vertical eddy diffusion coefficient. The horizontal dashed lines show the observed CO abundance of 1.3 ± 0.4 ppb on Jupiter. This is the unweighted mean of 1.0±0.3 ppb reported by Bjoraker *et al.* (1986a) and 1.6 ± 0.3 ppb reported by Noll *et al.* (1988). In this figure and in the following figures illustrating the results of kinetic calculations, the vertical dashed lines show the range of K_{eddy} values estimated from free convection theory and the observed heat fluxes on Jupiter and Saturn (Stone 1976, Flasar and Gierasch 1977, Prinn and Barshay 1977, Lewis and Fegley 1984, Prinn *et al.* 1984, Fegley and Prinn 1985).

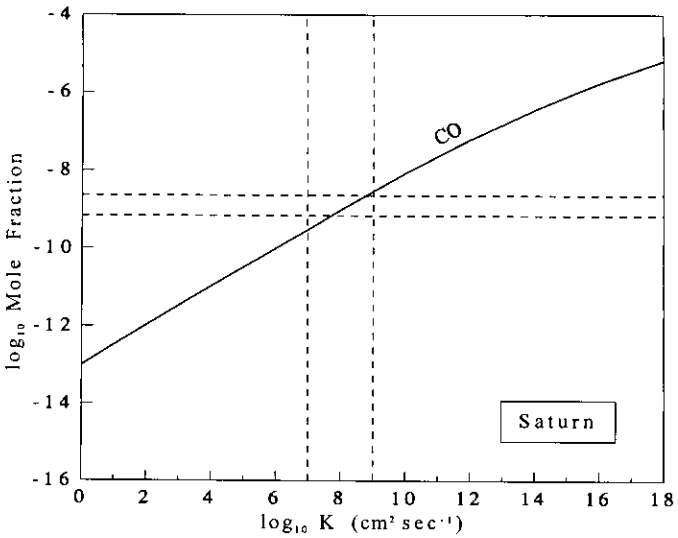

FIG. 19. The predicted CO mixing ratios in the visible atmosphere of Saturn as a function of K_{eddy} the vertical eddy diffusion coefficient. The horizontal dashed lines show the observed CO abundance of 1.5 ± 0.8 ppb on Saturn. This is the unweighted mean of 2.0 ± 0.7 ppb reported by Noll *et al.* (1986) and 1.0 ± 0.3 ppb reported by Noll and Larson (1990).

As shown by Fegley and Prinn (1985), the CO equilibrium abundance is proportional to E^2 while the CO chemical lifetime is independent of the enrichment factor. In fact, the CO mixing ratios predicted in the present calculations are about 10 times higher than those calculated by Fegley and Prinn (1985). This difference is due to the larger heavy element enrichment, which accounts for a factor of $(6/2.5)^2$–5.8 times, as well as to the slightly different P,T profile which accounts for the remaining factor of about 1.7 times. Thus, our use of the currently accepted elemental enrichment factors for Saturn is the major reason why the present calculations match the observed CO abundance on that planet. Our results for Jupiter and Saturn reinforce the concept that the CO observed on Jupiter and Saturn is due to rapid vertical transport from the deep atmospheres of these two planets, and not to extraplanetary sources.

Figures 20 and 21 show that the major Si gases on Jupiter are SiH_4, SiO, SiS, SiH_2, $SiFH_3$, and SiH_3. The same sequence also holds on Saturn. However, no Si gases are expected to be spectroscopically observable in the atmospheres of Jupiter and Saturn because precipitation of forsterite (Mg_2SiO_4) and enstatite ($MgSiO_3$) takes place above 2000 K on both planets and rapidly depletes the abundances of all Si gases. Thus, on Jupiter at the 1000-K level, less than 0.1 part per 10^{12} of total Si is left in the gas because all of the rest condensed out of the

jovian atmosphere as silicate clouds at much deeper levels.

The upper limit for SiH_4 on Jupiter is 2.5 ppb (Treffers *et al.* 1978) and the upper limit for SiH_4 on Saturn is 0.2 ppb (Noll and Larson 1990). The upper limits correspond to quenching the $SiH_4 \rightarrow$ silicate conversion at 1525–1435 K. However, kinetic modeling shows that the $SiH_4 \rightarrow$ silicate conversion cannot be quenched at such high temperatures. Reactions such as H atom abstraction from SiH_4 and Si hydride radicals, and the unimolecular decomposition of SiH_4,

$$SiH_4 + H = SiH_3 + H_2 \quad (7)$$

$$SiH_3 + H = SiH_2 + H_2 \quad (8)$$

$$SiH_2 + H = SiH + H_2 \quad (9)$$

$$SiH_4 = SiH_2 + H_2, \quad (10)$$

maintain equilibrium concentrations of SiH_4 and Si hydride radicals in the deep atmospheres of Jupiter and Saturn. Silane decomposition to $SiH_2 + H_2$ is the initial step in SiH_4 pyrolysis (e.g., Jasinski and Estes 1985, Neudorfl *et al.* 1980, Newman *et al.* 1979, Purnell and Walsh 1966, White *et al.* 1985), but it is easily shown that the H atom abstraction reactions are also important in the deep atmospheres of Jupiter and Saturn due to the large H atom equilibrium concentrations. The oxidation of reduced Si and the subsequent condensation of magnesian silicates plausibly proceeds via the reactions

$$SiH_2 + H_2O \rightarrow H_2Si{=}O + H_2 \quad (11)$$

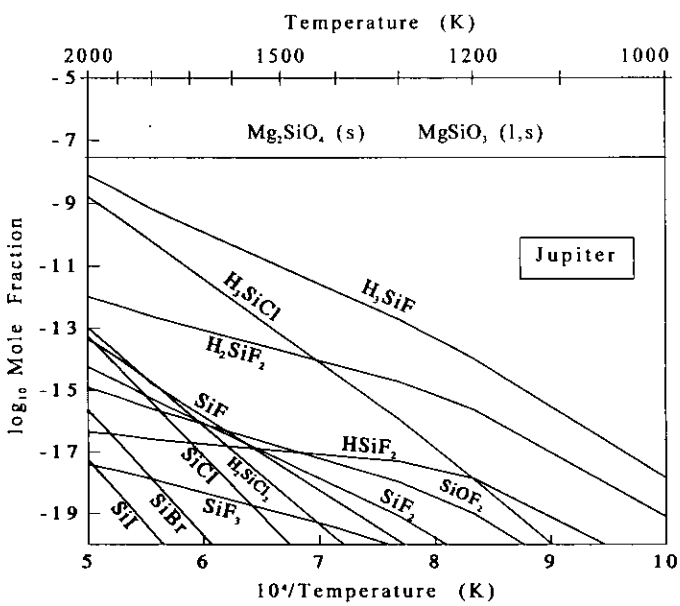

FIG. 20. The first of two graphs showing silicon chemistry along the jovian adiabat.

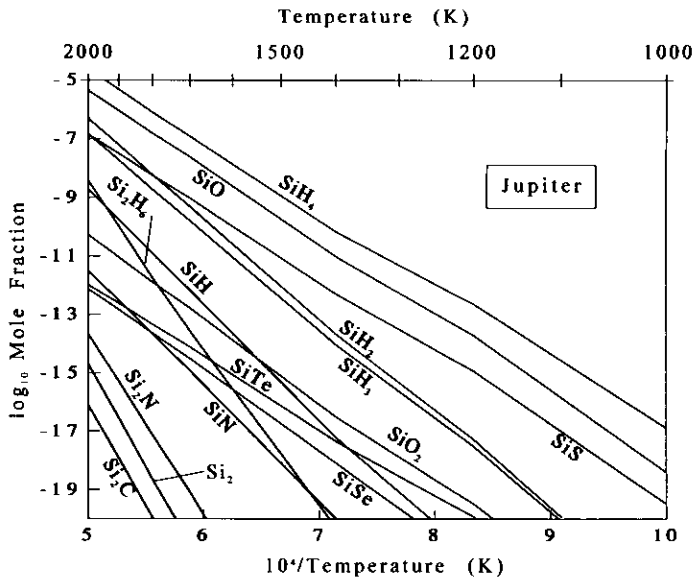

FIG. 21. The second graph showing silicon chemistry along the jovian adiabat.

$$H_2Si{=}O + H_2O \rightarrow HSiOOH + H_2 \quad (12)$$

$$HSiOOH \rightarrow SiO + H_2O \quad (13)$$

$$SiO + OH \rightarrow SiO_2 + H \quad (14)$$

$$SiO_2 \rightarrow SiO_2\,(s) \quad (15)$$

$$Mg(OH)_2 + SiO_2\,(s) \rightarrow MgSiO_3\,(s) + H_2O, \quad (16)$$

which are supported by experimental studies and theoretical models of SiH_4 pyrolysis and oxidation. Silanone ($H_2Si{=}O$), the Si analog to formaldehyde, is an intermediate observed during SiH_4 oxidation by O_3 (Glinski *et al.* 1985) and after ultraviolet irradiation of Ar matrices containing SiH_4 and O_3 (Withnall and Andrews 1985a,b). Silanone is also postulated to play an important role in SiH_4 combustion in silane–air flames (Fukutani *et al.* 1991a,b) and in SiH_4 oxidation by water vapor under high-temperature anaerobic conditions (Zachariah and Tsang 1993a,b).

Reaction (11) involving the formation of a Si=O bond is taken as the rate determining step with a rate constant of

$$k_{11} = 10^{-11.25} \exp(-5800/T)\ \mathrm{cm^3 sec^{-1}} \quad (17)$$

calculated by Zachariah and Tsang (1993a). The corresponding expression for the chemical lifetime of SiH_4 is

$$t_{\mathrm{chem}}(SiH_4) = [SiH_4]/k_{11}[SiH_2][H_2O]. \quad (18)$$

Figure 22 shows the results of the kinetic calculations.

The SiH_4 mole fractions that can be produced by quenching at K_{eddy} values of 10^7–10^9 cm^2sec^{-1} are below 10^{-20} while physically unrealistic K_{eddy} values of $>10^{18}$ cm^2sec^{-1} are required in order to produce 2.5 ppb SiH_4, which is the observational upper limit on Jupiter. It is clear that this conclusion is unchanged even if the adopted rate constant for reaction (11) is uncertain by a large factor. Thus, it can be confidently stated that the SiH_4 abundance due to rapid vertical transport in the atmospheres of Jupiter and Saturn is many orders of magnitude lower than the currently estimated upper limits. As discussed later under As chemistry, the absence of SiH_4 in the observable atmospheres of Jupiter and Saturn is a powerful argument against an extraplanetary origin for GeH_4, PH_3, and AsH_3 on these two planets because Si is much more abundant in meteoritic material than Ge, P, or As.

As noted above, the Ge monochalcogenides are important Ge gases. In fact, GeS is the major gas over most of the temperature range 298–2000 K and GeH_4 is the second most abundant Ge gas over most of the same range. The two major processes which destroy GeH_4 in the atmospheres of Jupiter and Saturn are conversion to GeS and GeSe, with sulfide formation being more important. Our proposed mechanism for GeH_4 conversion to GeS is different than that adopted by Fegley and Prinn (1985) but is analogous to the SiH_4 chemistry discussed above. Reactions such as H atom abstraction from GeH_4 and Ge hydride radicals and germane dissociation,

$$GeH_4 = GeH_2 + H_2 \quad (19)$$

$$GeH_4 + H = GeH_3 + H_2 \quad (20)$$

$$GeH_3 + H = GeH_2 + H_2 \quad (21)$$

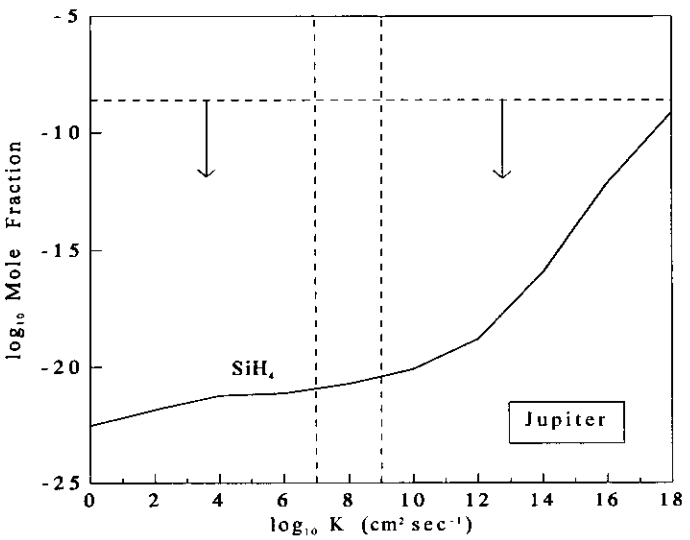

FIG. 22. Predicted SiH_4 mixing ratios in the visible atmosphere of Jupiter as a function of K_{eddy}, the vertical eddy diffusion coefficient.

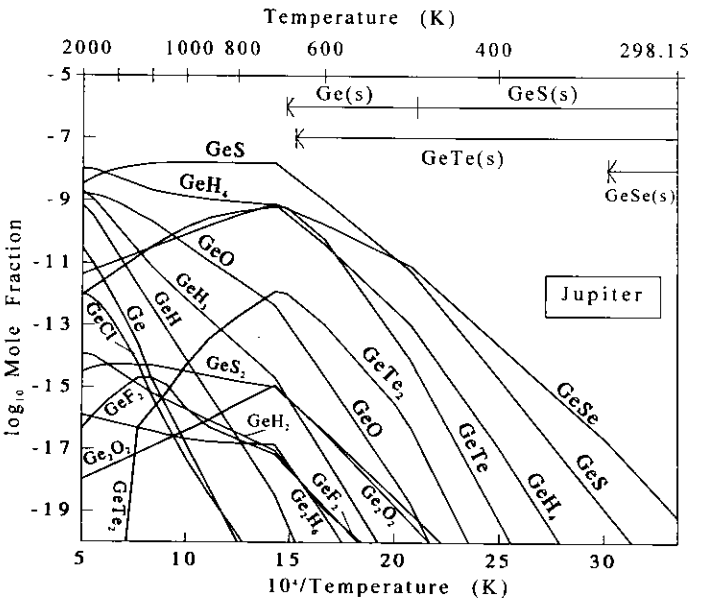

FIG. 23. Germanium equilibrium chemistry along the jovian adiabat.

$$GeH_2 + H = GeH + H_2, \quad (22)$$

maintain equilibrium concentrations of GeH_4 and Ge hydride radicals in the deep atmospheres of Jupiter and Saturn. Laboratory studies show that GeH_4 dissociation to $GeH_2 + H_2$ is the initial step in GeH_4 pyrolysis (Newman *et al.* 1980, Votintsev *et al.* 1984), but as mentioned above for silane, H atom abstraction reactions are also important in the deep atmospheres of Jupiter and Saturn because of the large H atom equilibrium concentrations. Germane sulfurization proceeds analogously to silane oxidation via the reactions

$$GeH_2 + H_2S \rightarrow H_2Ge{=}S + H_2 \quad (23)$$

$$H_2Ge{=}S \rightarrow \textit{trans}\text{-HGeSH} \quad (24)$$

$$\textit{trans}\text{-HGeSH} \rightarrow GeS + H_2, \quad (25)$$

which are followed by GeS condensation

$$GeS \rightarrow GeS\,(s). \quad (26)$$

Germathione ($H_2Ge{=}S$) is an analog to silanethione ($H_2Si{=}S$) and to germanone ($H_2Ge{=}O$), which is observed in UV-irradiated Ar matrices containing germane and oxygen (Withnall and Andrews 1990). Organogermathiones such as $(C_2H_5)_2Ge{=}S$ are believed to be intermediates in germanium organometallic chemistry (Barrau *et al.* 1979, 1980; Lavayssiere *et al.* 1978). Quantum mechanical calculations of the [Ge,H_2,S] potential energy surface (So 1993, Trinquier *et al.* 1981) predict the molecu-

lar structure, bond strengths, and vibrational frequencies for $H_2Ge{=}S$. Reactions (24)–(25) above are proposed instead of the single step

$$H_2Ge{=}S \rightarrow GeS + H_2 \qquad (27)$$

because the calculations by So (1993) predict that the $H_2Ge{=}S$ rearrangement to *trans*-HGeSH has an activation energy about 55 kJ mol^{-1} lower than unimolecular decomposition to GeS + H_2. The initial formation of the Ge=S bond via reaction (23) is taken as the rate-determining step with a rate constant of

$$k_{23} = 10^{-11} \exp(-6000(\pm 1000)/T)\ cm^3 sec^{-1} \qquad (28)$$

estimated by analogy with the rate constant calculated by Zachariah and Tsang (1993a) for $H_2Si{=}O$ formation via reaction (11). The expression for $t_{chem}(GeH_4)$ is

$$t_{chem}(GeH_4) = [GeH_4]/k_{23}[GeH_2][H_2S] \qquad (29)$$

and the results of the kinetic calculations are shown in Figs. 24 and 25. The predicted GeH_4 mole fractions on Jupiter and Saturn agree well with the observed values. The dotted lines show the effects of the ±1000-K uncertainty in the activation energy, which gives approximately a factor of 5 uncertainty in the rate constant. Within this uncertainty there is good agreement between the predicted and observed GeH_4 mole fractions on the two planets. We feel that our proposed mechanism for GeH_4 sulfurization is preferable to that suggested by Fegley and Prinn (1985) because it explains the GeH_4 observations on both Jupiter and Saturn and is analogous to the mechanisms proposed for CH_4 oxidation (via $H_2C{=}O$) by Prinn and Barshay (1977) and for SiH_4 oxidation via $H_2Si{=}O$ by Zachariah and Tsang (1993a,b). In any case, the two proposed mechanisms can be tested by laboratory studies of the kinetics and mechanism of the reaction between GeH_4 and H_2S.

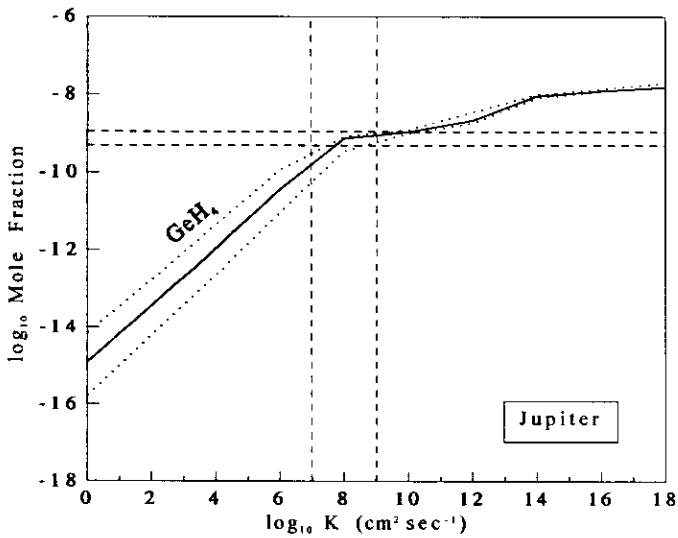

FIG. 24. The predicted GeH_4 mixing ratios in the visible atmosphere of Jupiter as a function of K_{eddy}, the vertical eddy diffusion coefficient. The horizontal dashed lines show the observed GeH_4 abundance of $0.7^{+0.4}_{-0.2}$ ppb reported by Bjoraker *et al.* (1986a). The dotted lines show the effect of the estimated ±1000 K uncertainty in the activation energy on the predicted GeH_4 abundance.

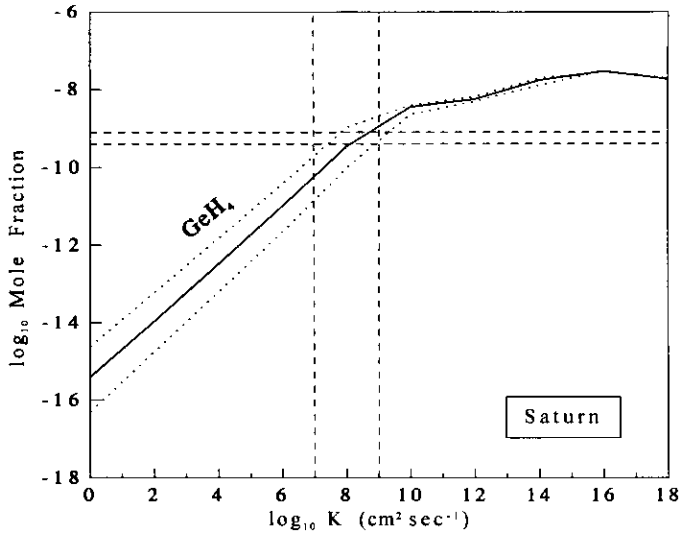

FIG. 25. The predicted GeH_4 mixing ratios in the visible atmosphere of Saturn as a function of K_{eddy}, the vertical eddy diffusion coefficient. The horizontal dashed lines show the observed GeH_4 abundance of 0.4 ± 0.4 ppb reported by Noll and Larson (1990). The dotted lines show the effect of the estimated ±1000 K uncertainty in the activation energy on the predicted GeH_4 abundance.

Tin equilibrium chemistry is illustrated in Fig. 26. Our results are in good agreement with the previous calculations of Fegley and Lewis (1979). Tin sulfide is always the major Sn gas, with the second most abundant gas shifting from SnH to SnTe and finally to SnSe with decreasing temperature. Condensation of elemental Sn removes tin from the atmospheres of Jupiter and Saturn. With decreasing temperature, the elemental Sn is successively replaced by SnS (s) and SnSe (s). Our calculations also confirm that stannane (SnH_4) is negligible relative to the tin chalcogenides and never constitutes more than a tiny fraction of the total Sn abundance.

Lead equilibrium chemistry is shown in Fig. 27. It is very similar to the chemistry of tin. Again, our results agree well with the previous calculations by Fegley and Lewis (1979). With decreasing temperature, the major lead gas switches from Pb to PbTe. Other important lead gases are PbH, PbS, and PbSe. Plumbane (PbH_4) is totally unimportant and never has a mole fraction $> 10^{-14}$. Elemental Pb is the first lead condensate, but is replaced

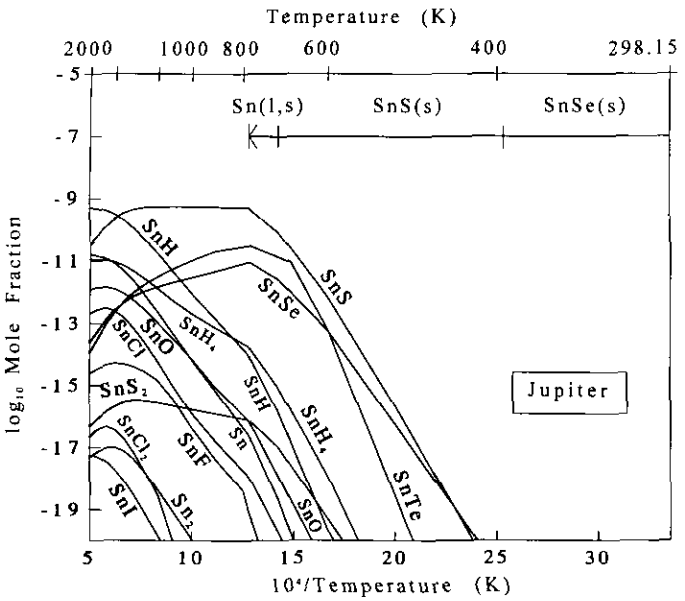

FIG. 26. Tin equilibrium chemistry along the jovian adiabat.

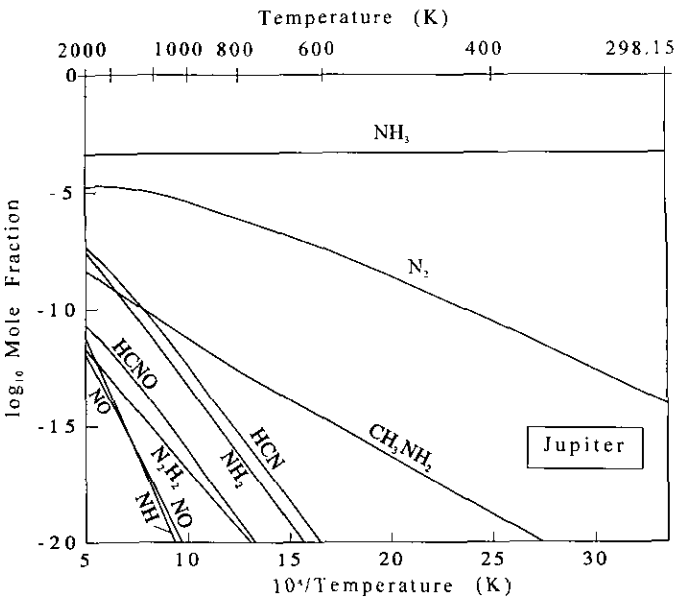

FIG. 28. Nitrogen equilibrium chemistry along the jovian adiabat.

shortly after its formation by PbTe (s), which in turn is replaced by PbSe (s).

Group VA elements. Figures 28–38 show the chemistry of N, P, As, Sb, and Bi on Jupiter and Saturn. The chemistry of these elements displays periodic trends exemplified by the decreasing stability of the trihydrides and the increasing stabilities of the elemental species and chalcogenides down the group. Ammonia is always the major N gas, while N_2 only composes a fraction of total nitrogen, and nitrogen oxides are totally insignificant. Phosphine is the major P gas down to ~ 1000 K where it is converted to P_4O_6 (g). Arsine is the major As gas down to ~400 K where either As_4 or As_2S_2 precipitates. Stibine is the major Sb gas down to ~700 K where SbS becomes as abundant and Sb_4 (g) becomes more abundant. Bismuthine is never a major Bi gas and is generally less abundant than Bi, Bi_2, BiS, BiSe, and BiTe. Also, elemental Bi is the first bismuth condensate. As discussed in more detail below, these trends have important consequences for spectroscopic observations of gases formed by the Group V elements.

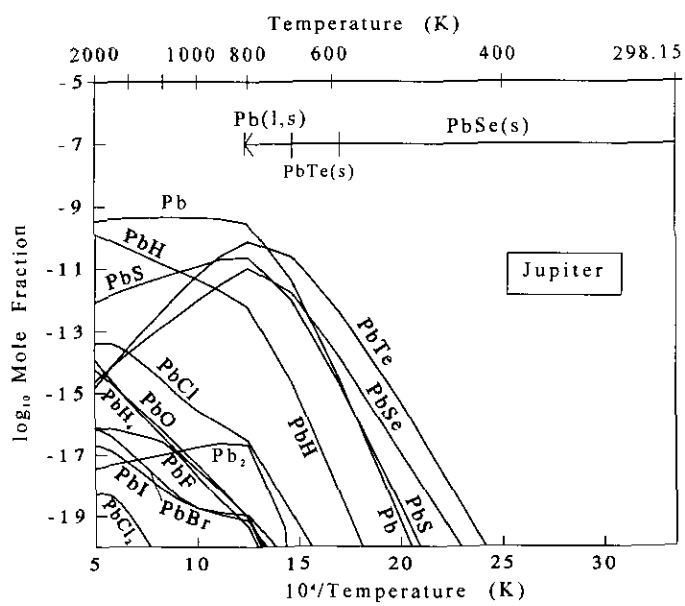

FIG. 27. Lead equilibrium chemistry along the jovian adiabat.

Nitrogen equilibrium chemistry on Jupiter is summarized in Fig. 28. Our results for Jupiter and Saturn agree with prior calculations for these two planets (Barshay and Lewis 1978, Fegley and Prinn 1985). The three nitrogen gases which are potential chemical probes of the deep atmospheres of Jupiter and Saturn are N_2, HCN, and CH_3NH_2 (methylamine). All three gases may also be produced by photochemical reactions in the stratospheres of Jupiter and Saturn (Atreya 1986; Kaye and Strobel 1983a,b, 1984). As discussed below, vertical mixing from the deep atmospheres is predicted to be the dominant source of N_2, HCN, and CH_3NH_2 in the tropospheres of these two planets.

Figure 28 shows that with decreasing temperature N_2 is converted back to NH_3. This may occur either homogeneously in the gas phase or heterogeneously on a grain surface if a suitable catalyst is available. In principle, the use of Fe-based catalysts in the industrial production of NH_3 by the Haber process and the relatively large Fe/H_2 ratio in solar composition material could lead to heteroge-

neous N_2 reduction on Fe grains in the atmospheres of the gas giant planets (e.g., see Prinn and Olaguer 1981, Fegley and Prinn 1985, Fegley *et al.* 1991). However, this is unlikely because the chemical equilibrium calculations show that all Fe is condensed out of the atmospheres of Jupiter and Saturn far below the 2000-K level. In fact, it is plausible that all the iron in the gas giant planets is sequestered in their cores. Thus, we have not repeated our earlier kinetic calculations for Fe grain-catalyzed N_2 reduction and have considered only gas phase reduction, which is the more likely mechanism.

The rate-determining step for the homogeneous gas phase $N_2 \rightarrow NH_3$ conversion (Lewis and Prinn 1980, Prinn and Olaguer 1981) is

$$N_2 + H_2 \rightarrow NH + NH \tag{30}$$

with a rate constant of

$$k_{30} = 8.45 \times 10^{-8} \exp(-81{,}515/T)\ \mathrm{cm^3 sec^{-1}}. \tag{31}$$

The chemical lifetime for N_2 is then

$$t_{\mathrm{chem}}(N_2) = 1/k_{30}[H_2]. \tag{32}$$

Likewise, HCN is also converted back into NH_3 with decreasing temperature on Jupiter and Saturn. In this case Prinn and Fegley (1981) proposed that the rate determining step is

$$HCN + H_2 \rightarrow CH_2 + NH \tag{33}$$

and that the rate constant and chemical lifetime are

$$k_{33} = 1.08 \times 10^{-8} \exp(-70{,}456/T)\ \mathrm{cm^3 sec^{-1}} \tag{34}$$

$$t_{\mathrm{chem}}(HCN) = 1/k_{33}[H_2]. \tag{35}$$

The predicted HCN and N_2 abundances as a function of the assumed K_{eddy} values on Jupiter and Saturn are displayed in Figs. 29 and 30. Considering HCN first, K_{eddy} values of 10^7–10^9 $\mathrm{cm^2 sec^{-1}}$ on Jupiter and Saturn provide 0.6–2.6 ppb HCN on both planets. This is virtually identical to the observed HCN abundance of 2^{+2}_{-1} ppb on Jupiter and consistent with the upper limit of <4 ppb on Saturn (Tokunaga *et al.* 1981). Fegley and Prinn (1985, 1988a) previously pointed out the plausibility of a deep atmospheric origin for HCN on Jupiter and Saturn, but we predict that more HCN is produced because of the larger elemental enrichment factors used in our models. As mentioned earlier, photochemical models also predict the production of HCN on Jupiter and Saturn (Kaye and Strobel 1983b,1984). The jovian HCN abundance can be produced photochemically if vertical mixing is slow above the NH_3 clouds ($K_{\mathrm{eddy}} \sim 10^4$ $\mathrm{cm^2 sec^{-1}}$). The predicted HCN abundance on Saturn is $<10^{-12}$ at the 500-mbar level and is also dependent upon the assumed K_{eddy} values. Although the variation of K_{eddy} below the homopause on Jupiter and Saturn is not presently known, there are several potentially diagnostic observations that in principle can distinguish between photochemical and deep atmospheric sources for HCN on the two planets.

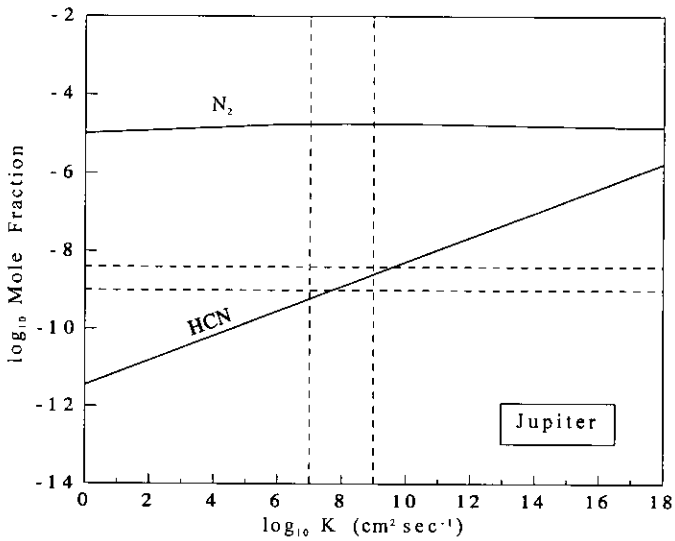

FIG. 29. The predicted N_2 and HCN mixing ratios in the visible atmosphere of Jupiter as a function of K_{eddy}, the vertical eddy diffusion coefficient. The horizontal dashed lines show the observed HCN abundance of 2^{+2}_{-1} ppb reported by Tokunaga *et al.* (1981). There are no observations of or upper limits for N_2 on Jupiter.

One diagnostic observation is to search again for HCN on Saturn to determine whether the amount of HCN predicted by vertical mixing from the deep atmosphere is actually present. The deep atmospheric source for HCN on Saturn is approximately 1000 times stronger than the photochemical source, so observations sensitive to HCN at the 0.6-ppb level can distinguish between the two mechanisms. A second diagnostic observation, which applies to Jupiter, is to use the neutral mass spectrometer on the Galileo probe to determine the vertical profile for HCN. This test probably requires concentrating samples of jovian atmosphere prior to mass spectrometer analysis (e.g., see Hunten *et al.* 1986). Yet a third diagnostic observation, which was proposed by Fegley and Prinn (1988b), is to determine the carbon and nitrogen isotopic composition of jovian HCN to see if it displays the predicted thermochemical isotopic fractionation established at the quench temperature.

Figures 29 and 30 also show that the predicted N_2 abundances on Jupiter and Saturn are ~20–30 ppm and are fairly insensitive to the assumed K_{eddy} values. Again, these predicted values are larger than those calculated pre-

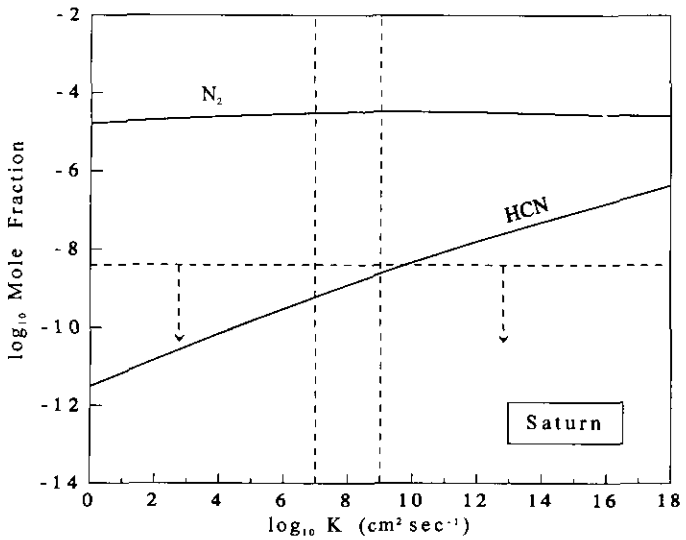

FIG. 30. The predicted N_2 and HCN mixing ratios in the visible atmosphere of Saturn as a function of K_{eddy}, the vertical eddy diffusion coefficient. The horizontal dashed line shows the upper limit of 4 ppb reported by Tokunaga *et al.* (1981). There are no observations of or upper limits for N_2 on Saturn.

viously (Prinn and Olaguer 1981, Fegley and Prinn 1985) because the nitrogen mole fraction is proportional to E^2 and larger elemental enrichment factors are used in the present models. For comparison, photochemical models predict significantly lower N_2 abundances on Jupiter and Saturn (Atreya 1986). The photochemically produced N_2 abundance on Jupiter and Saturn depends upon hydrazine (N_2H_4) supersaturation. If N_2H_4 is supersaturated, then a larger N_2 abundance up to ~0.1 ppm is predicted. However, if N_2H_4 supersaturation does not occur, then the abundance of photochemically produced N_2 is even lower, below 0.001 ppm.

Several potentially diagnostic observations can distinguish between photochemical and deep atmospheric sources of N_2. The neutral mass spectrometer experiment on the Galileo probe is capable of detecting N_2 at the 20- to 30 ppm-level (Hunten *et al.* 1986) predicted from deep atmospheric mixing and should also be able to give a vertical profile for N_2 in the atmosphere of Jupiter. A mass spectrometer on an entry probe sent into the atmosphere of Saturn would also be capable of distinguishing between photochemical and deep atmospheric sources. The $^{15}N/^{14}N$ ratios in N_2 coming from the deep atmosphere and from NH_3 photolysis are also predicted to be different (Fegley and Prinn 1988b).

Methylamine is another possible chemical probe of the deep atmospheres of Jupiter and Saturn. Figure 28 shows that CH_3NH_2 is more abundant than HCN below ~1200 K on Jupiter. The CH_3NH_2/HCN ratio on Saturn is also greater than unity below about 1500 K. If HCN and CH_3NH_2 maintain chemical equilibrium, then vertical mixing should provide more methylamine than hydrogen cyanide. This qualitative prediction suggests that deep atmospheric sources for CH_3NH_2 should dominate over photochemical sources on Jupiter and Saturn, because the CH_3NH_2/HCN ratio is 10^{-3} to 10^{-4} in the photochemical models (Kaye and Strobel 1983b, 1984).

Figure 31 illustrates phosphorus chemistry on Jupiter. Although phosphorus chemistry is fairly complex, PH_3 is the major P gas until it is converted to P_4O_6 (g) which later condenses as $NH_4H_2PO_4$ solid at about 494 K on Jupiter and at about 541 K on Saturn. The results shown are similar to those reported earlier (e.g., Lewis 1969a, Prinn and Owen 1976, Barshay and Lewis 1978, Fegley and Prinn 1985) because both the present and the prior studies used the thermodynamic data from the JANAF Tables.

However, during the course of our work, Borunov and Dorofeyeva (1991) and Borunov *et al.* (1993) reported dramatically different calculations for phosphorus chemistry on Jupiter. Their work uses thermodynamic data primarily taken from Gurvich *et al.* (1989–94) with some data such as that for PH_3 also being taken from JANAF. The major difference between our calculations and those of Borunov and colleagues is that P_4O_6 (g) is never stable in their models, so PH_3 remains the dominant P gas down to very low temperatures where P_4O_{10} (s) is predicted to form.

The differences between the two sets of calculations are almost totally due to the different values used for the enthalpy of formation ($\Delta H^0_{f,298}$) of P_4O_6 (g) in the JANAF

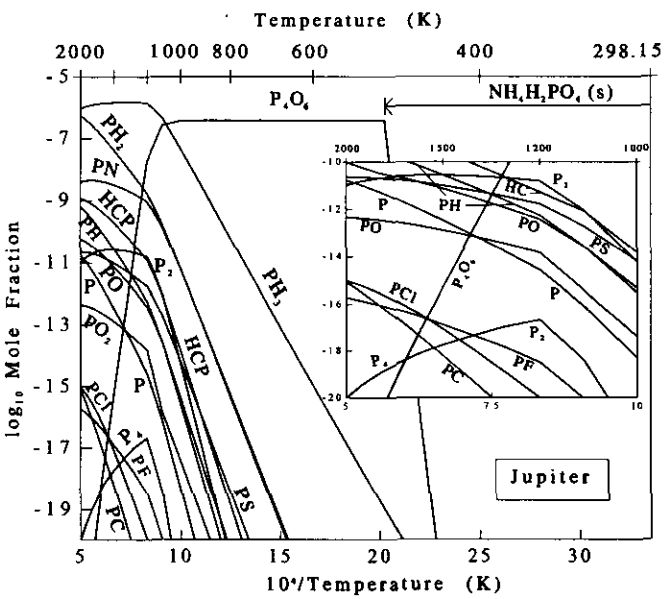

FIG. 31. Phosphorus equilibrium chemistry along the jovian adiabat. The inset shows a magnified view of the lower left portion of the figure.

Tables and in the analogous compilation by Gurvich *et al.* (1989–91). The JANAF Tables use an enthalpy of formation which is based on the calorimetric study of Koerner and Daniels (1952). In contrast, Gurvich *et al.* (1989–91) use a less negative enthalpy of formation based on the calorimetric data of Hartley and McCoubrey (1963). Gurvich *et al.* (1989–91) also cite two dissociation energy estimates made by Muenow et al (1970) and Smoes and Drowart (1974) in support of their adopted calorimetric value.

After performing calculations to verify that the differences in the adopted enthalpies of formation are indeed responsible for the different predictions about the stability of P_4O_6 (g) in the atmospheres of Jupiter and Saturn, we went back to the original calorimetry and mass spectrometry papers in order to try to determine which enthalpy value was preferable. We see no compelling reasons, such as a problem with experimental methods or with data reduction, to lead us to reject the work of Koerner and Daniels (1952) in favor of the study by Hartley and McCoubrey (1963). Also, the dissociation energy estimates are not based on direct experimental measurements of P_4O_6 (g), but are interpolated values from mass spectrometry studies of other phosphorus oxide gases. Furthermore, the JANAF data for P_4O_6 (g) have also been adopted in other recent thermodynamic data compilations (e.g., Barin 1989). Finally, the JANAF data yield results for the stability of PH_3 which are consistent with the periodic trends (discussed earlier) in the chemistry of the Group V elements. The discrepancy in the calorimetric data obviously needs to be resolved by a new experimental determination of the P_4O_6 (g) enthalpy of formation. However, at present we have decided to continue to use the data in the JANAF Tables in our calculations for the reasons mentioned above.

Our calculations using the Gurvich *et al.* (1989–94) data for P_4O_6 (g) do not support the prediction of Borunov and Dorofeyeva (1991) that PH_3 is always the most abundant P-bearing gas in the atmosphere of Jupiter until it is removed by condensation as P_4O_{10} solid. Instead we calculate that PH_3 is converted directly to $NH_4H_2PO_4$ (s). Solid P_4O_{10} is not stable in the jovian and saturnian atmospheres because it is highly reactive toward water (e.g., Cotton and Wilkinson 1988). It will rapidly react with the water vapor and NH_3 in the atmospheres of Jupiter and Saturn to form $NH_4H_2PO_4$ solid. Indeed P_4O_{10} is a highly effective desiccant (known somewhat misleadingly as phosphorus pentoxide) that is commonly used in chemical laboratories. Thus, even if the Gurvich *et al.* data for P_4O_6 (g) were adopted, which we do not feel is correct, the principal PH_3 loss process is still $NH_4H_2PO_4$ (s) condensation.

The kinetics and mechanism of PH_3 oxidation by water vapor are still unknown. However, experimental studies of PH_3 oxidation in O_3/O_2, O_3/N_2, and O/O_2 gas mixtures

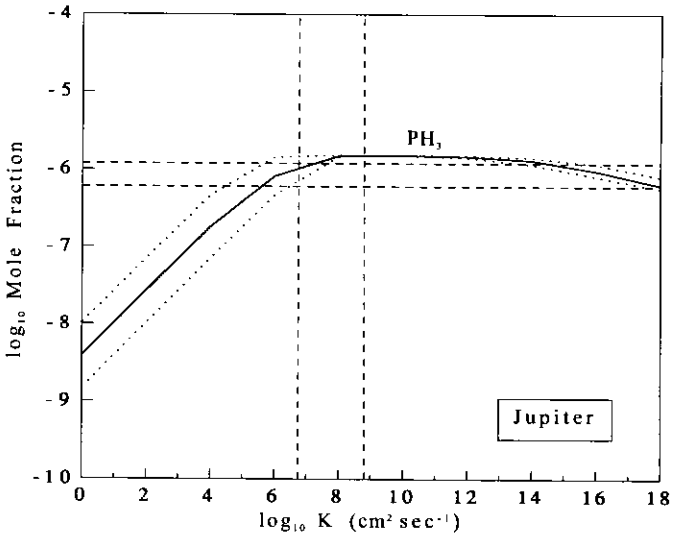

FIG. 32. The predicted PH_3 mixing ratio in the visible atmosphere of Jupiter as a function of K_{eddy}, the vertical eddy diffusion coefficient. The horizontal dashed lines show the observed PH_3 abundances on Jupiter, which range from 0.6 to 1.2 ppm (Bjoraker *et al.* 1986a, Drossart *et al.* 1990). The dotted lines show the effect of the estimated factor of 10 uncertainty in the rate constant on the predicted PH_3 abundance. The observed PH_3 abundances correspond to ~1–2 times the solar P/H_2 ratio.

and quantum mechanical calculations of the stabilities of gaseous P oxides and their anions show that PO and PO_2 are important intermediates in PH_3 oxidation (Fraser *et al.* 1983, 1984; Lohr 1984). A plausible mechanism was proposed by Prinn *et al.* (1984) and Fegley and Prinn (1985). It starts with the thermal decomposition of PH_3

$$PH_3 = PH + H_2, \tag{36}$$

followed by reaction of the PH radicals with OH radicals to eventually give P_4O_6

$$H_2O = OH + H \tag{37}$$

$$PH + OH \rightarrow PO + H_2 \tag{38}$$

$$PO + OH \rightarrow PO_2 + H \tag{39}$$

$$2PO + 2PO_2 + 2M \rightarrow P_4O_6 + 2M \tag{40}$$

Following Prinn *et al.* (1984) and Fegley and Prinn (1985), we assume that the initial formation of a P–O bond in reaction (38) is the rate determining step with a rate estimated as

$$k_{38} = 10^{-10\pm1}\ \mathrm{cm^3 sec^{-1}} \tag{41}$$

The chemical lifetime of PH_3 is then given by

$$t_{chem}(PH_3) = [PH_3]/k_{38}[PH][OH] \tag{42}$$

As illustrated in Figs. 32 and 33, there is generally good

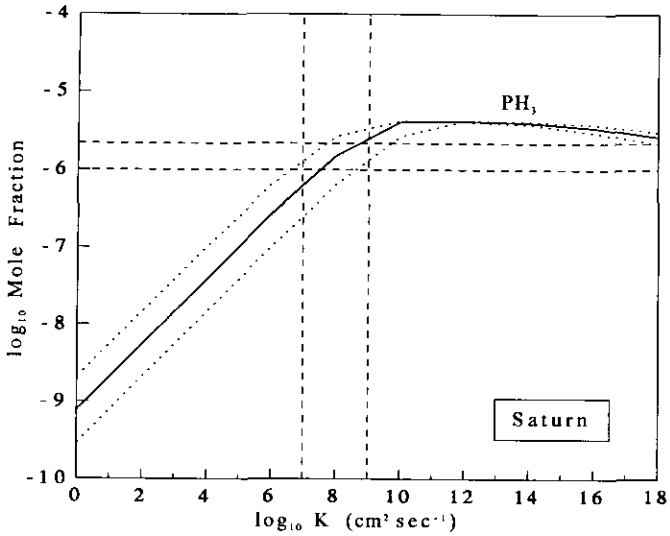

FIG. 33. The predicted PH_3 mixing ratio in the visible atmosphere of Saturn as a function of K_{eddy}, the vertical eddy diffusion coefficient. The horizontal dashed lines show the observed PH_3 abundances on Saturn which range from 1.0 to 2.2 ppm (Courtin *et al.* 1984, Larson *et al.* 1980, Noll and Larson 1990). The dotted lines show the effect of the estimated factor of 10 uncertainty in the rate constant on the predicted PH_3 abundance. The observed PH_3 abundances correspond to ~1.4–3 times the solar P/H_2 ratio.

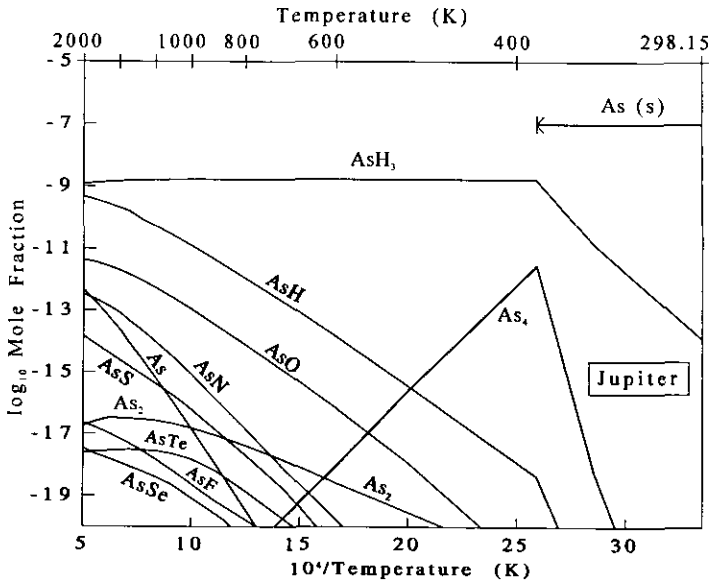

FIG. 34. Arsenic equilibrium chemistry along the jovian adiabat. The text explains the differences between the present results and those of Fegley and Lewis (1979).

agreement between the predicted and observed PH_3 mole fractions on Jupiter and Saturn. The dotted lines on the two figures show the effects of the estimated factor of 10 uncertainty in the rate constant. The drop-off in the PH_3 abundance at low K_{eddy} values is due to quenching at levels where P_4O_6 is the major P gas and PH_3 is a minor species. The drop-off in the PH_3 abundance at high K_{eddy} values is due to the increasing importance of PH_2, PN, and other P gases at very high temperatures. However, neither the very low nor the very high K_{eddy} values are physically realistic and they are included on the graph only to illustrate trends.

Arsenic equilibrium chemistry is shown in Fig. 34. Arsine (AsH_3) is the major arsenic gas over the entire temperature range considered on Jupiter and Saturn. The AsH radical is the second most abundant gas down to ~490 K where As_4 becomes more abundant. However, the present calculations do not include AsH_2 gas because only the dissociation energy and enthalpy of formation are available for AsH_2 (Berkowitz 1988), while entropy and heat capacity data are also needed to calculate the Gibbs free energy as a function of temperature to do chemical equilibrium calculations. If AsH_2 were included in the calculations, it would presumably have an abundance intermediate between those of AsH_3 and AsH over most of the temperature range considered. This is the case for NH_3, NH_2, and NH and for PH_3, PH_2, and PH.

Precipitation of either As_4 (s) or As_2S_2 (s) occurs just below 400 K on Jupiter and Saturn, and the abundances of AsH_3 and As_4 decrease below this point. Barshay and Lewis (1978) predicted that solid As condensation removed AsH_3 from the gas. However, As_2S_2 (s), which is calculated to condense 5° higher than As_4 (s), was not included in their calculations. The 5° difference is within the uncertainties of the thermodynamic data, and is not significant. However, because the As_2S_2 (s) data are partially estimated (Mills 1974), we model arsenic chemistry using solid arsenic condensation.

Fegley and Lewis (1979), who used thermodynamic data for AsF_3(g) from Wagman *et al.* (1968), predicted that AsH_3 was replaced by AsF_3 as the major As gas at about 360 K. However we find that AsF_3 is unimportant because an error in the tabulated $\Delta H^0_{f,298}$ for AsF_3 gas has recently been discovered and corrected. The older, incorrect value and the newer, corrected value for the $\Delta H^0_{f,298}$ of AsF_3(g) are shown in Table 3.

Because it is not certain whether AsH_3 is converted to As_4 (s) or to As_2S_2 (s), we propose two different mecha-

TABLE III
Values for the Enthalpy of Formation of AsF_3 (g) [kJ mol^{-1}][a]

$\Delta H^0_{f,298}$	Reference	Comments
−920.6	Wagman *et al.* 1968	Used by Fegley and Lewis 1979
−785.8	Barin 1989	Used in this work
−785.7	Knacke *et al.* 1991	Similar to value used in this work

[a] For formation of AsF_3 (g) from As (gray, s) and F_2 (g).

nisms for AsH_3 destruction on Jupiter and Saturn. Both schemes start with AsH_3 thermal dissociation and H atom abstraction reactions

$$AsH_3 = AsH + H_2 \quad (43)$$

$$AsH_3 + H = AsH_2 + H_2 \quad (44)$$

$$AsH_2 + H = AsH + H_2, \quad (45)$$

which maintain equilibrium concentrations of AsH_3, AsH_2, and AsH. If As_4 precipitation is actually responsible for AsH_3 destruction, these reactions are followed by

$$AsH + AsH_3 \rightarrow As_2H_2 + H_2 \quad (46)$$

$$As_2H_2 \rightarrow As_2 + H_2 \quad (47)$$

$$As_2 + As_2 + M \rightarrow As_4 + M \quad (48)$$

$$As_4 \rightarrow As_4\,(s) \quad (49)$$

The formation of an As–As bond in reaction (46) is taken as the rate determining step with a rate constant of

$$k_{46} = 10^{-10\pm1}\,cm^3sec^{-1}, \quad (50)$$

by analogy with the rate constant for SiH + SiH_4 (Jasinski 1994). We use this analogy because we have been unable to find data for the analogous PH + PH_3 or GeH + GeH_4 reactions. The chemical lifetime for AsH_3 is given by

$$t_{chem}(AsH_3) = 1/k_{46}[AsH]. \quad (51)$$

If As_2S_2 (s) precipitation is responsible for AsH_3 destruction instead, the following sequence occurs:

$$H_2S + H = HS + H_2 \quad (52)$$

$$AsH + HS \rightarrow AsS + H_2 \quad (53)$$

$$AsS + AsS + M \rightarrow As_2S_2 + M \quad (54)$$

$$As_2S_2 \rightarrow As_2S_2\,(s) \quad (55)$$

Reaction (53) leading to the formation of an As–S bond is assumed to be the rate determining step with a rate constant also estimated as

$$k_{53} = 10^{-10\pm1}\,cm^3sec^{-1}. \quad (56)$$

In this case the chemical lifetime of AsH_3 is

$$t_{chem}(AsH_3) = [AsH_3]/k_{53}[AsH][HS]. \quad (57)$$

Because the same value is used for the two rate constants, the lower HS molecular number densities lead to larger t_{chem} values and thus to higher quench temperatures. In fact, all the calculated quench temperatures for AsH_3 destruction via As_2S_2 precipitation are higher than 400 K. As a result, the predicted AsH_3 abundances are equal to the total assumed As abundance and are independent of the assumed K_{eddy} values. Thus, the kinetic calculations for As_2S_2 precipitation are not graphed.

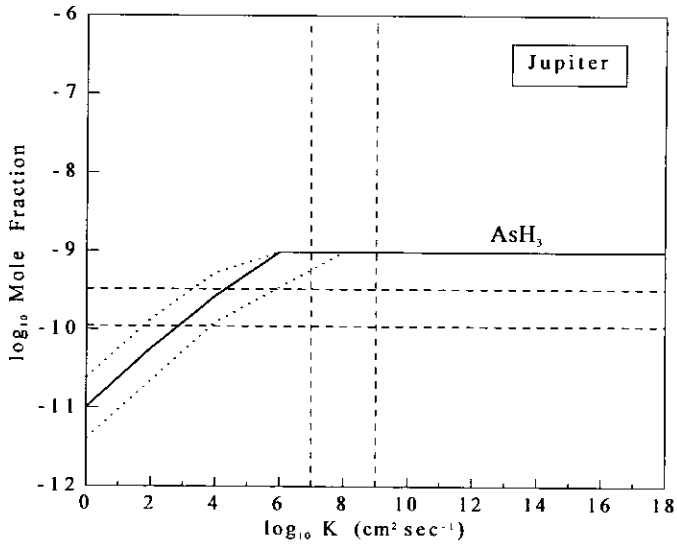

FIG. 35. The predicted AsH_3 mixing ratio in the visible atmosphere of Jupiter as a function of K_{eddy}, the vertical eddy diffusion coefficient. The horizontal dashed lines show the observed AsH_3 abundance of 0.22 ± 0.11 ppb (Noll *et al.* 1990). The dotted lines show the effect of the estimated factor of 10 uncertainty in the rate constant on the predicted AsH_3 abundance. The observed AsH_3 abundance corresponds to ~0.2–0.7 times the solar As/H_2 ratio.

Figures 35 and 36 show the kinetic calculations for AsH_3 destruction via As_4 precipitation on Jupiter and Saturn. Again, the dotted lines on the two figures show the effects of the estimated factor of 10 uncertainty in the rate constant. The predicted AsH_3 abundance on Jupiter is always greater than the observed value except at K_{eddy} values less than approximately $10^4\,cm^2sec^{-1}$. However, the predicted AsH_3 abundance on Saturn agrees well with the observed value.

Despite the disagreement between the observed and predicted AsH_3 abundances on Jupiter, the vertical transport of arsine is still the most plausible source for this species because AsH_3 production from an extraplanetary source, such as infalling meteoritic material, would lead to large amounts of unobserved species such as SiH_4 and H_2S. Arsenic is a siderophile element which is 50% condensed in Fe alloy at about 1012 K at 10^{-4} bars total pressure in the solar nebula (Fegley 1994a). Silicon and sulfur condense at 1529 K and 684 K, respectively, at the same total pressure, with all Si being incorporated into rock and all S forming FeS. The CI chondritic Si/As and S/As atomic ratios are about 152,400 and 78,500 (Anders

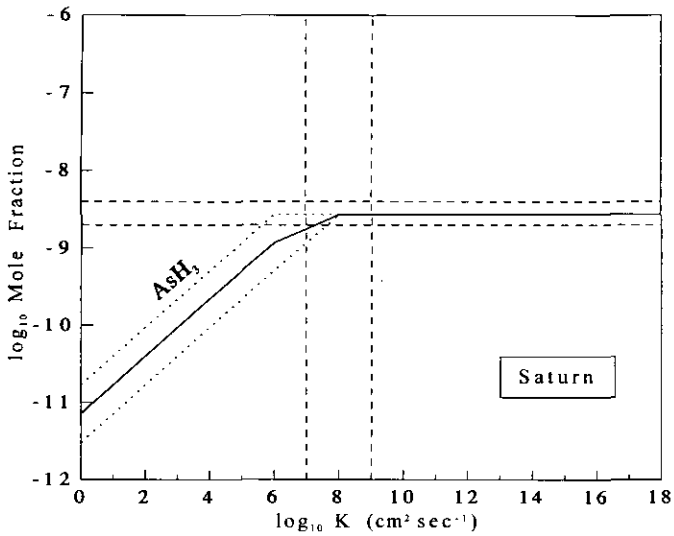

FIG. 36. The predicted AsH_3 mixing ratio in the visible atmosphere of Saturn as a function of K_{eddy}, the vertical eddy diffusion coefficient. The horizontal dashed lines show the observed AsH_3 abundance of 3 ± 1 ppb (Bézard *et al.* 1989, Noll and Larson 1990, Noll *et al.* 1989). The dotted lines show the effect of the estimated factor of 10 uncertainty in the rate constant on the predicted AsH_3 abundance. The observed AsH_3 abundance corresponds to ~4–8 times the solar As/H_2 ratio.

and Grevesse 1989). If the AsH_3 in the atmosphere of Jupiter were derived from infalling chrondritic material, much larger amounts of SiH_4 and H_2S would also be expected to be produced. However, neither of these gases are found in the observable region of Jupiter's atmosphere and the upper limits on them are in the ppb range. If the infalling material were assumed to be solely composed of iron meteorites, which is unlikely given that most observed falls are stony meteorites, the H_2S/AsH_3 ratio would still be much greater than unity because of the ubiquitous FeS inclusions found in iron meteorites. Thus, an extraplanetary source for AsH_3, GeH_4 and PH_3, on Jupiter and Saturn is implausible given the absence of SiH_4 and H_2S in the observable atmospheres of the two planets. The deep atmospheric source is preferable in all cases.

Instead, it is much more likely that the disagreement between the predicted and observed AsH_3 abundance on Jupiter is due to one of two factors. Either the observed AsH_3 abundance could be in error or the mechanism and kinetics of AsH_3 destruction could be in error. Initially, Noll *et al.* (1989) reported 0.7 ppb AsH_3 on Jupiter with an uncertainty which allowed an AsH_3 abundance as high as 1.4 ppb. This much AsH_3 is compatible with our predicted abundance for plausible K_{eddy} values of 10^7–10^9 cm^2sec^{-1}. However, the AsH_3 abundance reported by Noll *et al.* (1989) disagreed with an upper limit of <0.3 ppb derived by Bézard *et al.* (1989). Later, Noll *et al.* (1990) revised their AsH_3 abundance on Jupiter downward to 0.22 ± 0.11 ppb, which is the range shown by the horizontal dashed lines in Fig. 35.

The revised AsH_3 abundance is difficult to understand for the following reasons. Arsine and PH_3 are the major As and P gases in the atmospheres of Jupiter and Saturn because of the thermodynamic and kinetic factors described above. The observed PH_3/H_2 and AsH_3/H_2 ratios on Jupiter correspond to about 1–2 and 0.2–0.7 times the solar ratios, respectively. On Saturn the observed PH_3/H_2 and AsH_3/H_2 ratios correspond to about 1.4–3 and 4–8 times the solar ratios, respectively. The solar abundances of both elements are known to about 10%, so it is unlikely that the differences in their behavior can be attributed to errors in the solar elemental abundances. The large formal uncertainties preclude firm statements, but AsH_3 is apparently depleted relative to solar on Jupiter and enriched relative to solar on Saturn, while PH_3 is enriched relative to solar on both planets.

This pattern is difficult to explain because of the similar cosmochemical behavior of P and As. Both elements are siderophile and condense in Fe alloy within a few hundred degrees of each other (Fegley 1994a). Thus, to a first approximation, P and As are rock-forming elements that should behave similarly during accretion of Jupiter and Saturn. Until more accurate and precise observational data are available, we feel that errors in the AsH_3 abundance on Jupiter cannot be ruled out. However, it would be necessary to increase the jovian AsH_3 abundance by about a factor of 3 to agree with the predicted value.

Conversely, the mechanism and kinetics of AsH_3 destruction in the atmospheres of Jupiter and Saturn may be different than those proposed here. As noted earlier, AsH_2 could not be included in the chemical equilibrium calculations because only incomplete thermodynamic data are available for this species. If AsH_2 were more abundant than AsH, as expected by analogy with NH_3, NH_2, and NH and PH_3, PH_2, and PH, then AsH_3 destruction may proceed via the reactions

$$AsH_3 + H = AsH_2 + H_2 \quad (44)$$

$$AsH_2 + AsH_2 \rightarrow As_2H_2 + H_2 \quad (58)$$

$$As_2H_2 \rightarrow As_2 + H_2 \quad (47)$$

$$As_2 + As_2 + M \rightarrow As_4 + M \quad (48)$$

$$As_4 \rightarrow As_4(s). \quad (49)$$

In this case the higher number densities of AsH_2 would lead to more rapid AsH_3 destruction given similar values for the rate constant of reaction (58), the assumed rate determining step. This would lead to lower predicted AsH_3 abundances on Jupiter, but also to lower AsH_3 abundances on Saturn. Until the necessary entropy and heat

capacity data are available for AsH_2, this possibility cannot be quantitatively evaluated.

Figure 37 shows Sb chemistry on Jupiter. Our results for Sb chemistry are in good agreement with those of Fegley and Lewis (1979). Stibine (SbH_3) and SbS (g), which have similar abundances, are the two major Sb gases down to about 690 K where Sb_4 (g) becomes the major species. Solid Sb condensation takes place at a slightly lower temperature of ~670 K. The two possible Sb gases which may be transported upward by rapid vertical mixing are SbH_3 and SbS. It is unlikely that Sb_4 can be transported upward because once it becomes slightly supersaturated relative to the vapor pressure over Sb (s) it will probably condense out. No detailed mechanism is put forward for SbH_3 or SbS destruction because of a lack of thermodynamic data for SbH_2 and SbH and the lack of kinetic data or good analogies. However, stibine destruction in the upward moving gas parcels is plausibly initiated by thermal decomposition and H atom abstraction,

$$SbH_3 = SbH + H_2 \quad (59)$$

$$SbH_3 + H = SbH_2 + H_2, \quad (60)$$

followed by reactions of Sb hydride radicals to form elemental Sb_2 vapor

$$SbH + SbH_3 \rightarrow Sb_2H_2 + H_2 \quad (61)$$

$$SbH_2 + SbH_2 \rightarrow Sb_2H_2 + H_2 \quad (62)$$

$$Sb_2H_2 \rightarrow Sb_2 + H_2,$$

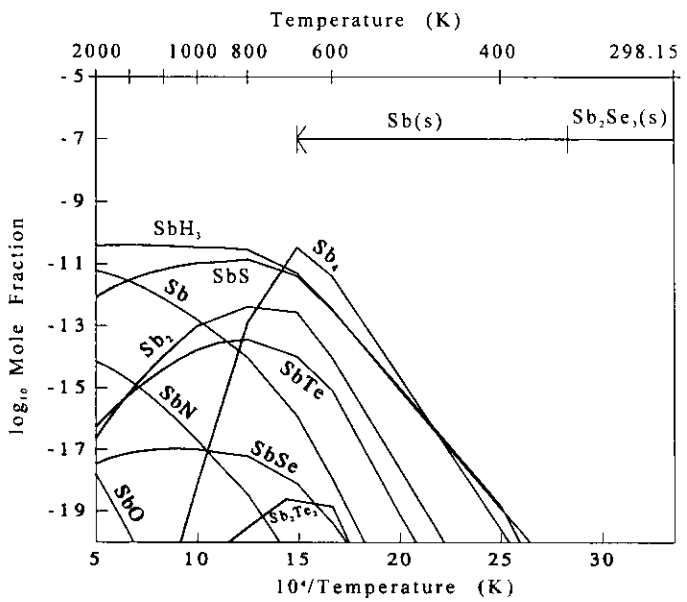

FIG. 37. Antimony equilibrium chemistry along the jovian adiabat.

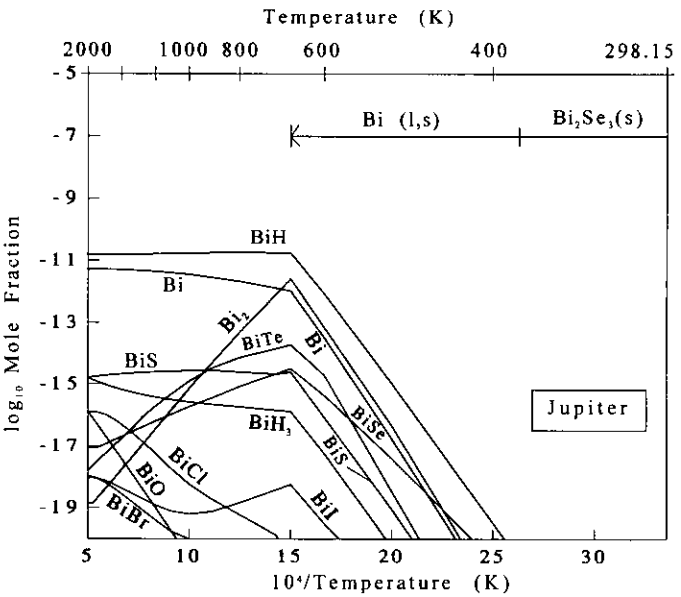

FIG. 38. Bismuth equilibrium chemistry along the jovian adiabat.

which then reacts with itself and a third body forming Sb_4,

$$Sb_2 + Sb_2 + M \rightarrow Sb_4 + M \quad (63)$$

$$Sb_4 \rightarrow Sb_4(s). \quad (64)$$

The assumed rate determining step is either reaction (61) or (62), which both lead to the formation of an Sb–Sb bond.

The destruction of SbS in upward moving gas parcels may proceed via the reactions

$$SbS + H \rightarrow Sb + HS \quad (65)$$

$$Sb + Sb + M \rightarrow Sb_2 + M \quad (66)$$

$$Sb_2 + Sb_2 + M \rightarrow Sb_4 + M \quad (63)$$

$$Sb_4 \rightarrow Sb_4(s). \quad (64)$$

Stibine destruction is plausibly a rapid process because of the weak Sb–H bond strength. Antimony sulfide destruction is more difficult to evaluate because of the lack of kinetic data or of good analogies, but the Sb–S bond is fairly strong. However, given the detection of three other group V trihydrides on Jupiter and Saturn, efforts to detect SbH_3 also seem warranted. The ν_1 and ν_3 fundamentals nears 1890 cm^{-1} could be used to search for SbH_3 (Treffers et al. 1978).

Figure 38 depicts Bi chemistry on Jupiter and Saturn. The major gas at all temperatures is BiH. Bismuthine (BiH_3) is much more unstable than any of the other Group

V trihydrides and only reaches a mole fraction of 10^{-15} at 2000 K. The only other Bi gases which make up more than 1% of total Bi at some point over the range 300 to 2000 K are Bi and Bi_2. Solid Bi condensation at ~670 K reduces the abundances of all Bi gases. It is unlikely that the BiH radical can be quenched in upward moving gas parcels, and we do not expect that Earth-based observations can detect any Bi compounds in the atmospheres of Jupiter and Saturn.

Group VIA elements. Periodic trends in the chemistry of the Group VIA elements are exemplified by the decreasing stability of the dihydrides (H_2O, H_2S, H_2Se, and H_2Te) down the group and the increasing importance of monochalcogenide gases down the group with monoxides being generally less important than monosulfides, monoselenides, and monotellurides. The dissociation energy data also indicate that monohydrides (OH, HS, HSe, and HTe) become more important down the group, but entropy and heat capacity data are not tabulated for HSe and HTe so equilibrium calculations were not done for these two gases.

Water vapor is the dominant oxygen gas and H_2S is the dominant sulfur gas on both Jupiter and Saturn. The results for these two elements (Figs. 39 and 40) are virtually identical to those reported earlier (Barshay and Lewis 1978, Fegley and Prinn 1985). Liquid water condenses at about 293 K on Jupiter and 334 K on Saturn and leads to the formation of aqueous solution clouds. Cloud condensation chemistry on Jupiter and Saturn has been discussed by many authors (e.g., Lewis 1969a,b, Weidenschilling and Lewis 1973, Atreya 1986) and is not covered in this paper.

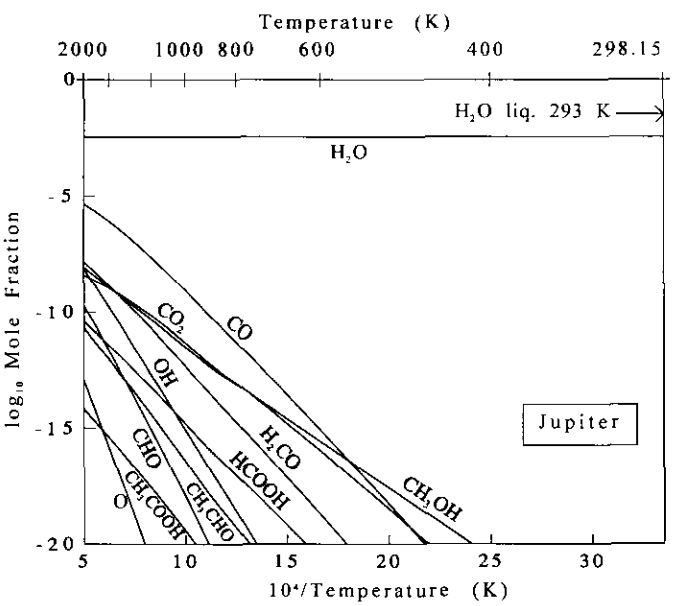

FIG. 39. Oxygen equilibrium chemistry along the jovian adiabat. Water vapor condenses to form aqueous solutions clouds at 293 K on Jupiter and 334 K on Saturn.

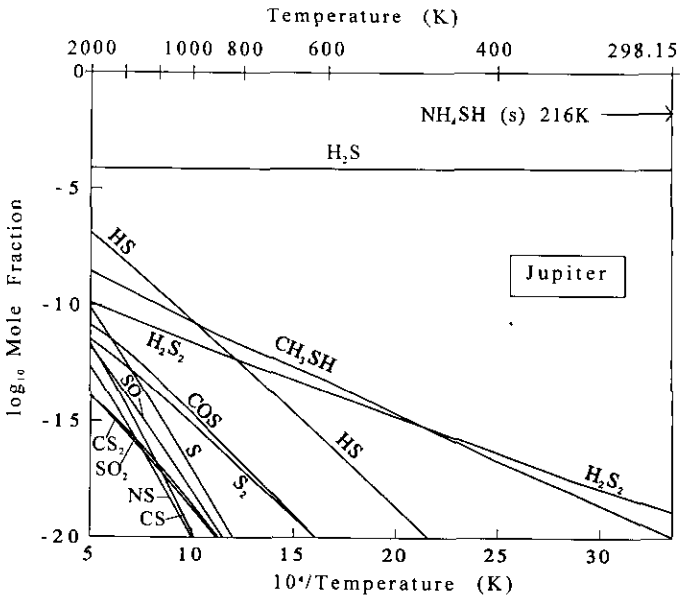

FIG. 40. Sulfur equilibrium chemistry along the jovian adiabat. Hydrogen sulfide condenses to form NH_4SH at 216 K.

Spectroscopic searches for H_2S on Jupiter and Saturn (Bézard *et al.* 1983, Larson *et al.* 1984, Owen *et al.* 1977) give upper limits of <40 ppb on Jupiter and <0.2 ppm on Saturn. The failure to detect H_2S and the low upper limits are plausibly due to chemical effects in the atmospheres of Jupiter and Saturn instead of to bulk sulfur depletions on the two planets. One important factor is that no significant H_2S absorption occurs in the 5-μm window in the atmospheres of Jupiter and Saturn (e.g., Larson *et al.* 1984). This is the wavelength region which probes deepest into the atmospheres of the two planets. Searches for H_2S must be done at either longer or shorter wavelengths which probe higher (and cooler) regions where NH_4SH condensation is taking place and where photodissociation of H_2S may also occur. Larson *et al.* (1984) searched for H_2S in the 2.7-μm window on Jupiter, which sounds the 175-K region, and found an upper limit consistent with the H_2S vapor pressure over solid NH_4SH. We calculate that NH_4SH condenses at about 216 K on Jupiter, in good agreement with Larson *et al.* (1984) who calculated 210 K. Thus, we agree with Larson *et al.* (1984) that NH_4SH condensation is responsible for the depletion of H_2S in the upper troposphere of Jupiter.

Figures 41 and 42 show Se and Te equilibrium chemistry on Jupiter. With the exception of some changes in the abundance of some metal selenide and telluride vapors, the results are very similar to those reported by Fegley and Lewis (1978) for Jupiter and Fegley and Prinn (1985) for Saturn. Hydrogen selenide is the major Se gas over

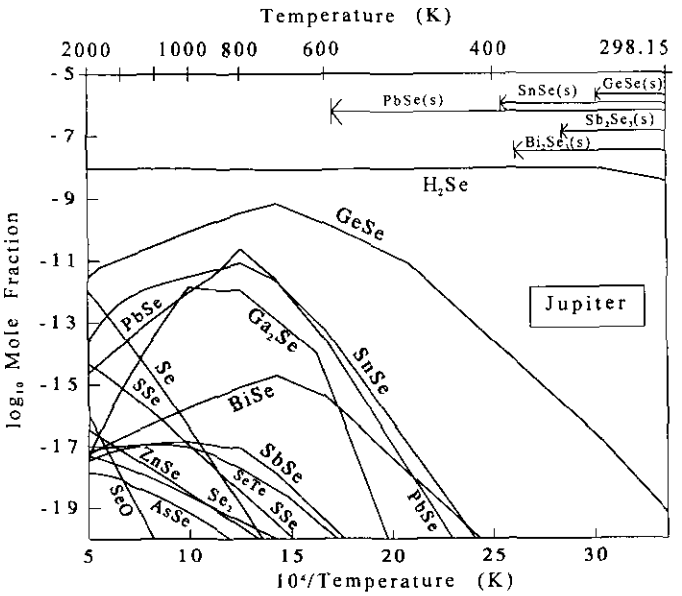

FIG. 41. Selenium equilibrium chemistry along the jovian adiabat.

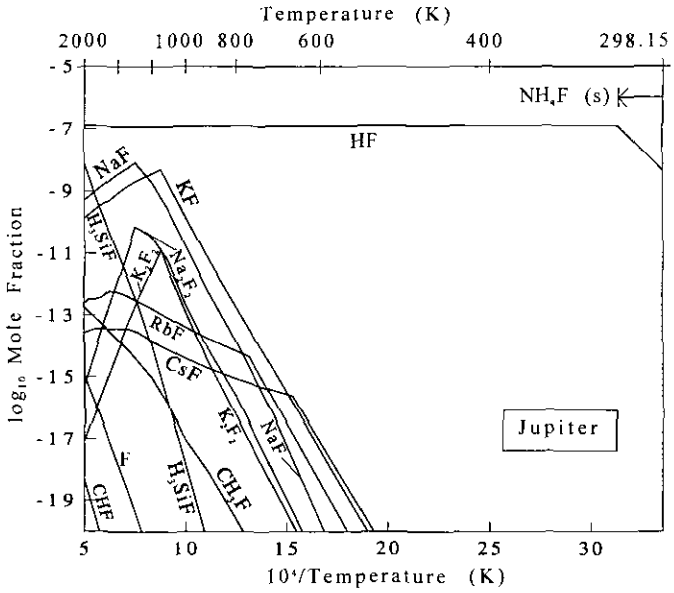

FIG. 43. Fluorine equilibrium chemistry along the jovian adiabat. Solid NH_4F condenses at 319 K and probably dissolves in the aqueous solution clouds.

the entire temperature range considered while H_2Te is briefly replaced by GeTe as the major Te gas in the range 700–900 K range. Both H_2Se and H_2Te are possibly detectable, but are subject to photodissociation and condensation as NH_4HSe and NH_4HTe, respectively. We are unaware of spectroscopic upper limits for either gas. However, Bézard *et al.* (1986) proposed that both H_2Se and H_2Te could be detected, if present at 1–5 times solar abundance, by high resolution submillimeter observations of Jupiter and Saturn.

Group VIIA elements. Figures 43–46 illustrate the equilibrium chemistry for the halogens in the jovian atmosphere. The periodic trends displayed by the halogens are the decreasing stability of the hydrogen halides down the group, the increasing stability of alkali halide vapors down the group, and the decreasing condensation temperatures for ammonium halides going from Cl to Br to I. Our results

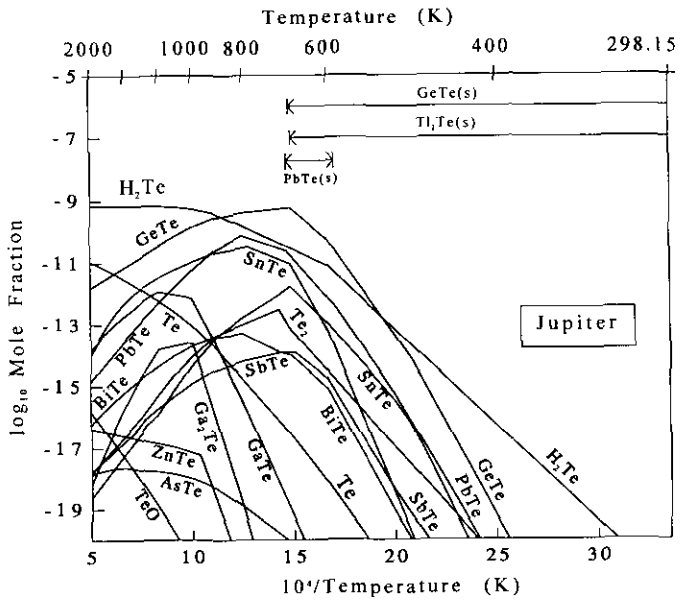

FIG. 42. Tellurium equilibrium chemistry along the jovian adiabat.

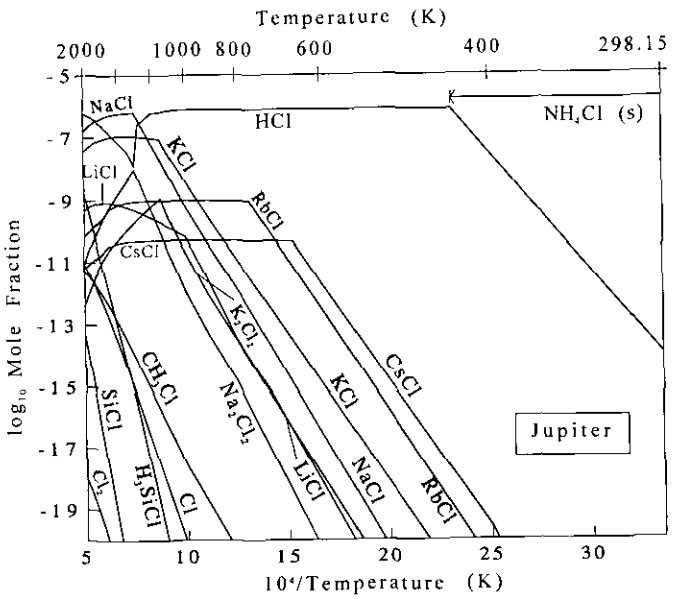

FIG. 44. Chlorine equilibrium chemistry along the jovian adiabat. Ammonium chloride condenses at 432 K.

TABLE IV
Predicted Chemical Probes on Jupiter and Saturn

Gas	Class	Comments	Gas	Class	Comments
CO	A, E	see Figs. 18-19	NaCN	D	See Fig. 3
HCN	A, E	see Figs. 29-30	MBO_2	D	M = Na, K, Rb, See Fig. 12
PH_3	A, E	see Figs. 32-33	GaN	D	See Fig. 14
AsH_3	A, E	see Figs. 35-36	Ga_2O	D	See Fig. 14
GeH_4	A, E	see Figs. 24-25	Ga_2S	D	See Fig. 14
C_2H_6	A, E	Photochemical product in stratosphere, See Fig. 17	Tl_2S	D	See Fig. 16
C_2H_4	A, E	Photochemical product in stratosphere, See Fig. 17	GeH_3	D	See Fig. 23
H_3BO_3	B	dissolves in aq. soln. clouds	P_2	D	See Fig. 31
N_2	B	see Figs. 29-30	PH_2	D	See Fig. 31
H_2S	B, E?	condenses as NH_4SH	PN	D	See Fig. 31
HF	B,C?	sub-mm observations?	AsH_2	D	AsH_2 > AsH?
HCl	B,C?	sub-mm observations?	MS	D	M = Ge, Sn, Pb, Sb
HBr	B,C?	sub-mm observations?	HS	D	See Fig. 40
CH_3NH_2	C, E?	predict CH_3NH_2/HCN >1	H_2S_2	D	See Fig. 40
SbH_3	C?, E?	no available upper limits	MSe	D	M = Ge, Sn, Pb
CO_2	C?,D, E?	See Fig. 17	Ga_2Se	D	See Fig. 14
CH_3OH	C?,D, E?	See Fig. 17	H_2Te	C?,D, E?	See Fig. 42
CH_3SH	C?,D, E?	CH_3SH/CH_3NH_2 ~1	MTe	D	M = Ga, Ge, Sn, Pb
CH_3	D	See Fig. 17	Te_2	D	See Fig. 42
H_2Se	C, E?	sub-mm observations?	MF	D	M = Li, Na, K, Rb, Ga
M	D	M = Na, K, Rb, Cs, Ag, Zn, Cd, Hg, In, Tl, Pb, Bi	$(MF)_2$	D	M = Li, Na, K
MOH	D	M = Li, Na, K, Rb, Cs, Ga, In	MCl	D	M = Li, Na, K, Rb, Cs, In
MH	D	M = Li, Na, K, Rb, Ga, In, Cu, Au, Ga, In, Tl, Sn, Pb, As, Bi	$(MCl)_2$	D	M = Na, K, Rb
$(MOH)_2$	D	M = Li, Na, K	MBr	D	M = Na, K, Rb
$Mg(OH)_2$	D	See Fig. 8	HI	C?,D	sub-mm observations?
Na_2	D	See Fig. 3	MI	D	M = Na, K

A: Observed on Jupiter and/or Saturn

B: Considered detectable by the Galileo Probe ($X_i \geq 10^{-9}$ at some point above the 20-bar level on Jupiter).

C: Considered detectable by Earth-based observations ($X_i \geq 10^{-12}$ at some point above the aqueous solution clouds on Jupiter and/or Saturn).

D: Considerable detectable by deep atmospheric entry probes ($X_i \geq 10^{-12}$ at some point above the 500-bar (~1000 K) level on Jupiter and/or Saturn).

E: Considered detectable by the Cassini Orbiter around Saturn ($X_i \geq 10^{-10}$ at some point above the aqueous solution clouds on Saturn).

agree well with the prior calculations by Barshay and Lewis (1978) and Fegley and Prinn (1985). The hydrogen halides are generally the major gases except at high temperatures (~1500–1900 K) where alkali chlorides, bromides, and iodides are dominant. Alkali fluorides never replace HF as the major fluorine gas. At low temperatures, the hydrogen halides are removed from the atmospheres of Jupiter and Saturn by condensation. On Jupiter the condensation points for the ammonium halides are NH_4F (319 K), NH_4Cl (432 K), NH_4Br (415 K), and NH_4I (368 K). Again, we are unaware of any spectroscopic upper limits for the hydrogen halides on Jupiter and Saturn. However, Bézard *et al.* (1986) also predict that all of the hydrogen halides are potentially detectable in the submillimeter region.

SUMMARY AND SUGGESTIONS FOR FUTURE OBSERVATIONS

Table 4 presents a summary of the predicted chemical probes on Jupiter and Saturn. This listing was compiled from a careful and thorough examination of the results of our chemical equilibrium calculations for 2000 compounds of all naturally occurring elements in the periodic table. It is divided into five classes of compounds: (A) observed species, (B) species considered detectable by the Galileo probe in Jupiter's atmosphere, (C) species considered detectable by Earth-based and Earth-orbital spectroscopic observations, (D) species considered detectable by the next generation of deep atmospheric entry probes, and (E) species considered detectable by the Cassini orbiter around Saturn.

The gases in Table 4 include molecules, radicals, and monatomic vapors. Excluding isotopically substituted gases (e.g., see Fegley and Prinn 1988b) and charged species, the ~100 different gases in Table 4, which have not yet been observed on Jupiter or Saturn, appear to be the best prospects for discovering new chemical probes of the deep atmospheres of these two planets. At present, with the exception of a few species (e.g., P_2H_4, AsH_2, As_2H_4, SbH, SbH_2, HSe, HTe) for which only incomplete thermodynamic data are available, all potentially important inorganic gases have probably been considered in our calculations. Although only a relatively small number of organic compounds have been included in our calculations and in the work of Barshay and Lewis (1978), the thermochemical equilibrium calculations show that the hot hydrogen-rich deep atmospheres of Jupiter and Saturn are hostile environments for the survival of complex organic molecules. Instead of being formed in the deep atmospheres of Jupiter and Saturn, organic compounds will be broken down into methane and hydrogen.

Further advances in the study of chemical probes of the deep atmospheres of Jupiter and Saturn thus lie in areas other than theoretical modeling. Laboratory kinetic studies are necessary to test the proposed thermochemical kinetic schemes for the observed and predicted chemical probes of atmospheric dynamics. Earth-based and Earth-orbital planetary spectroscopy are needed to quantify temporal and spatial variations in the abundances of observed chemical probes and to search for new chemical probes. New spacecraft capable of carrying out long-term observations of the atmospheres of the jovian planets are needed to complement the Earth-based observing programs. Finally, it is essential to design a new generation of atmospheric entry probes capable of penetrating to great depths in the atmospheres of the jovian planets in order to directly measure the nature, abundance, and vertical profiles of the predicted chemical probes. Hopefully, this paper will prove a stimulus for workers in these diverse fields.

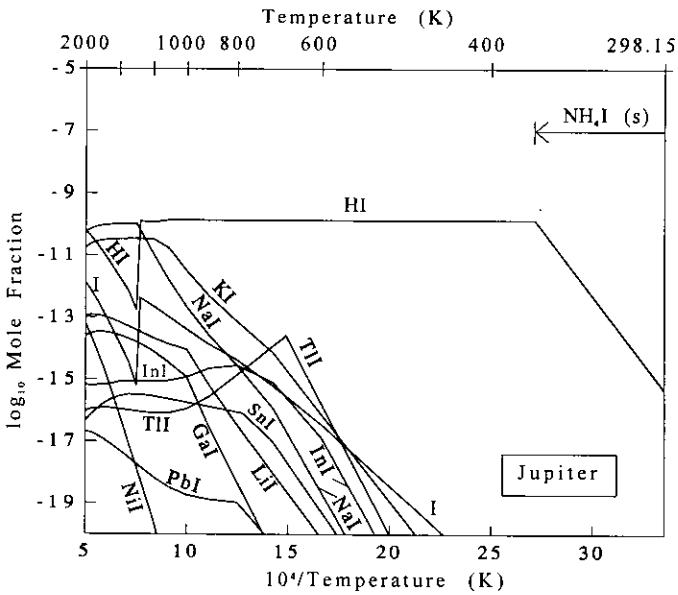

FIG. 46. Iodine equilibrium chemistry along the jovian adiabat. Ammonium iodide condenses at 368 K.

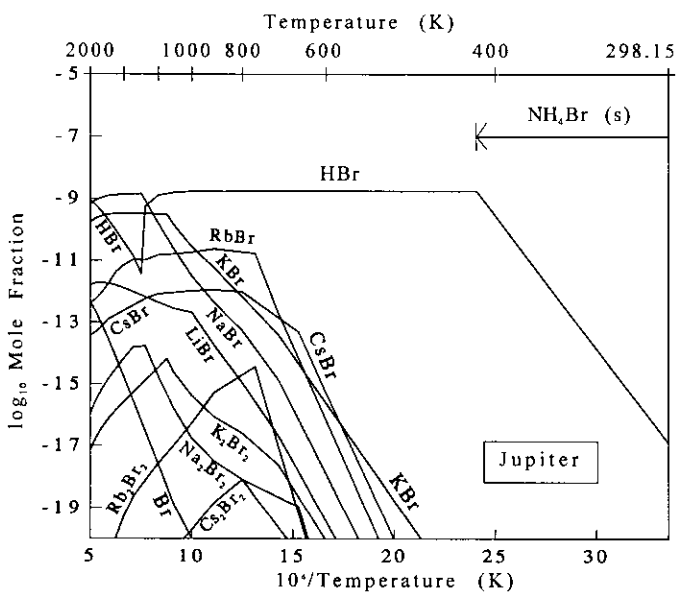

FIG. 45. Bromine equilibrium chemistry along the jovian adiabat. Ammonium bromide condenses at 415 K.

ACKNOWLEDGMENTS

This work was supported by a grant from the NASA Planetary Atmospheres Program (B. Fegley, P.I.). We thank B. Bézard, G. Bjoraker, E. Lellouch, and H. Palme for useful discussions. We acknowledge help from S. Hinds, L. Lu, S. Saenton, and K. Sper, who are Washington University undergraduates, in expanding and maintaining our bibliographic and thermodynamic databases.

REFERENCES

ALLER, L. H. 1961. *The Abundances of the Elements*. Wiley–Interscience, New York.

ANDERS, E., AND N. GREVESSE 1989. Abundances of the elements: Meteoritic and solar. *Geochim. Cosmochim. Acta* **53**, 197–214.

ATREYA, S. K. 1986. *Atmospheres and Ionospheres of the Outer Planets and Their Satellites*. Springer-Verlag, Berlin.

BARIN, I. 1989. *Thermochemical Data of Pure Substances*, 2 vols. VCH, Weinheim, Germany.

BARRAU, J., M. BOUCHAUT, H. LAVAYSSIÈRE, G. DOUSSE, AND J. SATGÉ 1979. Réactiions de germylénes avec divers oxirannes et le thiirane. Mise en évidence de germanones et germathiones intermédiaires. *Helv. Chim. Acta* **62**, 152–154.

BARRAU, J., M. BOUCHAUT, H. LAVAYSSIÈRE, G. DOUSSE, AND J. SATGÉ 1980. Deshydrocondensation de thiols β-germanies a liason

APPENDIX

Appendix. Thermodynamic Database and Literature Sources

GASES:

Ag	Pankratz 1982
AgBr	Barin 1989
AgCl	Barin 1989
AgF	Barin 1989
AgI	Barin 1989
AgS	Mills 1974
Al	JANAF
Al-	JANAF
Al+	JANAF
AlBr	JANAF
AlBr3	JANAF
AlC	JANAF
AlCl	JANAF
AlCl+	JANAF
AlClF	JANAF
AlClF+	JANAF
AlClF2	JANAF
AlClO	JANAF
AlCl2	JANAF
AlCl2-	JANAF
AlCl2+	JANAF
AlCl2F	JANAF
AlCl3	JANAF
AlF	JANAF
AlF+	JANAF
AlF2	JANAF
AlF2+	JANAF
AlF2-	JANAF
AlF2O	JANAF
AlF2O-	JANAF
AlF3	JANAF
AlF4-	JANAF
AlF4Na	JANAF
AlH	JANAF
AlHO+	JANAF
AlI	JANAF
AlI3	JANAF
AlLiF4	JANAF
AlN	JANAF
AlO	JANAF
AlO-	JANAF
AlO+	JANAF
AlOF	JANAF
AlOH	JANAF
AlOH-	JANAF
AlO2	JANAF
AlO2-	JANAF
AlS	JANAF
AlS2	Gurvich et al.
AlSe	Knacke et al. 1991
AlTe	Mills 1974
Al2	JANAF
Al2Br6	JANAF
Al2Cl6	JANAF
Al2F6	JANAF
Al2I6	JANAF
Al2O	JANAF
Al2O+	JANAF
Al2O2	JANAF
Al2O2+	JANAF
Al2S	Gurvich et al.
Al2S2	Gurvich et al.
Al2Se	Knacke et al. 1991
Al2Se2	Barin 1989
Ar	JANAF
Ar+	JANAF
As	Hultgren et al. 1973
AsBr3	Barin 1989
AsCl	Shaulov & Mosin 1973
AsCl2	Shaulov & Mosin 1973
AsCl3	Barin 1989
AsF	O'Hare 1968
AsF2	O'Hare 1968
AsF3	Barin 1989
AsF5	Barin 1989
AsH	Sauval & Tatum 1984
AsH3	Barin 1989
AsI3	Pankratz 1984
AsN	Wagman et al. 1968, Kelley 1960
AsO	Barin 1989
AsS	Pankratz 1984
AsSe	Mills 1974
AsTe	Mills 1974
As2	Hultgren et al. 1973
As3	Hultgren et al. 1973
As4	Hultgren et al. 1973
As4O6	Barin 1989
As4S4	Pankratz et al. 1987
Au	Pankratz 1982
AuH	Knacke et al. 1991
AuS	Mills 1974
B	JANAF
B+	JANAF
B-	JANAF
BAlO2	JANAF
BBeO2	JANAF
BBr	JANAF
BBrCl	JANAF
BBrCl2	JANAF
BBrF	JANAF
BBrF2	JANAF
BBrO	JANAF
BBr2	JANAF
BBr2Cl	JANAF
BBr2F	JANAF
BBr2H	JANAF
BBr3	JANAF
BC	JANAF
BCl	JANAF
BCl+	JANAF
BClF	JANAF
BClO	JANAF
BCl2	JANAF
BCl2+	JANAF
BCl2-	JANAF
BCl2F	JANAF
BCl2H	JANAF
BCl3	JANAF
BCsO2	Cordfunke & Konings 1990
BF	JANAF
BFO	JANAF
BF2	JANAF
BF2+	JANAF
BF2-	JANAF
BF2H	JANAF
BF2O	JANAF
BF3	JANAF
BF4-	Gurvich et al.
BF4K	JANAF
BH	JANAF
BHO+	JANAF
BHO-	JANAF
BHO2	JANAF
BHS	JANAF
BHS+	JANAF
BH2	JANAF
BH2O2	JANAF
BH3	JANAF
BH3O3	JANAF
BI	JANAF
BI2	JANAF
BI3	JANAF
BKO2	JANAF
BLiO2	JANAF
BN	JANAF
BNaO2	JANAF
BO	JANAF
BO-	Gurvich et al.
BO2	JANAF
BO2-	JANAF
BS	JANAF
BS2	Pankratz et al. 1987
B2	JANAF
B2BeO4	JANAF
B2Cl4	JANAF
B2F4	JANAF
B2F4O	JANAF
B2H6	JANAF
B2H4O4	JANAF
B2O	JANAF
B2O2	JANAF
B2O3	JANAF
B2S	Gurvich et al.
B2S2	Gurvich et al.
B2S3	Gurvich et al.
B3Cl3O3	JANAF
B3FH2O3	JANAF
B3F2HO3	JANAF
B3F3O3	JANAF
B3H3O3	JANAF
B3H3O6	JANAF
B3H6N3	JANAF
B5H9	JANAF
B10H14	JANAF
Ba	JANAF
Ba+	JANAF
BaBr	JANAF
BaBr2	JANAF
BaCl	JANAF
BaCl2	JANAF
BaF	JANAF
BaF+	JANAF
BaF2	JANAF
BaH	Barin 1989
BaI	JANAF
BaI2	JANAF
BaO	JANAF
BaOH	JANAF
BaOH+	JANAF
Ba(OH)2	JANAF
BaS	JANAF
Be	JANAF
Be+	JANAF
BeBr	JANAF
BeBr2	JANAF
BeC2	JANAF
BeCl	JANAF
BeCl+	JANAF
BeClF	JANAF
BeCl2	JANAF
BeF	JANAF
BeF2	JANAF
BeF3Li	JANAF
BeH	JANAF
BeH+	JANAF
BeH2	JANAF
BeI	JANAF
BeI2	JANAF
BeN	JANAF
BeO	JANAF
BeOH	JANAF
BeOH+	JANAF
Be(OH)2	JANAF
BeS	JANAF
Be2	JANAF
Be2Cl4	JANAF
Be2F2O	JANAF
Be2F4	Gurvich et al.
Be2O	JANAF
Be2O2	JANAF
Be3O3	JANAF
Be4O4	JANAF
Be5O5	JANAF
Be6O6	JANAF
Bi	Pankratz 1982
BiBr	Barin 1989
BiBr3	Pankratz 1984
BiCl	Barin 1989
BiCl3	Barin 1989
BiF	Barin 1989
BiF3	Pankratz 1984
BiH	Lindgren & Nilsson 1975
BiH3	Knacke et al. 1991
BiI	Barin 1989
BiI3	Pankratz 1984
BiO	Uy & Drowart 1969
BiS	Pankratz et al. 1987
BiSe	Knacke et al.1991
BiTe	Knacke et al.1991
Bi2	Hultgren et al. 1973
Bi2S2	Pankratz et al. 1987
Bi2S3	Pankratz et al. 1987
Br	JANAF
Br-	JANAF
Br+	JANAF
BrCN	JANAF
BrCl	JANAF

BrF	JANAF	COClF	JANAF	CaH	Barin 1989	CsOH+	JANAF
BrF3	JANAF	COF	JANAF	CaI	JANAF	Cs2	JANAF
BrF5	JANAF	COF2	JANAF	CaI2	JANAF	Cs2Br2	Gurvich et al.
Br2	JANAF	COS	JANAF	CaO	JANAF	Cs2Cl2	JANAF
C	JANAF	CO2	JANAF	CaOH	JANAF	Cs2CrO4	Cordfunke & Konings
C+	JANAF	CO2-	JANAF	CaOH+	JANAF		1990
C-	JANAF	CS	JANAF	Ca(OH)2	JANAF	Cs2F2	JANAF
CBr	JANAF	CSe	Pankratz et al. 1984	CaS	JANAF	Cs2I2	Cordfunke & Konings
CBrF3	JANAF	CS2	JANAF	Ca2	JANAF		1990
CBr4	JANAF	CSe2	Pankratz et al. 1984	Cd	Pankratz 1982	Cs2MoO4	Cordfunke & Konings
CCO	JANAF	C2	JANAF	CdBr2	Knacke et al. 1991		1990
CCl	JANAF	C2-	JANAF	CdCl2	Knacke et al. 1991	Cs2O	JANAF
CClF3	JANAF	C2Cl2	JANAF	CdF2	Knacke et al. 1991	Cs2O+	Gurvich et al.
CCl2	JANAF	C2Cl4	JANAF	CdI2	Knacke et al. 1991	Cs2O2	Cordfunke & Konings
CCl2F2	JANAF	C2Cl6	JANAF	CdO	Barin 1989		1990
CCl3	JANAF	C2F2	JANAF	CdS	Barin 1989	Cs2(OH)2	JANAF
CCl3F	JANAF	C2F4	JANAF	CdSe	Knacke et al. 1991	Cs2SO4	JANAF
CCl4	JANAF	C2F6	JANAF	CdTe	Knacke et al. 1991	Cu	JANAF
CF	JANAF	C2H	JANAF	Cl	JANAF	Cu-	JANAF
CF+	JANAF	C2HCl	JANAF	Cl+	JANAF	Cu+	JANAF
CFN	JANAF	C2HF	JANAF	Cl-	JANAF	CuBr	Pankratz 1984
CF2	JANAF	C2H2	JANAF	ClCN	JANAF	CuCl	JANAF
CF2+	JANAF	C2H2O	Barin 1989	ClF	JANAF	CuF	JANAF
CF3	JANAF	C2H3Cl	Barin 1989	ClF3	JANAF	CuF2	JANAF
CF3+	JANAF	C2H3N	Stull et al. 1969	ClF5	JANAF	CuH	Knacke et al. 1991
CF3CN	JANAF	C2H4	JANAF	ClO	JANAF	CuI	Pankratz 1984
CF3OF	JANAF	C2H4O	Oxirane, JANAF	ClO2	JANAF	CuO	JANAF
CF3SF5	JANAF	C2H5Cl	Barin 1989	ClO3F	JANAF	CuS	Mills 1974
CF4	JANAF	C2H6	Glushko et al.	Cl2	JANAF	CuSe	Knacke et al. 1991
CH	JANAF	C2H6O	Barin 1989	Cl2O	JANAF	CuTe	Knacke et al. 1991
CH+	JANAF	C2N	JANAF	Co	JANAF	Cu2	JANAF
CHCl	JANAF	C2N2	JANAF	Co-	JANAF	Cu3Br3	Pankratz 1984
CHClF2	JANAF	C3	JANAF	Co+	JANAF	Cu3Cl3	JANAF
CHCl2F	JANAF	C3H4	Barin 1989	CoCl	JANAF	Cu3I3	Pankratz 1984
CHCl3	JANAF	{Py}C3H4	Barin 1989	CoCl2	JANAF	e-	JANAF
CHF	JANAF	C3H6	Rossini et al. 1953	CoCl3	JANAF	F	JANAF
CHF3	JANAF	C3H6O	Barin 1989	CoF2	JANAF	F-	JANAF
CHO	JANAF	C3H8	Chao et al. 1973	Co2Cl4	JANAF	F+	JANAF
CH2	JANAF	C3O2	JANAF	Cr	JANAF	{c}FNNF	JANAF
CH2ClF	JANAF	C4	JANAF	Cr-	JANAF	{t}FNNF	JANAF
CH2Cl2	JANAF	C4H6	Barin 1989	Cr+	JANAF	FONO2	JANAF
CH2F2	JANAF	C4H8	Barin 1989	CrBr4	Pankratz 1984	FSSF	JANAF
CH2O	JANAF	C4 H10	Rossini et al. 1953	Cr(CO)6	Knacke et al. 1991	F2 (g	JANAF
CH2O2	Barin 1989	C4N2	JANAF	CrCl2	Knacke et al. 1991	Fe	JANAF
CH3	JANAF	C5	JANAF	CrCl2O2	Barin 1989	Fe+	JANAF
CH3CHO	Stull et al. 1969	C5H8	Barin 1989	CrCl3	Knacke et al. 1991	Fe-	JANAF
CH3Cl	JANAF	C5 H12	Barin 1989	CrCl4	Pankratz 1984	FeBr2	JANAF
CH3F	JANAF	C6H14	Rossini et al. 1953	CrN	JANAF	Fe(CO)5	JANAF
CH3NH2	Stull et al. 1969	C6H6	Rossini et al. 1953	CrO	JANAF	FeCl	JANAF
CH3OH	Glushko et al.	C6H6O	Barin 1989	CrO2	JANAF	FeCl2	JANAF
CH3SH	Stull et al. 1969	C7H16	Barin 1989	CrO3	JANAF	FeCl3	JANAF
CH4	JANAF	C8H14	Barin 1989	CrS	Mills 1974	FeF	JANAF
CH4CO2	Chao & Zwolinski	C8H18	Barin 1989	Cs	JANAF	FeF2	JANAF
	1978	C9H16	Barin 1989	Cs-	JANAF	FeF3	JANAF
ClF3	JANAF	C9H20	Barin 1989	Cs+	JANAF	FeI2	JANAF
Cl4	Pankratz 1984	C10H22	Barin 1989	CsBr	Barin 1989	FeO	JANAF
CN	JANAF	Ca	JANAF	CsCl	JANAF	Fe(OH)2	JANAF
CN+	JANAF	Ca+	JANAF	CsF	JANAF	FeS	JANAF
CN-	JANAF	CaBr	JANAF	CsH	Knacke et al. 1991	Fe2Br4	JANAF
CNI	JANAF	CaBr2	JANAF	CsI	Barin 1989	Fe2Cl4	JANAF
CNN	JANAF	CaCl	JANAF	CsNO2	Gurvich et al.	Fe2Cl6	JANAF
CO	JANAF	CaCl2	JANAF	CsNO3	Gurvich et al.	Fe2I4	JANAF
COCl	JANAF	CaF	JANAF	CsO	JANAF	Ga	Gurvich et al.
COCl2	JANAF	CaF2	JANAF	CsOH	JANAF	Ga+	Gurvich et al.

Ga-	JANAF	HAlO	JANAF	Hf-	JANAF	K-	JANAF
GaBr	Knacke et al. 1991	HAlO2	JANAF	HfBr4	Pankratz 1984	K+	JANAF
GaBr3	Knacke et al. 1991	HBO	JANAF	HfCl2	Barin 1989	KBr	JANAF
GaCl	Gurvich et al.	HBr	JANAF	HfCl3	Barin 1989	(KBr)2	JANAF
GaCl2	Gurvich et al.	HCN	JANAF	HfCl4	Pankratz 1984	KCN	JANAF
GaCl3	Gurvich et al.	HCNO	JANAF	HfF4	Pankratz 1984	(KCN)2	JANAF
GaF	Gurvich et al.	HCO+	JANAF	HfI4	Pankratz 1984	KCl	JANAF
GaF2	Gurvich et al.	HCOF	JANAF	HfO	Glushko et al.	(KCl)2	JANAF
GaF3	Gurvich et al.	HCOOH	Glushko et al.	HfO2	Glushko et al.	KF	JANAF
GaH	Gurvich et al.	HCP	JANAF	Hg	JANAF	(KF)2	JANAF
GaI	Knacke et al. 1991	HC3N	Harland 1986, Benson 1978	Hg+	JANAF	KF2-	JANAF
GaI3	Knacke et al. 1991			HgBr	JANAF	KH	JANAF
GaN	Wagman et al. 1968	HC5N	Harland 1986, Benson 1978	HgBr2	JANAF	KI	JANAF
GaO	Gurvich et al.			HgCl	JANAF	(KI)2	JANAF
GaOH	Gurvich et al.	HC7N	Harland 1986, Benson 1978	HgCl2	JANAF	KO	JANAF
GaTe	Knacke et al. 1991			HgF	JANAF	KO-	JANAF
Ga2Br6	Knacke et al. 1991	HC9N	Harland 1986, Benson 1978	HgF2	JANAF	KOH	JANAF
Ga2Cl6	Gurvich et al.			HgH	JANAF	KOH+	JANAF
Ga2O	Gurvich et al.	HC11N	Harland 1986, Benson 1978	HgI	JANAF	(KOH)2	JANAF
Ga2S	Knacke et al. 1991			HgI2	JANAF	KS	Pankratz et al. 1987
Ga2Se	Knacke et al. 1991	HC13N	Harland 1986, Benson 1978	HgO	JANAF	K2	JANAF
Ga2Te	Knacke et al. 1991			HgS	Pankratz et al. 1987	K2S	Pankratz et al. 1987
Ge	Gurvich et al.	HCl	JANAF	HgSe	Mills 1974	K2SO4	JANAF
Ge+	Gurvich et al.	HF	JANAF	HgTe	Mills 1974	Kr	JANAF
GeBr	Gurvich et al.	HI	JANAF	I	JANAF	Kr+	JANAF
GeBr2	Gurvich et al.	HNO	JANAF	I-	JANAF	Li	JANAF
GeBr3	Gurvich et al.	{t}HNO2	JANAF	I+	JANAF	Li+	JANAF
GeBr4	Gurvich et al.	{c}HNO2	JANAF	IBr	JANAF	Li-	JANAF
GeCl	Gurvich et al.	HNO3	JANAF	ICl	JANAF	LiBr	JANAF
GeCl2	Gurvich et al.	HOCl	JANAF	IF	JANAF	LiCl	JANAF
GeCl3	Gurvich et al.	HOF	JANAF	IF5	JANAF	LiClO	JANAF
GeCl4	Gurvich et al.	HO2	JANAF	IF7	JANAF	LiF	JANAF
GeF	Gurvich et al.	HPO	Gurvich et al.	I2	JANAF	LiF2-	JANAF
GeF2	Gurvich et al.	HReO4	Smith et al. 1952	In	Gurvich et al.	LiFO	JANAF
GeF3	Gurvich et al.	HS	JANAF	In+	Gurvich et al.	LiH	JANAF
GeF4	Gurvich et al.	HSO3F	JANAF	InBr	Barin 1989	LiI	JANAF
GeH	Glushko et al.	HSiCl3	JANAF	InBr3	Knacke et al. 1991	LiN	JANAF
GeH2	Ruscic et al. 1990	HSiF3	JANAF	InCl	Gurvich et al.	LiNO	JANAF
GeH3	Ruscic et al. 1990; Shabur & Morozov 1978	H2	JANAF	InCl2	Gurvich et al.	LiNO2	Gurvich et al.
		H2+	JANAF	InCl3	Gurvich et al.	LiNO3	Gurvich et al.
		H2-	JANAF	InF	Gurvich et al.	LiNaO	JANAF
GeH4	Barin 1989	H2F2	JANAF	InF2	Gurvich et al.	LiO	JANAF
GeI	Gurvich et al.	H2O	JANAF	InF3	Gurvich et al.	LiO-	JANAF
GeI2	Knacke et al. 1991	H2O2	JANAF	InH	Gurvich et al.	LiOH	JANAF
GeI3	Gurvich et al.	H2S	JANAF	InI	Barin 1989	LiOH+	JANAF
GeI4	Barin 1989	H2SO4	JANAF	InI2	Pankratz 1984	Li2+	Gurvich et al.
GeO	Gurvich et al.	H2S2	Mills 1974	InI3	Pankratz 1984	Li2	JANAF
GeO2	Gurvich et al.	H2Se	Mills 1974	InO	Gurvich et al.	Li2Br2	JANAF
GeS	Gurvich et al.	H2SiCl2	JANAF	InOH	Gurvich et al.	Li2ClF	JANAF
GeS2	Gurvich et al.	H2SiF2	JANAF	InS	Mills 1974	Li2Cl2	JANAF
GeSe	Mills 1974	H2Te	Mills 1974	InSe	Barin 1989	Li2F2	JANAF
GeTe	Mills 1974	H3F3	JANAF	InTe	Knacke et al. 1991	Li2I2	JANAF
GeTe2	Knacke et al. 1991	H3+	Gurvich et al.	In2Cl6	Gurvich et al.	Li2O	JANAF
Ge2	Gurvich et al.	H3O+	JANAF	In2O	Gurvich et al.	Li2O+	Gurvich et al.
Ge2H6	Galasso et al. 1966	H3SiCl	JANAF	In2S	Knacke et al. 1991	Li2O2	JANAF
Ge2O2	Ramakhrishnan & Chandrasekharaiah 1975	H3SiF	JANAF	In2Se	Pankratz et al. 1984	Li2(OH)2	JANAF
		H4F4	JANAF	In2Te	Knacke et al. 1991	Li2SO4	JANAF
		H5F5	JANAF	Ir	Hultgren et al. 1973	Li3+	Gurvich et al.
Ge3O3	Ramakhrishnan & Chandrasekharaiah 1975	H6F6	JANAF	IrF6	Barin 1989	Li3Br3	Gurvich et al.
		H7F7	JANAF	IrO3	Chandrasekharaiah et al. 1981	Li3Cl3	JANAF
		He	JANAF			Li3F3	JANAF
H	JANAF	He+	JANAF	Ir2O3	Chandrasekharaiah et al. 1981	Li3I3	Gurvich et al.
H+	JANAF	Hf	JANAF			Mg	JANAF
H-	JANAF	Hf+	JANAF	K	JANAF	Mg+	JANAF

MgBr	JANAF	MoF4	JANAF	NaOH	JANAF	PBr	JANAF
MgBr2	JANAF	MoF4O	JANAF	NaOH+	JANAF	PBr3	JANAF
MgBr2+	JANAF	MoF5	JANAF	Na2	JANAF	PC	JANAF
MgCl	JANAF	MoF6	JANAF	Na2Br2	JANAF	PCl	JANAF
MgCl+	JANAF	MoI	JANAF	Na2(CN)2	JANAF	PCl2	Gurvich et al.
MgClF	JANAF	MoI2	JANAF	Na2Cl2	JANAF	PCl3	JANAF
MgCl2	JANAF	MoI3	JANAF	Na2F2	JANAF	PCl5	JANAF
MgF	JANAF	MoI4	JANAF	Na2(OH)2	JANAF	PF	JANAF
MgF+	JANAF	MoO	JANAF	Na2SO4	JANAF	PF-	JANAF
MgF2	JANAF	MoO2	JANAF	Nb	JANAF	PF+	JANAF
MgF2+	JANAF	MoO2Cl2	JANAF	Nb-	JANAF	PF2	JANAF
MgH	JANAF	MoO3	JANAF	Nb+	JANAF	PF2+	JANAF
MgI	JANAF	MoO3-	Gurvich et al.	NbBr5	JANAF	PF2-	JANAF
MgI2	JANAF	MoO4H2	JANAF	NbC	Gupta & Gingerich 1981	PF3	JANAF
MgN	JANAF	Mo2F10	JANAF			PF5	JANAF
MgO	JANAF	Mo2O6	Gurvich et al.	NbC2	Gupta & Gingerich 1981	PH	JANAF
MgOH	JANAF	Mo3F15	JANAF			PH2	JANAF
MgOH+	JANAF	Mo3O9	Gurvich et al.	NbCl4	Barin 1989	PH3	JANAF
Mg(OH)2	JANAF	Mo4O12	Gurvich et al.	NbCl5	JANAF	PI3	Barin 1989
MgS	JANAF	Mo5O15	Gurvich et al.	NbF5	Barin 1989	PN	JANAF
Mg2	JANAF	N	JANAF	NbO	JANAF	PO	JANAF
Mg2Br4	JANAF	N+	JANAF	NbOCl3	Barin 1989	POBr3	JANAF
Mg2Cl4	JANAF	N-	JANAF	NbO2	JANAF	POClF2	JANAF
Mg2F4	JANAF	NBr	JANAF	NbS	Mills 1974	POCl2F	JANAF
Mn	JANAF	NCN	JANAF	Ne	JANAF	POCl3	JANAF
Mn+	JANAF	NCO	JANAF	Ne+	JANAF	POF3	JANAF
MnBr	Wagman et al. 1969,	NF	JANAF	Ni	JANAF	PO2	JANAF
	Kelley 1960, Kelley &	NF2	JANAF	Ni-	JANAF	PS	JANAF
	King 1961	NF3	JANAF	Ni+	JANAF	PSBr3	JANAF
MnBr2	Barin 1989	NF3O	JANAF	NiBr	Pankratz 1984	PSF	JANAF
MnCl	Wagman et al. 1969,	NH	JANAF	NiBr2	Pankratz 1984	PSF3	JANAF
	Kelley 1960, Kelley &	NH2	JANAF	NiCl	JANAF	P2	JANAF
	King 1961	NH3	JANAF	NiCl2	JANAF	P2O3	Gurvich et al.
MnCl2	Barin 1989	NO	JANAF	Ni(CO)4	JANAF	P2O4	Gurvich et al.
MnF	Wagman et al. 1969,	NO+	JANAF	NiF	Pankratz 1984	P2O5	Gurvich et al.
	Kelley 1960, Kelley &	NO2	JANAF	NiF2	Pankratz 1984	P3	Gurvich et al.
	King 1961	NO2-	JANAF	NiH	Knacke et al. 1991	P3O6	Gurvich et al.
MnF2	Pankratz 1984	NO2Cl	JANAF	NiI	Pankratz 1984	P4	JANAF
MnO	Wagman et al. 1969,	NO2F	JANAF	NiO	Pankratz 1982	P4O6	Gurvich et al.
	Kelley 1960, Kelley &	NO3	JANAF	Ni(OH)2	Knacke et al. 1991	P4O7	Gurvich et al.
	King1961	NS	JANAF	NiS	JANAF	P4O8	Gurvich et al.
MnS	Mills 1974	N2	JANAF	O	JANAF	P4O9	Gurvich et al.
MnSe	Knacke et al. 1991	N2-	JANAF	O+	JANAF	P4O10	JANAF
Mo	JANAF	N2+	JANAF	O-	JANAF	P4O10	Gurvich et al.
Mo-	JANAF	N2F4	JANAF	OD	JANAF	P4S3	JANAF
Mo+	JANAF	N2H4	JANAF	OF	JANAF	Pb	JANAF
MoBr	JANAF	N2O	JANAF	OF2	JANAF	Pb-	JANAF
MoBr2	JANAF	N2O+	JANAF	OH	JANAF	Pb+	JANAF
MoBr3	JANAF	N2O3	JANAF	OH+	JANAF	PbBr	JANAF
MoBr4	JANAF	N2O4	JANAF	OH-	JANAF	PbBr2	JANAF
MoC	Gupta & Gingerich 1981	N2O5	JANAF	ONBr	JANAF	PbBr3	Gurvich et al.
		N3	JANAF	ONCl	JANAF	PbBr4	JANAF
MoC2	Gupta & Gingerich 1981	Na	JANAF	ONF	JANAF	PbCl	JANAF
		Na+	JANAF	ONI	JANAF	PbCl+	JANAF
Mo(CO)6	Barin 1989	Na-	JANAF	O2	JANAF	PbCl2	JANAF
MoCl	Knacke et al. 1991	NaBr	JANAF	O2+	JANAF	PbCl2+	JANAF
MoCl2	Knacke et al. 1991	NaCN	JANAF	O2-	JANAF	PbCl3	Gurvich et al.
MoCl3	Knacke et al. 1991	NaCl	JANAF	O2F	JANAF	PbCl4	JANAF
MoCl4	JANAF	NaF	JANAF	O3	JANAF	PbF	JANAF
MoCl5	JANAF	NaF2-	JANAF	Os	Hultgren et al. 1973	PbF2	JANAF
MoCl6	JANAF	NaH	JANAF	OsO4	Barin 1989	PbF3	Gurvich et al.
MoF	JANAF	NaI	Pankratz 1984	P	JANAF	PbF4	JANAF
MoF2	JANAF	NaO	JANAF	P-	JANAF	PbH	JANAF
MoF3	JANAF	NaO-	JANAF	P+	JANAF	PbH4	Shiskin et al. 1973

PbI	JANAF	SCl+	JANAF	Sb2S3	Pankratz et al. 1987	SiF3	JANAF
PbI2	JANAF	SClF5	JANAF	Sb2S4	Pankratz et al. 1987	SiF4	JANAF
PbI3	Gurvich et al.	SCl2	JANAF	Sb2Te2	Sullivan et al. 1974	SiH	JANAF
PbI4	JANAF	SCl2+	JANAF	Sb3S2	Pankratz et al. 1987	SiH+	JANAF
PbO	JANAF	SD	JANAF	Sb3S3	Pankratz et al. 1987	SiHBr3	JANAF
PbO2	Gurvich et al.	SF	JANAF	Sb4	Pankratz 1984	SiHI3	JANAF
PbS	JANAF	SF+	JANAF	Sb4O6	Pankratz 1982	SiH2	Pankratz et al. 1984
PbS2	Gurvich et al.	SF-	JANAF	Sb4S3	Pankratz et al. 1987	SiH2Br2	JANAF
PbSe	Mills 1974	SF2	JANAF	Sb4S4	Pankratz et al. 1987	SiH2I2	JANAF
PbTe	Mills 1974	SF2+	JANAF	Sc	Pankratz 1982	SiH3	Pankratz et al. 1984
Pb2	JANAF	SF2-	JANAF	ScBr3	Knacke et al. 1991	SiH3Br	JANAF
Pb2I4	Barin 1989	SF3	JANAF	ScC2	Haque & Gingerich 1981	SiH3I	JANAF
Pb2S2	Knacke et al. 1991	SF3+	JANAF	ScC3	Haque & Gingerich 1981	SiH4	JANAF
Pd	Pankratz 1982	SF3-	JANAF	ScC4	Haque & Gingerich 1981	SiI	JANAF
PdCl2	Knacke et al. 1991	SF4	JANAF	ScC5	Haque & Gingerich 1981	SiI2	JANAF
PdO	Wagman et al. 1969	SF4+	JANAF	ScC6	Haque & Gingerich 1981	SiI3	JANAF
Pt	Pankratz 1982	SF4-	JANAF	ScCl3	Knacke et al. 1991	SiI4	JANAF
PtO2	Barin 1989	SF5	JANAF	ScF3	Pankratz 1984	SiN	JANAF
Rb	Gurvich et al.	SF5+	JANAF	ScO	Pedley & Marshall 1983	SiO	JANAF
Rb+	Gurvich et al.	SF5-	JANAF	ScS	Mills 1974	SiOF2	JANAF
Rb-	JANAF	SF6	JANAF	Se	Mills 1974	SiO2	JANAF
RbBO2	Gurvich et al.	SF	JANAF	SeBr2	Mills 1974	SiS	JANAF
RbBr	Gurvich et al.	SO	JANAF	SeCl2	Mills 1974	SiS2	Gurvich et al.
RbCl	Gurvich et al.	SOCl2	Barin 1989	SeF	Mills 1974	SiSe	Mills 1974
RbF	Gurvich et al.	SOF2	JANAF	SeF2	Pankratz 1984	SiTe	Pankratz et al. 1984
RbH	Gurvich et al.	SO2	JANAF	SeF4	Mills 1974	Si2	JANAF
RbI	Gurvich et al.	SO2Cl2	JANAF	SeF5	Mills 1974	Si2C	JANAF
RbK	Gurvich et al.	SO2FCl	JANAF	SeF6	Mills 1974	Si2H6	Barin 1989
RbLi	Gurvich et al.	SO2F2	JANAF	SeO	Mills 1974	Si2N	JANAF
RbNO2	Gurvich et al.	SO3	JANAF	SeO2	Pankratz 1982	Si3	JANAF
RbNO3	Gurvich et al.	SPCl3	JANAF	SeTe	Drowart & Smoes 1977	Sn	Gurvich et al.
RbNa	Gurvich et al.	SSF2	JANAF	Se2	Mills 1974	Sn+	Gurvich et al.
RbO	Gurvich et al.	SSe	Drowart & Smoes 1977	Se2Br2	Mills 1974	SnBr	Gurvich et al.
RbOH	Gurvich et al.	S2	JANAF	Se2Cl2	Mills 1974	SnBr2	Knacke et al. 1991
Rb2	Gurvich et al.	S2Br2	Mills 1974	Se3	Mills 1974	SnBr3	Gurvich et al.
Rb2Br2	Gurvich et al.	S2Cl	JANAF	Se4	Mills 1974	SnBr4	Pankratz 1984
Rb2Cl2	Gurvich et al.	S2Cl2	JANAF	Se5	Mills 1974	SnCl	Gurvich et al.
Rb2F2	Gurvich et al.	S2F10	JANAF	Se6	Mills 1974	SnCl2	Gurvich et al.
Rb2I2	Gurvich et al.	S2O	JANAF	Se7	Mills 1974	SnCl3	Gurvich et al.
Rb2O	Gurvich et al.	S3	JANAF	Se8	Mills 1974	SnCl4	Pankratz 1984
Rb2(OH)2	Gurvich et al.	S4	JANAF	Si	JANAF	SnF	Gurvich et al.
Rb2O2	Gurvich et al.	S5	JANAF	Si+	JANAF	SnF2	Gurvich et al.
Rb2SO4	Gurvich et al.	S6	JANAF	Si-	JANAF	SnF3	Gurvich et al.
Re	Pankratz 1982	S7	JANAF	SiBr	JANAF	SnF4	Gurvich et al.
Re2O7	Wagman et al. 1969	S8	JANAF	SiBr2	JANAF	SnH	Saalfeld & Svec 1963, Kelley 1960, Kelley & King 1961
Rh	Hultgren et al. 1973	Sb	Hultgren et al. 1973	SiBr3	JANAF	SnH4	Barin 1989
RhCl2	Barin 1989	SbBr3	Pankratz 1984	SiBr4	JANAF	SnI	Gurvich et al.
RhCl3	Barin 1989	SbCl	Barin 1989	SiC	JANAF	SnI2	Barin 1989
RhO	Knacke et al. 1991	SbCl3	Barin 1989	SiC2	JANAF	SnI3	Gurvich et al.
RhO2	Barin 1989	SbCl5	Barin 1989	SiCl	JANAF	SnI4	Pankratz 1984
Rn	JANAF	SbF	Barin 1989	SiClF3	JANAF	SnO	Gurvich et al.
Rn+	JANAF	SbF3	Pankratz 1984	SiCl2	JANAF	SnO2	Gurvich et al.
Ru	Hultgren et al. 1973	SbH3	Barin 1989	SiCl3	JANAF	SnS	Gurvich et al.
RuCl3	Barin 1989	SbI3	Pankratz 1984	SiCl3F	JANAF	SnS2	Gurvich et al.
RuCl4	Barin 1989	SbN	Wagman et al. 1968, Kelley 1960, Kelley & King 1961	SiCl4	JANAF	SnSe	Mills 1974
RuF5	Knacke et al. 1991	SbO	Barin 1989	SiF	JANAF	SnTe	Mills 1974
RuO3	Barin 1989	SbS	Hino et al. 1986	SiF2	JANAF	Sn2	Gurvich et al.
RuO4	Barin 1989	SbSe	Mills 1974			Sn2I4	Barin 1989
S	JANAF	SbTe	Sullivan et al. 1974			Sn2Te2	Mills 1974
S+	JANAF	Sb2	Hultgren et al. 1973			Sr	JANAF
S-	JANAF	Sb2S2	Pankratz et al. 1987			Sr+	JANAF
SBrF5	JANAF					SrBr	JANAF
SBr2	Mills 1974						
SCl	JANAF						

SrBr2	JANAF
SrCl	JANAF
SrCl2	JANAF
SrF	JANAF
SrF+	JANAF
SrF2	JANAF
SrH	Pankratz et al. 1984
SrI	JANAF
SrI2	JANAF
SrO	JANAF
SrOH	JANAF
SrOH+	JANAF
Sr(OH)2	JANAF
SrS	JANAF
Ta	JANAF
Ta+	JANAF
Ta-	JANAF
TaCl	Pankratz 1984
TaCl2	Pankratz 1984
TaCl3	Pankratz 1984
TaCl4	Pankratz 1984
TaCl5	JANAF
TaBr5	Pankratz 1984
TaF5	Barin 1989
TaI5	Barin 1989
TaO	JANAF
TaOCl3	Barin 1989
TaO2	JANAF
TaS	Mills 1974
Te	Mills 1974
TeCl2	Mills 174
TeCl4	Mills 1974
TeF	Mills 1974
TeF2	Mills 1974
TeF4	Mills 1974
TeF5	Mills 1974
TeF6	Mills 1974
TeH2O3	Cordfunke & Konings 1990
TeI4	Cordfunke & Konings 1990
TeO	Mills 1974
TeO2	Mills 1974
Te2	Mills 1974
Te2F10	Pankratz et al. 1984
Te2O2	Mills 1974
Te2O4	Knacke et al. 1991
Ti	JANAF
Ti+	JANAF
Ti-	JANAF
TiBr	JANAF
TiBr2	JANAF
TiBr3	JANAF
TiBr4	JANAF
TiC2	Kohl & Stearns 1974
TiC4	Kohl & Stearns 1974
TiCl	JANAF
TiClO	JANAF
TiCl2	JANAF
TiCl2O	JANAF
TiCl3	JANAF
TiCl4	JANAF
TiF	JANAF
TiF2	JANAF
TiF3	JANAF
TiF4	JANAF
TiI	JANAF
TiI2	JANAF
TiI3	JANAF
TiI4	JANAF
TiO	JANAF
TiOF	JANAF
TiOF2	JANAF
TiO2	JANAF
TiS	Mills 1974
Tl	Gurvich et al.
Tl+	Gurvich et al.
TlBr	Cubicciotti & Eding 1965
TlCl	Gurvich et al.
TlF	Gurvich et al.
TlH	Gurvich et al.
TlI	Barin 1989
TlO	Gurvich et al.
TlOH	Gurvich et al.
Tl2Cl2	Gurvich et al.
Tl2F2	Gurvich et al.
Tl2O	Gurvich et al.
Tl2S	Knacke et al. 1991
V	JANAF
V+	JANAF
V-	JANAF
VBr4	Barin 1989
VC	Gupta & Gingerich 1981
VC2	Gupta & Gingerich 1981
VCl2	Barin 1989
VCl4	Pankratz 1984
VF5	Pankratz 1984
VI2	Barin 1989
VN	JANAF
VO	JANAF
VOCl3	Barin 1989
VO2	JANAF
VS	Mills 1974
W	JANAF
W+	JANAF
W-	JANAF
WBr	JANAF
WBr5	JANAF
WBr6	JANAF
W(CO)6	Barin 1989
WCl	JANAF
WCl2	JANAF
WCl4	JANAF
WCl5	JANAF
WCl6	JANAF
WF	JANAF
WF4O	JANAF
WF6	JANAF
WO	JANAF
WOCl4	JANAF
WO2	JANAF
WO2Cl2	JANAF
WO2I2	Barin 1989
WO3	JANAF
WO4H2	JANAF
W2Cl10	JANAF
W2O6	JANAF
W3O8	JANAF
W3O9	JANAF
W4O12	JANAF
W5O15	Gurvich et al.
Y	Pankratz 1982
YCl	Knacke et al. 1991
YCl3	Knacke et al. 1991
YF	Knacke et al. 1991
YF3	Knacke et al. 1991
YI3	Knacke et al. 1991
YO	Gurvich et al.
YS	Mills 1974
Xe	JANAF
XeF2	Pankratz 1984
Xe+	JANAF
Zn	JANAF
Zn+	JANAF
Zn-	JANAF
ZnBr2	Barin 1989
ZnCl2	Barin 1989
ZnF2	Barin 1989
ZnI2	Barin 1989
ZnO	Lamoreux et al. 1987
ZnS	Mills 1974
ZnSe	Mills 1974
ZnTe	Mills 1974
Zr	JANAF
Zr+	JANAF
Zr-	JANAF
ZrBr	JANAF
ZrBr2	JANAF
ZrBr3	JANAF
ZrBr4	JANAF
ZrCl	JANAF
ZrCl2	JANAF
ZrCl3	JANAF
ZrCl4	JANAF
ZrF	JANAF
ZrF2	JANAF
ZrF3	JANAF
ZrF4	JANAF
ZrH	JANAF
ZrI	JANAF
ZrI2	JANAF
ZrI3	JANAF
ZrI4	JANAF
ZrN	JANAF
ZrO	JANAF
ZrO2	JANAF
ZrS	Mills 1974

SOLIDS & LIQUIDS:

Ag	Pankratz 1982
Al	JANAF
AlN	JANAF
Al2O3	JANAF
Al2S3	Pankratz et al 1987
Al4C3	Barin 1989
As	Barin 1989
AsI3	Barin 1989
{c}As2O3	Arsenolite, Pankratz 1982
{m}As2O3	Claudetite, Pankratz 1982
As2O5	Pankratz 1982
As2S2	Mills 1974, Pankratz et al. 1987
As2S3	Origment, Pankratz et al. 1987
As2Se3	Mills 1974
As2Te3	Barin 1989
As4O6	Knacke et al. 1991
As4S4	Realgar, Pankratz et al. 1987
Au	Pankratz 1982
B	JANAF
HBO2	JANAF
H3BO3	JANAF
BN	JANAF
B2Al4O9	Knacke et al. 1991
B2O3	JANAF
B2(OH)4	JANAF
B2S3	Mills 1974
B4Al18O33	Knacke et al. 1991
B4C	JANAF
B10H14	JANAF
Ba	JANAF
BaC2	Barin 1989
BaH2	Barin 1989
BaO	JANAF
BaS	JANAF
BaTiO3	Barin 1989
Ba3N2	Barin 1989
Be	JANAF
BeAl2O4	JANAF
BeBr2	JANAF
BeCl2	JANAF
BeF2	JANAF
BeH	Pankratz et al. 1984
BeH2	Pankratz et al. 1984
BeI2	JANAF
BeN	Pankratz et al. 1984
BeO	JANAF
Be(OH)2	JANAF
BeS	JANAF
BeSO4	JANAF
Be2C	JANAF
Be3B2O6	JANAF
Be3N2	JANAF
Bi	Bankratz 1982
BiBr3	Pankratz 1984
BiCl3	Barin 1989
BiF3	Pankratz 1984
BiI	Barin 1989
BiI3	Pankratz 1984
Bi2O3	Pankratz 1982
Bi2S3	Pankratz et al. 1987
Bi2Se3	Mills 1974
Bi2Te3	Mills 1974
Br2	JANAF
NH4Br	JANAF
PH4Br	Wagman et al. 1968
C	JANAF
Ca	JANAF
CaC2	Barin 1989

CaAl2Si2O8	Anorthite, Hemingway et al. 1982	Cu3P	Barin 1989	In	Pankratz 1982	MnB	Knacke et al. 1991
		F2	JANAF	InAs	Barin 1989	MnB2	Knacke et al. 1991
CaAl12O19	Hibonite, Hallsted 1990	NH4F	Knacke et al. 1991	InBr	Barin 1989	MnS	Pankratz et al. 1987
		Fe	JANAF	InBr3	Barin 1989	Mn2B	Knacke et al. 1991
CaB2O4	Barin 1989	FeB	Barin 1989	InCl	Pankratz 1984	Mn3C	Knacke et al. 1991
CaH2	Barin 1989	FeS	JANAF	InCl2	Knacke et al. 1991	Mn3O4	Pankratz 1982
CaMgSi2O6	Diopside, Robie et al. 1979	Fe3C	Robie et al. 1979	InCl3	Barin 1989	Mo	JANAF
		Fe4N	Knacke et al. 1991	InF3	Pankratz 1984	MoB	Knacke et al. 1991
CaO	JANAF	Ga	JANAF	InI	Knacke et al. 1991	MoC	Pankratz et al. 1984
CaS	Oldhamite, JANAF	GaAs	Barin 1989	InI3	Barin 1989	MoO2	JANAF
CaTiO3	Perovskite, Robie et al. 1979	GaBr3	Barin 1989	InN	Barin 1989	MoS2	JANAF
		GaCl3	Barin 1989	InP	Barin 1989	Mo2C	Pankratz et al. 1984
Ca2Al2SiO7	Gehlenite, Hemingway et al. 1982	GaF3	Pankratz 1984	InS	Pankratz et al. 1987	Mo2N	Barin 1989
		GaI3	Knacke et al. 1991	InSb	Knacke et al. 1991	Na	JANAF
Ca2MgSi2O7	Akermanite, Robie et al. 1979	GaN	Barin 1989	InSe	Mills 1974	NaAlSi3O8	Albite, Robie et al. 1979
		GaP	Barin 1989	InTe	Mills 1974		
Ca3N2	Barin 1989	GaS	Pankratz et al. 1987	In2O3	Pankratz 1982	NaBH4	JANAF
Cd	Pankratz 1982	GaSb	Knacke et al. 1991	In2S3	Pankratz et al. 1987	NaBO2	JANAF
CdBr2	Barin 1989	GaSe	Mills 1974	In2Se3	Mills 1974	NaBr	JANAF
CdCO3	Barin 1989	GaTe	Mills 1974	In2Te3	Barin 1989	NaCl	JANAF
CdCl2	Barin 1989	Ga2O3	Pankratz 1982	Ir	Pankratz 1982	NaF	JANAF
CdF2	Barin 1989	Ga2S3	Mills 1974	K	JANAF	NaH	JANAF
CdI2	Barin 1989	Ga2Se3	Mills 1974	KAlSi3O8	Microcline, Robie et al. 1979	NaI	JANAF
CdO	Pankratz 1982	Ga2Te3	Mills 1974			NaOH	JANAF
Cd(OH)2	Barin 1989	Ge	Pankratz 1982	KBF4	JANAF	Na2B4O7	JANAF
CdS	Pankratz et al. 1987	GeI2	Knacke et al. 1991	KBH4	JANAF	Na2O	JANAF
CdSO4	Barin 1989	GeI4	Knacke et al. 1991	KBO2	JANAF	Na2S	JANAF
CdSb	Barin 1989	GeO	Knacke et al. 1991	KBr	JANAF	Na2SO4	JANAF
CdSe	Mills 1974	{h}GeO2	hexagonal, Pankratz 1982	KCl	JANAF	Na2SiO3	JANAF
CdSiO3	Barin 1989			KH	JANAF	Na2Si2O5	JANAF
CdTe	Barin 1989	{t}GeO2	tetragonal, Pankratz 1982	KF	JANAF	Nb	JANAF
Cd3As2	Knacke et al. 1991			KI	JANAF	NbB2	Barin 1989
Cl2	JANAF	{v}GeO2	vitreous, Pankratz 1982	KOH	JANAF	NbC	Barin 1989
NH4Cl	JANAF			K2B4O7	JANAF	NbN	Barin 1989
PH4Cl	Wagman et al. 1968	GeS	Pankratz et al. 1987	K2O	JANAF	NbO	JANAF
Co	JANAF	GeP	Barin 1989	K2S	Pankratz et al. 1987	NbO2	JANAF
Cr	JANAF	GeS2	Murray & O'Hare 1984	K2SO4	JANAF	Nb2C	Barin 1989
CrB	Barin 1989			K2SiO3	JANAF	Nb2N	Barin 1989
CrB2	Barin 1989	GeSe	O'Hare et al. 1989	Li	JANAF	Nb2O5	JANAF
CrN	JANAF	GeSe2	Mills 1974	LiBH4	JANAF	Ni	JANAF
CrS	Mills 1974	GeTe	Mills 1974	LiBO2	JANAF	Os	Pankratz 1982
Cr2O3	JANAF	H2O	Weast et al. 1974-1975	LiBr	JANAF	P	JANAF
Cr2N	JANAF	Hf	JANAF	LiCl	JANAF	NH4H2PO4	Wagman et al. 1968
Cr3C2	JANAF	HfB2	Barin 1989	LiF	JANAF	NH4SH	Wagman et al. 1968
Cs	JANAF	HfC	Barin 1989	LiH	JANAF	Pb	JANAF
CsBr	Barin 1989	HfN	Pankratz et al. 1984	LiI	JANAF	PbB2O4	JANAF
CsCl	JANAF	HfO2	Barin 1989	LiOH	JANAF	PbB4O7	JANAF
CsF	JANAF	HfS2	Pankratz et al. 1987	Li2O	JANAF	PbB6O10	JANAF
CsI	Barin 1989	Hg	JANAF	Li2S	Barin 1989	PbBr2	JANAF
Cs2O	Pankratz 1982	HgBr2	JANAF	Li2SO4	JANAF	PbCO3	Barin 1989
Cs2SO4	JANAF	HgCl2	JANAF	Li2SiO3	JANAF	PbCl2	JANAF
Cs2SiO3	Knacke et al. 1991	HgF2	JANAF	Li2Se	Barin 1989	PbF2	JANAF
Cu	JANAF	HgI2	JANAF	Li2Te	Mills 1974	PbI2	JANAF
CuBr	Pankratz 1984	HgO	Pankratz 1982	Li3N	JANAF	PbO	JANAF
CuCl	JANAF	HgS	Mills 1974	Mg	JANAF	PbO2	JANAF
CuF	JANAF	HgSe	Mills 1974	MgAl2O4	Spinel, JANAF	PbS	JANAF
CuI	Barin 1989	HgTe	Miills 1974	MgB2	JANAF	PbSO4	Barin 1989
CuP2	Barin 1989	Hg2Br2	JANAF	MgC2	Barin 1989	PbSe	Mills 1974
CuS	Barin 1989	Hg2Cl2	JANAF	MgS	JANAF	PbSiO3	JANAF
CuSe	Mills 1974	Hg2F2	JANAF	MgSiO3	Enstatite cpx, JANAF	PbTe	Mills 1974
CuTe	Mills 1974	Hg2I2	JANAF	Mg2C3	JANAF	Pb2SiO4	JANAF
Cu2S	Pankratz et al. 1987	I2	JANAF	Mg2SiO4	Forsterite, JANAF	Pb3O4	JANAF
Cu2Se	Mills 1974	NH4I	JANAF	Mg3N2	Pankratz et al. 1984	Pd	Pankratz 1982
Cu3As	Barin 1989	PH4I	Wagman et al. 1968	Mn	JANAF	Pt	Pankratz 1982

Rb	JANAF	TaB2	Barin 1989
RbBr	Barin 1989	TaC	JANAF
RbCl	Barin 1989	TaN	Barin 1989
RbF	Barin 1989	TaS2	Barin 1989
RbI	Barin 1989	Ta2C	Barin 1989
Rb2O	Barin 1989	Ta2N	Barin 1989
Rb2SO4	Barin 1989	Ta2O5	JANAF
Rb2SiO3	Barin 1989	Te	Mills 1974
Re	Pankratz 1982	TeBr4	Barin 1989
ReO2	Barin 1989	TeCl4	Mills 1974
ReS2	Mills 1974	TeO2	Pankratz 1982
Rh	Pankratz 1982	Ti	JANAF
Ru	Pankratz 1982	TiB	JANAF
S	JANAF	TiB2	JANAF
Sb	Barin 1989	TiC	JANAF
SbBr3	Barin 1989	TiH2	JANAF
SbCl3	Barin 1989	TiO2	Rutile, JANAF
SbF3	Barin 1989	TiN	Osbornite, JANAF
SbI3	Pankratz 1984	TiS	Mills 1974
Sb2O3	Pankratz 1982	Tl	Pankratz 1982
Sb2O4	Pankratz 1982	TlBr	Pankratz 1984
Sb2O5	Barin 1989	TlCl	Pankratz 1984
Sb2S3	Pankratz et al. 1987	TlCl3	Barin 1989
Sb2Se3	Mills 1974	TlF	Pankratz 1984
Sb2Te3	Knacke et al. 1991	TlI	Pankratz 1984
Sc	Pankratz 1982	TlSe	Pankratz et al. 1984
ScN	Kubaschewski & Alcock 1979	Tl2O	Pankratz 1982
		Tl2O3	Pankratz 1982
Sc2O3	Pankratz 1982	Tl2S	Pankratz et al. 1987
Se	Mills 1974	Tl2SO4	Barin 1989
SeCl4	Mills 1974	Tl2Se	Mills 1974
SeO2	Pankratz 1982	Tl2Te	Mills 1974
Se2Cl2	Mills 1974	V	JANAF
Si	JANAF	VB	Barin 1989
{a}SiC	alpha, JANAF	VB2	Barin 1989
{b}SiC	beta, JANAF	VC088	Pankratz et al. 1984
Si2N2O	Sinoite, Fegley 1981	VN0465	JANAF
Si3N4	JANAF	VN	JANAF
Sn	Pankratz 1982	VO	JANAF
SnBr2	Pankratz 1984	V2B3	Knacke et al. 1991
SnBr4	Barin 1989	V2C	Pankratz et al. 1984
SnCl2	Pankratz 1984	V2O3	JANAF
SnCl4	Pankratz1984	V2O4	JANAF
SnF2	Pankratz 1984	V2O5	JANAF
SnI2	Pankratz 1984	V3B2	Barin 1989
SnI4	Pankratz 1984	V3B4	Barin 1989
SnO	Barin 1989	V5B6	Knacke et al. 1991
SnO2	Pankratz 1982	W	JANAF
SnS	Pankratz et al. 1987	WB	Knacke et al. 1991
SnS2	Mills 1974	WC	Barin 1989
SnSO4	Barin 1989	WO2	JANAF
SnSe	Mills 1974	WO3	JANAF
SnSe2	Barin 1989	WS2	Mills 1974
SnTe	Mills 1974	W2B	Knacke et al. 1991
Sn2S3	Mills 1974	W2C	Knacke et al. 1991
Sn3S4	Mills 1974	Y	Pankratz 1982
Sr	JANAF	YC2	Gschneidner & Kippenhan 1971
SrC2	Barin 1989		
SrH2	Barin 1989	YS	Gschneidner & Kippenhan 1971
SrO	JANAF		
SrS	JANAF	YN	Barin 1989
SrTiO3	Barin 1989	Y2O3	Pankratz 1982
Sr3N2	Barin 1989	Zn	JANAF
Ta	JANAF	ZnBr2	Barin 1989
ZnCl2	Barin 1989		
ZnF2	Barin 1989		
ZnI2	Barin 1989		
ZnO	Pankratz 1982		
ZnP2	Barin 1989		
ZnS	Sphalerite, Pankratz et al. 1987		
ZnSO4	JANAF		
ZnSe	Mills 1974		
ZnTe	Mills 1974		
Zn3As2	Barin 1989		
Zn3P2	Barin 1989		
Zn3N2	Barin 1989		
Zr	JANAF		
ZrB2	JANAF		
ZrC	JANAF		
ZrN	JANAF		
ZrO2	JANAF		
ZrS2	Mills 1974		
ZrSiO4	JANAF		

for REE and Actinide compounds see Lodders and Fegley 1993.

References to Appendix:

Barin I. (1989), Thermochemical data of pure substances. Vol. I&II, 1739 pp., VCH Weinheim, Germany.

Benson (1976) Thermochemical kinetics. 320 pp., J. Wiley Pub., New York., U.S.A.

Chandrasekharaiah M.S., Karkhanavala M.D., and Tripathi S.N. (1981) The pressure of iridium oxides over iridium at high temperatures in 1 atm. of dry oxygen. J. Less Common. Metals 80, P6-P17.

Chao J., Wilhoit R.C. and Zwolinski B.J. (1973) Ideal gas thermodynamic properties of ethane and propane. J. Chem. Ref. Data 2, 427-437.

Chao J. and Zwolinski B.J. (1978) *Ideal gas thermodynamic properties* of methanoic and ethanoic acids. J. Phys. Chem. Ref. Data 7, 363-377.

Cordfunke E.H.P and Konings R.J.M. (eds.) (1990) Thermochemical data for reactor materials and fission products. North Holland, Amsterdam, The Nederlands. pp. 695.

Cubicciotti D. and Eding H (1965) Enthalpies, entropies and free energy functions of TlF, TlBr, and TlI above room temperature. J. Chem. Eng. Data 10, 343-345.

Drowart J. and Smoes S. (1977) Determination by the mass spectrometric Knudsen cell method and discussion of the dissociation energies of the molecules Se_2 (g), SSe (g), and SeTe (g). J. Chem. Soc. Faraday Trans. II, 73, 1755-1767.

Fegley M.B. (1981) The thermodynamic properties of silicon oxynitride. Comm. Am. Ceram. Soc. *64, C124-C126.*

Galasso V., Bigotto A. and DeAlti G. (1966) Normal vibrations and thermodynamic properties of GeH_3CN, Ge_2H_6 and GeH_3CH_3. Z. *Physik.* Chem. *50, 38-45.*

Geschneidner K.A. and Kippenhan N. (1971) Thermochemistry of the rare earth carbides, nitrides and sulfides for steelmaking. 25 pp., Rare Earth Inf. Cent., Ames IA, Rep. IS-RIC-5.

Glushko V.P, Gurvich L.V., Bergman G.A., Veitz I.V., Medvedev V.A., Khachcurvzov G.A., and Yungman V.S (1970-1982) Thermodynamic properties of individual substances. Vol. 1-10, High Temperature Inst. Moscow, Russia.

Gupta S.K. and Gingerich K.A. (1981) Mass spectrometric study of the stabilities of gaseous carbides of vanadium, niobium, and molybdenum. J. Chem. Phys. 74, 3584-3590.

Gurvich et al. (1978 - 1990) Termodinamicheskie sovoistava indinvidual'nykh veshshestv. Vol. 1-4, Nauka, Moscow, Russia.

Hallsted B. (1990) Assessment of the CaO-Al2O3 system. J. Am. Ceramic. Soc. 37, 15-23.

Haque R. and Gingerich K.A. (1981) Identification and atomization energies of gaseous molecules *ScC2, ScC3, ScC4, ScC5,* and *ScC6* by high temperature mass spectrometry. J. Chem. Phys. 74, 6407-6414.

Harland (1986) Appearance energies and enthalpies of formation from ionization of cyanoacetylene by "monochromatic" electron impact. Int. J. Mass. Spec. Ion Process 70, 231-236.

Hemingway B.S., Haas J.L., and Robinson G.R. (1982) Thermodynamic properties of selected minerals in the system Al_2O_3-CaO-SiO_2-H_2O at 298.15 K and 1 bar (10^5 Pascals) pressure and at higher temperatures. Geol. Surv. Bull. 1544, 70 pp.

Hilsenrath J., Messina C.G., and Evans W.H. (1964) Tables of ideal gas thermodynamic functions for 73 atoms and their first and second ions to 10000°K. Vol. AFWL TDR-64-44. Air Force Weapons Laboratory, Kirtland Air Force Base, NM. pp. 441.

Hino M. Nagamori M. and Toguri J.M. (1986) Thermodynamics of

gaseous SbS. Metall. Trans. 17B, 913-914,
Hultgren R., Desai P.D., Hawkins D.T., Gleiser M., Kelley K.K., and Wagman D.D. (1973) Selected values of the thermodynamic properties of the elements. 636 pp., Am. Soc. Metals, Metals Park, Ohio, U.S.A.
JANAF Thermochemical tables (1975), M.W. Chase et al. eds.), 3rd ed., J. Phys. Chem. Ref. Data 14, suppl. No. 1.
Kelley K.K. (1960) Contributions to the data on theoretical metallurgy, XIII., high-temperature heat-content, heat-capacity, and entropy data for the elements and inorganic compounds. U.S. Bur. Mines Bull. No. 584, Washington D.C.
Kelley K.K. and King E.G. (1961) Contributions to the data on theoretical metallurgy, XIV. Entropies of the elements and inorganic compounds. U.S. Bur. Mines, No. 592, Washington D.C.
Knacke O., Kubaschewski O, and Hesselmann K (1991) Thermochemical properties of inorganic substances. Vol. I & II, 2412 pp., Springer Vlg Berlin, Germany.
Kohl F.J. and Stearns C.A. (1974) Vaporization and dissociation energies of the molecular carbides of titanium, zirconium, hafnium, and thorium. High Temp. Sci. 6, 284-302.
Kubaschewski O and Alcock C.B. (1979) Metallurgical thermochemistry. 183 pp., Pergamon New York, NY.
Lamoreux R.H., Hildenbrand D.L., and Brewer L. (1987) High-temperature vaporization behavior of oxides II. Oxides of Be, Mg, Ca, Sr, Ba, B, Al, Ga, In, Tl, Si, Ge, Sn, Pb, Zn, Cd, and Hg. J. Phys. Chem. Ref. Data 16, 419-443.
Lindgren B. and Nilsson C. (1975) On the spectra of BiH and BiD. J. Mol. Spectros. 55, 407-419.
Lodders K. and Fegley B. (1993) Lanthanide and actinide chemistry at high C/O ratios in the solar nebula. Earth Planet. Sci. Lett. 117, 125-145.
Mills K.C. (1974) Thermodynamic data for inorganic sulphides, selenides and tellurides. 845 pp., Butterworths, London.
Murray W.T. and O'Hare P.A.G. (1984) Thermochemistry of inorganic sulfur compounds II. Standard enthalpy of formation of germanium disulfide. J. Chem. Thermo. 16, 335-341.
O'Hare P.A.G. (1968) The thermodynamic properties of As2, As4, and some arsenic fluorides. U.S. AEC ANL Rep. 7456.
O'Hare P.A.G., Susman S., and Volin K.J. (1989) Thermochemistry of germanium monoselenide, and the Ge-Se bond dissociation enthalpy. J. Chem. Thermo. 21, 827-836.
Pankratz L.B. (1982) Thermodynamic properties of elements and oxides. US Bur. Mines Bull. 672, 509 pp.
Pankratz L.B. (1984) Thermodynamic properties of halides. US Bur. Mines Bull. 674, 826 pp.
Pankratz L.B., Stuve J.M., Gokcen N.A. (1984) Thermodynamic data for mineral technology. US Bur. Mines Bull. 677, 355 pp.
Pankratz L.B., Mah A.D., and Watson S.W (1987) Thermodynamic properties of sulfides. US Bur. Mines Bull. 689, 472 pp.
Pedley J.B. and Marshall E.M. (1983) Thermochemical data for gaseous monoxides. J. Chem. Ref. Data 12, 967-1031.
Powers D.A. (1992) The thermodynamic properties of technetium, High Temp. Sci. 31, 105-120.
Ramakhrishnan E.S. and Chandrasekharaiah M.S. (1975) Thermodynamic stability of amorphous germanium monoxide. Trans. Indian Inst. Metals 28, 58-63.
Robie R.A., Hemingway B.S., and Fisher J.R. (1979) Thermodynamic properties of minerals and related substances at 298.15 K and 1 bar (10^5 Pascals) pressure and at higher temperatures. Geol. Surv. Bull. 1452, 456 pp.
Rossini F.D., Pitzer K.S., Arnett R.L., Braun R.M. and Pimentel G.C. (1953) Selected values of physical and thermodynamic properties of hydrocarbons and related compounds. Am. Petroleum Inst. Res. Project 44, Carnegie Press, Pittsburgh PA.
Ruscic B, Schwarz M, and Berkowitz J. (1990) Photoionization studies of GeH_n (n=2-4). J. Chem Phys. 92, 1865-1875.
Saalfeld F.E. and Svec H.J. (1963) The mass spectra of volatile hydrides. I. The monoelemental hydrides of the group IVB and VB elements. Inorg. Chem. 2, 46-50.
Sauval H.R. and Tatum J.B (1984) A set of partition functions and equilibrium constants for 300 diatomic molecules of astronomical interest. Ap. J. suppl. ser. 56, 193-209.
Shabur V.N and Morozov V.P (1978) Thermodynamic functions of XY_n radicals. Teplofisika Vysokikh Temperatur 16(5), 946-950.
Shaulov Y. K. and Mosin A.M. (1973) Thermodynamic functions of arsenic chlorides. Russ. J. Phys. Chem. 47, 644-645.
Shiskin Y.A., Marusin V.V. and Kolyshev A.N. (1973) Thermodynamics of lead (IV) hydride at high temperatures. VINITI 6966-9673.
Smith W.T., Line L.E. and Bell, W.A. (1952) The vapor pressure of rhenium heptoxide and perrhenic acid. J. Am. Chem. Soc. 74, 4964-4966.
Stull D.R., Westrum E.F., and Sinke G.C. (1969) The chemical thermodynamics of organic compounds. Reprint 1987 with corrections, R.E. Krieger Pub. Company, Malabar, Fl., pp. 865.
Sullivan C.L., Zehe M.J. and Carlson K.D. (1974) Heats of reaction for gaseous species in the vaporization of solid antimony telluride (Sb_2Te_3). High Temp. Sci. 6, 80.
Uy O.M. and Drowart J. (1969) Mass spectrometric determination of the dissociation energies of the molecules BiO, BiS, BiSe, and BiTe. Trans. Faraday Soc. 65, 3221-3230.
Weast R.C. et al (1974-1975) Handbook of Chemistry and Physics, 55th ed., CRC Press.
Wagman D.D., Evans W.H., Parker V.B., Halow I., Bailey S.M., and Schumm R.H. (1968) Selected values of chemical thermodynamic properties. NBS TN 270-3, pp. 264.
Wagman D.D., W.H. Evans, V.B. Parker, I. Halow, S.M. Bailey, and Schumm R.H. (1969) Selected values of chemical thermodynamic properties. NBS TN 270-4, pp. 141.

Ge–H: Synthese de germathietannes et digermadithiannes nouvelle voie d'acces aux germathiones. *Synth. React. Inorg. Met.-Org. Chem.* **10,** 515–529.

BARSHAY, S. S., AND J. S. LEWIS 1978. Chemical structure of the deep atmosphere of Jupiter. *Icarus* **33,** 593–611.

BEER, R. 1976. Jupiter and the boron problem. *Icarus* **29,** 193–199.

BERKOWITZ, J. 1988. Photoionization mass spectrometric studies of AsH_n (n = 1–3). *J. Chem. Phys.* **89,** 7065–7076.

BÉZARD, B., P. DROSSART, E. LELLOUCH, G. TARRAGO, AND J. P. MAILLARD 1989. Detection of arsine in Saturn. *Astrophys. J.* **346,** 509–513.

BÉZARD, B., D. GAUTIER, AND A. MARTEN 1986. Detectability of HD and non-equilibrium species in the upper atmospheres of the giant planets from their submillimeter spectrum. *Astron. Astrophys.* **161,** 387–402.

BÉZARD, B., A. MARTEN, J. P. BALUTEAU, D. GAUTIER, J. M. FLAUD, AND C. CAMY-PEYRET 1983. On the detectability of H_2S in Jupiter. *Icarus* **55,** 259–271.

BJORAKER, G. L., H. P. LARSON, AND V. G. KUNDE 1986a. The gas composition of Jupiter as derived from 5-μm airborne spectroscopic observations. *Icarus* **66,** 579–609.

BJORAKER, G. L., H. P. LARSON, AND V. G. KUNDE 1986b. The abundance and distribution of water vapor in Jupiter's atmosphere. *Astrophys. J.* **311,** 1058–1072.

BORUNOV, S. P., AND V. A. DOROFEYEVA 1991. Phosphorus compounds in Jovian atmosphere. *Lunar Planet. Sci.* **22,** 125–126.

BORUNOV, S. P., V. DOROFEYEVA, I. KHODAKOVSKY, P. DROSSART, E. LELLOUCH, AND TH. ENCRENAZ 1993. Phosphorus compounds in the atmosphere of Jupiter. *Bull. Am. Astron. Soc.* **25,** 1029.

CAMERON, A. G. W. 1973. Abundances of the elements in the solar system. *Space Sci. Rev.* **15,** 121–146.

CHASE, M. W., JR., C. A. DAVIES, J. R. DOWNEY, JR., D. J. FRURIP,

R. A. McDonald, and A. N. Syverud 1985. *JANAF Thermochemical Tables*, 3rd ed., *J. Phys. Chem. Ref. Data* **14**, Suppl. 1, Am. Chem. Soc. and Am. Inst. of Phys., Washington, DC.

Conrath, B., D. Gautier, R. A. Hanel, and J. S. Hornstein 1984. The helium abundance of Saturn from Voyager Measurements. *Astrophys. J.* **282**, 807–815.

Cordfunke, E. H. P., and R. J. M. Konings 1990. *Thermochemical Data for Reactor Materials and Fission Products*. North-Holland, Amsterdam.

Cotton, F. A., and G. Wilkinson 1988. *Advanced Inorganic Chemistry*, 5th ed. Wiley–Interscience, New York.

Courtin, R., D. Gautier, A. Marten, B. Bézard, and R. Hanel 1984. The composition of Saturn's atmosphere at northern temperate latitudes from Voyager IRIS spectra: NH_3, PH_3, C_2H_2, C_2H_6, CH_3D, CH_4, and the Saturnian D/H isotopic ratio, *Astrophys. J.* **287**, 899–916.

Drossart, P., E. Lellouch, B. Bézard, J. P. Maillard, and G. Tarrago 1990. Jupiter: Evidence for a phosphine enhancement at high northern latitudes. *Icarus* **83**, 248–253.

Fegley, M. B. 1981. The thermodynamic properties of silicon oxynitride. *J. Am. Ceram. Soc.* **64**, C124–C126.

Fegley, B., Jr. 1988. The chemistry of arsine (AsH_3) in the deep atmospheres of Saturn and Jupiter. *Bull. Am. Astron. Soc.* **20**, 879.

Fegley, B., Jr. 1990. The applications of chemical thermodynamics and chemical kinetics to planetary atmospheres research. In *First International Conference on Laboratory Research for Planetary Atmospheres* (K. Fox, Ed.), NASA CP3077, pp. 267–302.

Fegley B., Jr. 1994a. Cosmochemistry. In *Encyclopedia of Planetary Sciences* (J.H. Shirley and R.W. Fairbridge, Eds.). Chapman and Hall, New York, in press.

Fegley, B., Jr. 1994b. Properties and composition of the terrestrial oceans and of the atmospheres of the Earth and other planets. In *AGU Handbook of Physical Constants* (T. Ahrens, Ed.). AGU, Washington, DC, in press.

Fegley, B., Jr., D. Gautier, T. Owen, and R. G. Prinn 1991. Spectroscopy and chemistry of the lower atmosphere of Uranus. In *Uranus* (J. Bergstralh, E. Miner, and M. S. Matthews, Eds.), pp. 147–203. Univ. of Arizona Press, Tucson.

Fegley, B., Jr., and J. S. Lewis 1979. Thermodynamics of selected trace elements in the jovian atmosphere. *Icarus* **38**, 166–179.

Fegley, B., Jr., and R. G. Prinn 1985. Equilibrium and non-equilibrium chemistry of Saturn's atmosphere: Implications for the observability of PH_3, N_2, CO, and GeH_4. *Astrophys. J.* **299**, 1067–1078.

Fegley, B., Jr., and R. G. Prinn 1988a. Chemical constraints on the water and total oxygen abundance in the deep atmosphere of Jupiter. *Astrophys. J.* **324**, 621–625.

Fegley, B., Jr., and R. G. Prinn 1988b. The predicted abundances of deuterium-bearing gases in the atmospheres of Jupiter and Saturn. *Astrophys. J.* **326**, 490–508.

Flasar, M., and P. J. Gierasch 1977. Eddy diffusivities within Jupiter. In *Proceedings Symposium on Planetary Atmospheres* (A. V. Jones, Ed.), pp. 85–87. Royal Society of Canada, Ottawa.

Fraser, M. E., and D. H. Stedman 1983. Spectroscopy and mechanism of chemiluminescent reactions between group V hydrides and ozone. *J. Chem. Soc. Faraday Trans. I* **79**, 527–542.

Fraser, M. E., D. H. Stedman, and T. M. Dunn 1984. Quantum-yield studies of group V hydride chemiluminescent reactions. *J. Chem. Soc. Faraday Trans. I* **80**, 285–295.

Fukutani, S., N. Kunioshi, Y. Uodome, and H. Jinno 1991a. Combustion reactions in silane–air flames. II. Counterflow diffusion flame. *Bull. Chem. Soc. Jpn.* **64**, 2335–2340.

Fukutani, S., Y. Uodome, N. Kunioshi, and H. Jinno 1991b. Combustion reactions in silane–air flames. I. Flat premixed flames. *Bull. Chem. Soc. Jpn.* **64**, 2328–2334.

Gautier, D., B. Conrath, M. Flasar, R. Hanel, V. Kunde, A. Chedin, and N. Scott 1981. The helium abundance of Jupiter from Voyager. *J. Geophys. Res.* **86**, 8713–8720.

Gautier, D., B. Bézard, A. Marten, J. P. Baluteau, N. Scott, A. Chedin, V. Kunde, and R. Hanel 1982. The C/H ratio in Jupiter from the Voyager infrared investigation. *Astrophys. J.* **257**, 901–912.

Glinski, R. J., J. L. Gole, and D. A. Dixon 1985. Oxidation processes in the gas-phase silane–ozone system. Chemiluminescent emission and the molecular structure of H_2SiO. *J. Am. Chem. Soc.* **107**, 5891–5894.

Gurvich, L. V., I. V. Veyts, and C. B. Alcock 1989–1994. *Thermodynamic Properties of Individual Substances*, 4th ed., 3 vols. Hemisphere Publishing, New York.

Hartley, S. B., and J. C. McCoubrey 1963. Enthalpy of formation of phosphorus oxide. *Nature* **198**, 476.

Hunten, D. M., L. Colin, and J. E. Hansen 1986. Atmospheric science on the Galileo mission. *Space Sci. Rev.* **44**, 191–240.

Jasinski, J. M. 1994. Gas phase and gas surface kinetics of transient silicon hydride species. *Proc. Mater. Res. Symp.*, in press.

Jasinski, J. M., and R. D. Estes 1985. Laser powered homogeneous pyrolysis of silane. *Chem. Phys. Lett.* **117**, 495–499.

Kaye, J. A., and D. F. Strobel 1983a. HCN formation on Jupiter. The coupled photochemistry of ammonia and acetylene. *Icarus* **54**, 417–433.

Kaye, J. A., and D. F. Strobel 1983b. Formation and photochemistry of methylamine in Jupiter's atmosphere. *Icarus* **55**, 399–419.

Kaye, J. A., and D. F. Strobel 1984. Phosphine photochemistry in the atmosphere of Saturn. *Icarus* **59**, 314–335.

Knacke, O., O. Kubaschewski, and K. Hesselmann 1991. *Thermochemical Properties of Inorganic Substances*, 2 vols. Springer-Verlag Berlin.

Koerner, W. E., and F. Daniels 1952. The heat of formation of nitric oxide and phosphorus trioxide. *J. Chem. Phys.* **20**, 113–115.

Larson, H. P., D. S. Davis, R. Hofman, and G. L. Bjoraker 1984. The jovian atmospheric window at 2.7 μm: A search for H_2S. *Icarus* **60**, 621–639.

Larson, H. P., U. Fink, H. A. Smith, and D. S. Davis 1980. The middle-infrared spectrum of Saturn: Evidence for phosphine and upper limits to other trace atmospheric constituents. *Astrophys. J.* **240**, 327–337.

Lavayssière, H., G. Dousse, J. Barrau, J. Satgé, and M. Bouchaut 1978. La diethylgermathione $Et_2Ge{=}S$: Formation et caracterisation. *J. Organomet. Chem.* **161**, C59–C62.

Lewis, J. S. 1969a. Observability of spectroscopically active compounds in the atmosphere of Jupiter. *Icarus* **10**, 393–409.

Lewis, J. S. 1969b. The clouds of Jupiter and the NH_3–H_2O and NH_3–H_2S systems. *Icarus* **10**, 365–378.

Lewis, J. S., and M. B. Fegley 1984. Vertical distribution of disequilibrium species in Jupiter's troposphere. *Space Sci. Rev.* **39**, 163–192.

Lewis, J. S., and R. G. Prinn 1980. Kinetic inhibition of CO and N_2 reduction in the solar nebula. *Astrophys. J.* **238**, 357–364.

Lodders, K., and H. Palme 1991. The role of sulfur in planetary core formation. *Meteoritics* **26**, 366.

Lohr, L. L. 1984. A theoretical study of the gaseous oxides PO_2 and PO, their anions, and their role in the combustion of phosphorus and phosphine. *J. Phys. Chem.* **88**, 5569–5574.

Muenow, D. W., O. M. Uy, and J. L. Margrave 1970. Mass spectro-

metric studies of the vaporization of phosphorus oxides. *J. Inorg. Nucl. Chem.* **32,** 3459–3467.

MURATA, K. J. 1960. Occurrence of CuCl emission in volcanic flames. *Am. J. Sci.* **258,** 769–772.

NEUDORFL, P., A. JODHAN, AND O. P. STRAUSZ 1980. Mechanism of the thermal decomposition of monosilane. *J. Phys. Chem.* **84,** 338–339.

NEWMAN, C. G., J. DZARNOSKI, M. A. RING, AND H. E. O'NEAL 1980. Kinetics and mechanism of the germane decomposition. *Int. J. Chem. Kinet.* **12,** 661–670.

NEWMAN, C. G., H. E. O'NEAL, M. A. RING, F. LESKA, AND N. SHIPLEY 1979. Kinetics and mechanism of the silane decomposition. *Int. J. Chem. Kinet.* **11,** 1167–1182.

NOLL, K. S., T. R. GEBALLE, AND R. F. KNACKE 1989. Arsine in Saturn and Jupiter. *Astrophys. J.* **338,** L71–L74.

NOLL, K. S., R. F. KNACKE, T. R. GEBALLE, AND A. T. TOKUNAGA 1986. Detection of carbon monoxide in Saturn. *Astrophys. J.* **309,** L91–L94.

NOLL, K. S., R. F. KNACKE, T. R. GEBALLE, AND A. T. TOKUNAGA 1988. The origin and vertical distribution of carbon monoxide in Jupiter. *Astrophys. J.* **324,** 1210–1218.

NOLL, K. S., AND H. P. LARSON 1990. The spectrum of Saturn from 1990 to 2230 cm^{-1}: Abundances of AsH_3, CH_3D, CO, GeH_4, NH_3, and PH_3. *Icarus* **89,** 168–189.

NOLL, K. S., H. P. LARSON, AND T. R. GEBALLE 1990. The abundance of AsH_3 in Jupiter. *Icarus* **83,** 494–499.

OWEN, T., A. R. W. MCKELLAR, TH. ENCRENAZ, J. LECACHEUX, C. DEBERGH, AND J. P. MAILLARD 1977. A study of the 1.56-μm NH_3 band on Jupiter and Saturn. *Astron. Astrophys.* **54,** 291–295.

PALME, H., AND B. FEGLEY, JR. 1990. High-Temperature Condensation of Iron-Rich Olivine in the Solar Nebula. *Earth Planet. Sci. Lett.* **101,** 180–195.

PRINN, R. G., AND S. S. BARSHAY 1977. Carbon monoxide on Jupiter and implications for atmospheric convection. *Science* **198,** 1031–1034.

PRINN, R. G., AND B. FEGLEY, JR. 1981. Kinetic inhibition of CO and N_2 reduction in circumplanetary nebulae: Implications for satellite composition. *Astrophys. J.* **249,** 308–317.

PRINN, R. G., H. P. LARSON, J. J. CALDWELL, AND D. GAUTIER 1984. Composition and chemistry of Saturn's atmosphere. In *Saturn* (T. Gehrels and M.S. Matthews, Eds.), pp. 88–149. Univ. of Arizona Press, Tucson.

PRINN, R. G., AND E. P. OLAGUER 1981. Nitrogen on Jupiter: A deep atmospheric source. *J. Geophys. Res.* **86,** 9895–9899.

PRINN, R. G., AND T. OWEN 1976. Chemistry and spectroscopy of the Jovian atmosphere. In *Jupiter* (T. Gehrels, Ed.), pp. 319–371. Univ. of Arizona Press, Tucson.

PURNELL, J. H., AND R. WALSH 1966. The pyrolysis of monosilane. *Proc. R. Soc.* **293,** 543–561.

RUSCIC, B., M. SCHWARZ, AND J. BERKOWITZ 1990. Photoionization studies of GeH_n (n = 2–4). *J. Chem. Phys.* **92,** 1865–1875.

SCHMITT, W., H. PALME, AND H. WÄNKE 1989. Experimental determination of metal/silicate partition coefficients for P, Co, Ni, Cu, Ga, Mo, and W and some implications for the early evolution of the Earth. *Geochim. Cosmochim. Acta* **53,** 173–185.

SMITH, W. R. AND R. W. MISSEN 1982. *Chemical Reaction Equilibrium Analysis: Theory and Algorithms.* Wiley, New York.

SMOES, S. AND J. DROWART 1974. Atomization energies of phosphorus oxides. *J. Chem. Soc. Faraday Trans. I,* 139–148.

SO, S. P. 1993. Theoretical study of the [Ge,H_2,S] potential energy surface: Comparison with [Ge,H_2,O]. *J. Phys. Chem.* **97,** 4643–4646.

STONE, P. H. 1976. Meteorology of the jovian atmosphere. In *Jupiter* (T. Gehrels, Ed.), pp. 586–618. Univ. of Arizona Press, Tucson.

SUESS, H. E., AND H. C. UREY 1956. Abundances of the elements. *Rev. Mod. Phys.* **28,** 53–74.

TAZIEFF, H. 1960. Exploration geophysique et geochimique du volcan Niragongo (Congo belge). *Bull. Volcanol.* **23,** 69–71.

TOKUNAGA, A. T., S. C. BECK, T. R. GEBALLE, J. H. LACY, AND E. SERABYN 1981. The detection of HCN on Jupiter. *Icarus* **48,** 283–289.

TREFFERS, R. R., H. P. LARSON, U. FINK, AND T. N. GAUTIER 1978. Upper limits to trace constituents in Jupiter's atmosphere from an analysis of its 5-μm spectrum. *Icarus* **34,** 331–343.

TRINQUIER, G., M. PELISSIER, B. SAINT-ROCH, AND H. LAVAYSSIERE 1981. Structure of germanone and germathione through ab initio calculations. *J. Organomet. Chem.* **214,** 169–181.

VAN ZEGGEREN, F., AND S. H. STOREY 1970. *The Computation of Chemical Equilibria.* Cambridge Univ. Press, Cambridge.

VOTINTSEV, V. N., I. S. ZASLONKO, V. S. MIKHEEV, AND V. N. SMIRNOV 1984. Mechanism of the decomposition of germane. *Kinet. Catal.* **26,** 1114.

WAGMAN, D. D., W. H. EVANS, V. B. PARKER, I. HALOW, S. M. BAILEY, AND R. H. SCHUMM 1968. *Selected Values of Chemical Thermodynamic Properties.* National Bureau of Standards (U.S.) Technical Note 270-3, Government Printing Office, Washington, DC.

WEIDENSCHILLING, S. J., AND J. S. LEWIS 1973. Atmospheric and cloud structure of the jovian planets. *Icarus* **20,** 465–476.

WHITE, R. T., R. L. ESPINO-RIOS, D. S. ROGERS, M. A. RING, AND H. E. O'NEAL 1985. Mechanism of the silane decomposition. I. Silane loss kinetics and rate inhibition by hydrogen. II. Modeling of the silane decomposition (all stages of reaction) *Int. J. Chem. Kinet.* **17,** 1029–1065.

WITHNALL, R., AND L. ANDREWS 1985a. Infrared spectroscopic evidence for silicon–oxygen double bonds: Silanone and the silanoic and silicic acid molecules. *J. Am. Chem. Soc.* **107,** 2567–2568.

WITHNALL, R., AND L. ANDREWS 1985b. Matrix reactions of silane and oxygen atoms. Infrared spectroscopic evidence for the silanol, silanone, and silanoic and silicic acid molecules. *J. Phys. Chem.* **89,** 3261–3268.

WITHNALL, R., AND L. ANDREWS 1990. Matrix reactions of germane and oxygen atoms. Infrared spectroscopic evidence for germylene–water complex, germanone, germanol, hydroxygermylene, and germanic acid. *J. Phys. Chem.* **94,** 2351–2357.

WOJSLAW, R. S., AND B. F. PEERY 1976. Identification of novel molecules in the spectrum of 19 Piscium. *Astrophys. J. Suppl.* **31,** 75–92.

ZACHARIAH, M. R. AND W. TSANG 1993a. Ab initio computation of thermochemistry and kinetics in the oxidation of gas phase silicon species. *Mater. Res. Soc. Symp. Proc.* **282,** 493–498.

ZACHARIAH, M. R., AND W. TSANG 1993b. Application of ab initio molecular orbital and reaction rate theories to nucleation kinetics. *Aerosol Sci. Technol.* **19,** 499–513.